

X-ray spectrometry at external-beam IBA facilities for cultural heritage applications

Massimo Chiari / *I.N.F.N. Florence*

 chiari@fi.infn.it

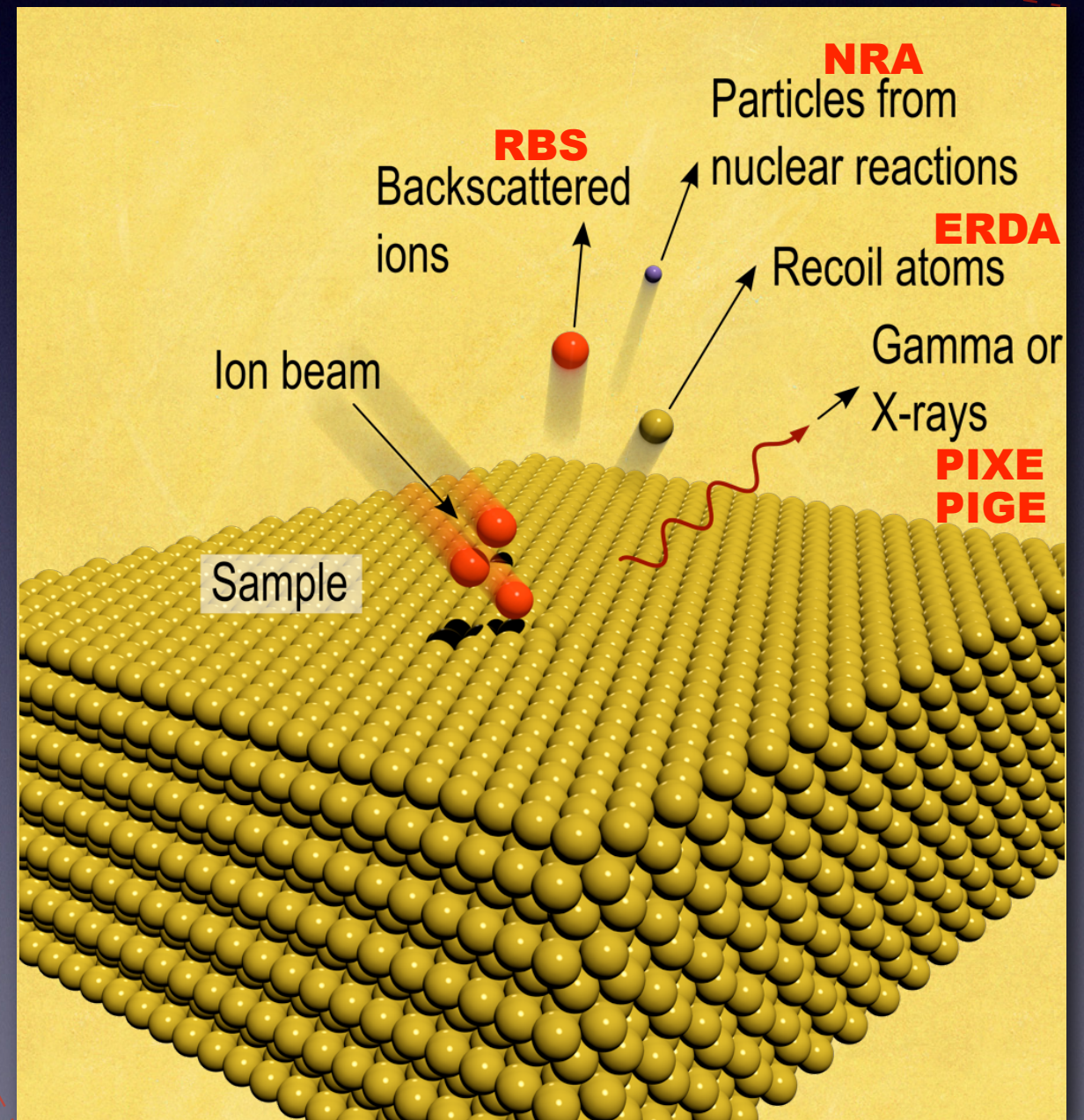
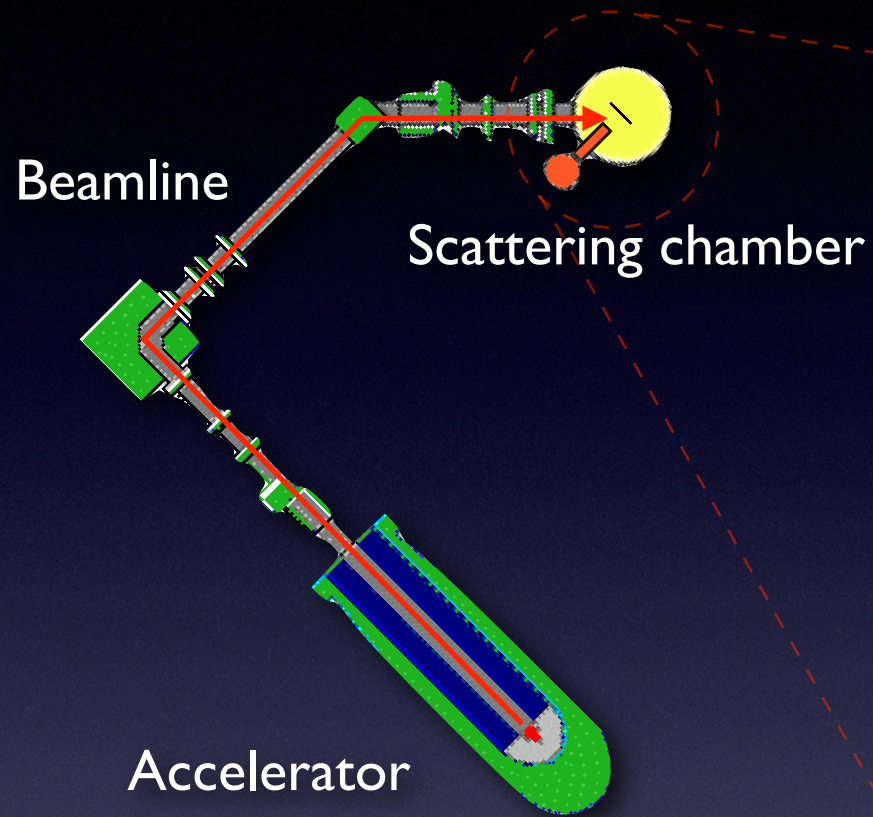
 [max0068](https://www.skype.com/people/max0068)

Outline

- Introduction to Ion Beam Analysis and to Particle Induced X-ray Emission technique
- External beams
- External-beam PIXE analysis of Cultural Heritage
- Synergy with other IBA techniques

Ion Beam Analysis techniques



Beam IN	Beam OUT	Analytical technique
ion	ion	RBS, NRA
ion	target	ERDA, SIMS, SNMS
ion	X-ray	PIXE
ion	Gamma-ray	PIGE, Activation Analysis
ion	hν	Ionoluminescence (IL)

General features of IBA

- Multielemental
- Quantitative analysis (“traceability”)
- High sensitivity (1-100 ppm in at/cm³; 10¹¹-10¹² in at/cm²)
- Surface analysis (10 Å - 10 μm)
- Depth profiling
- Non-destructive
- No sample pre-treatment
- Microanalysis (lateral resolution <1 μm)
- 2D mapping

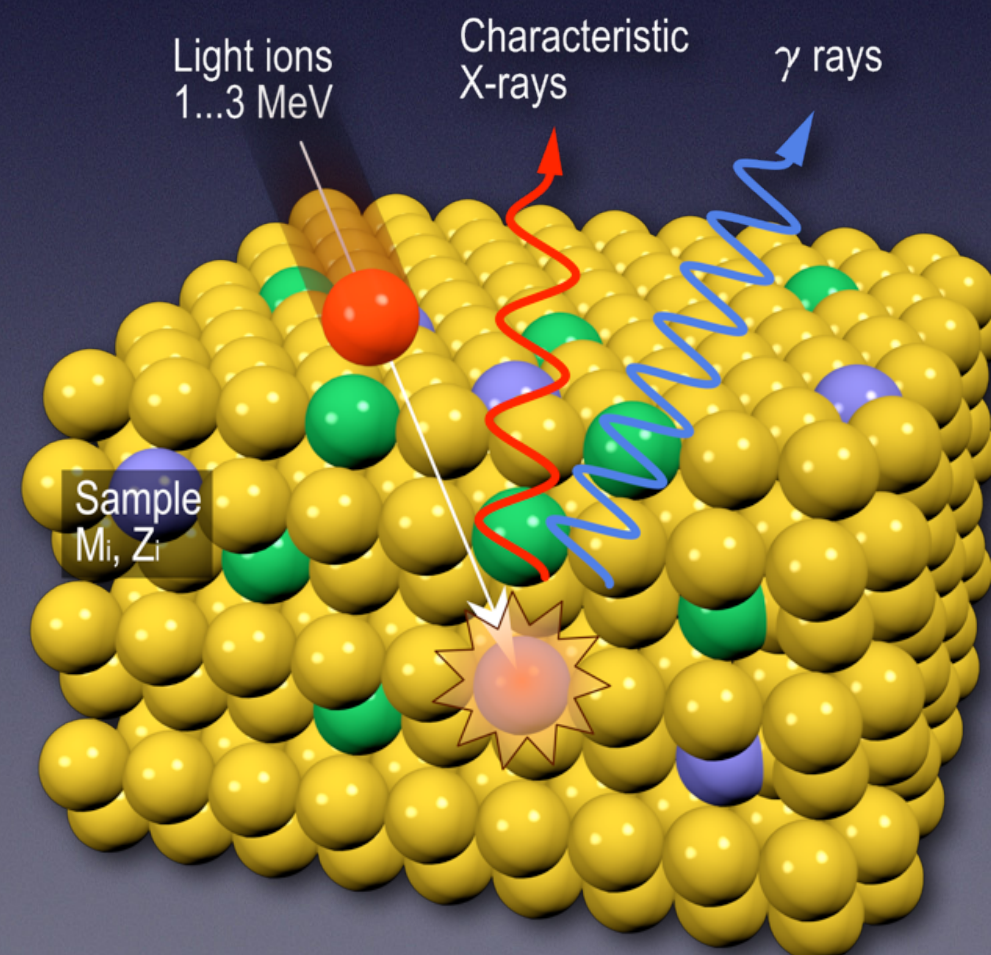
PIXE

Particle Induced X-ray Emission

Emission of characteristic X-rays
following ionization from incident ions

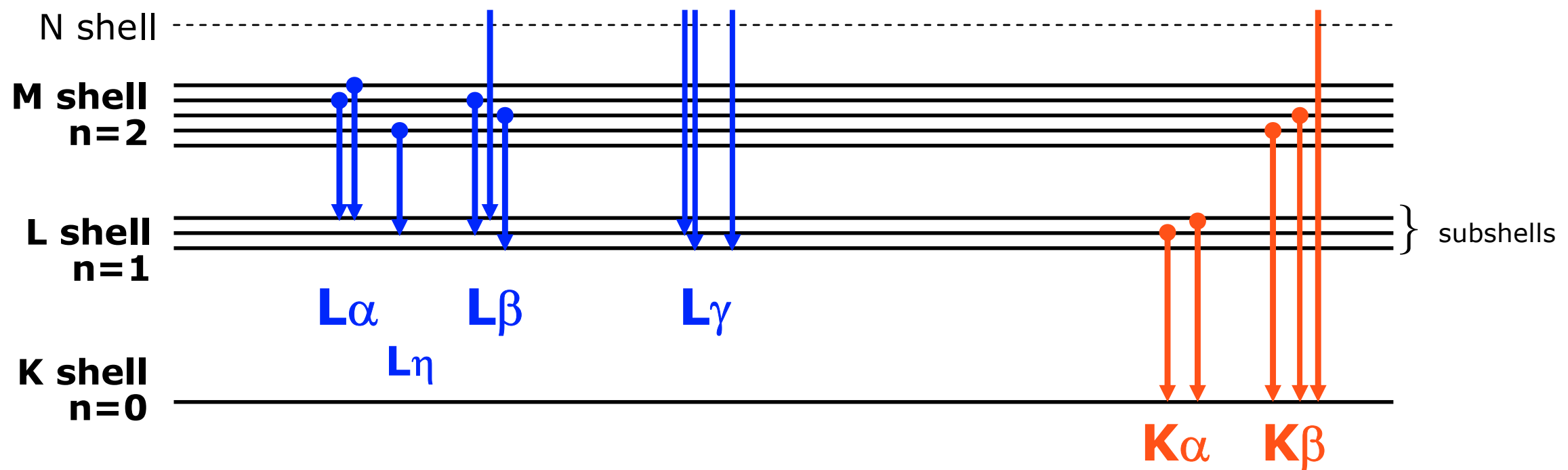


$Z > 10$



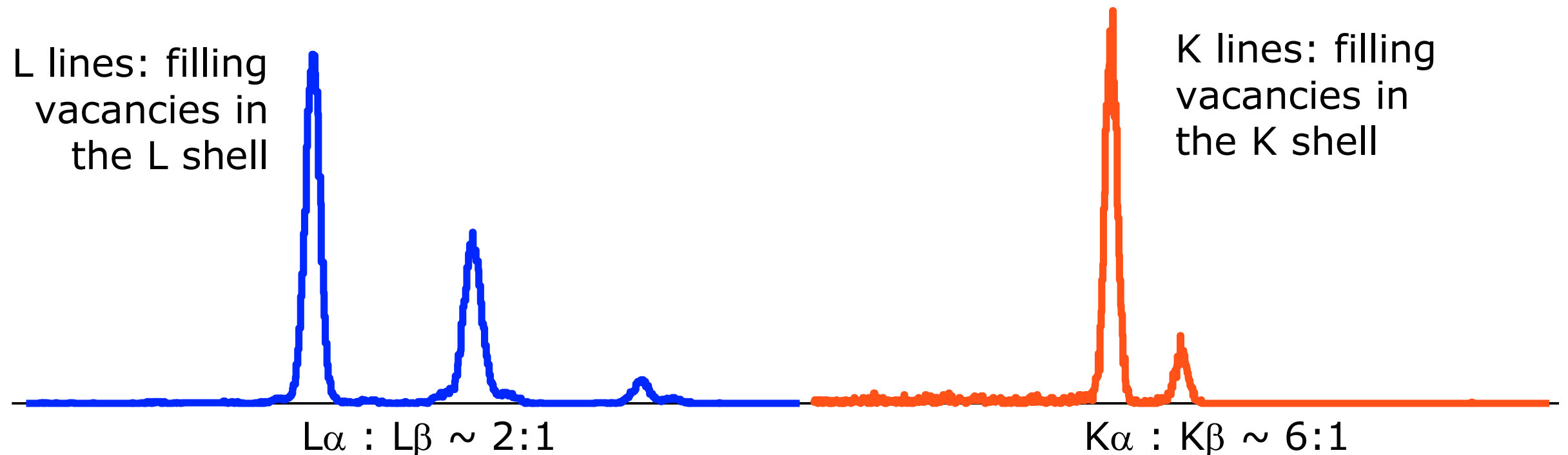
Energy of characteristic X-rays

Energy levels of core electrons

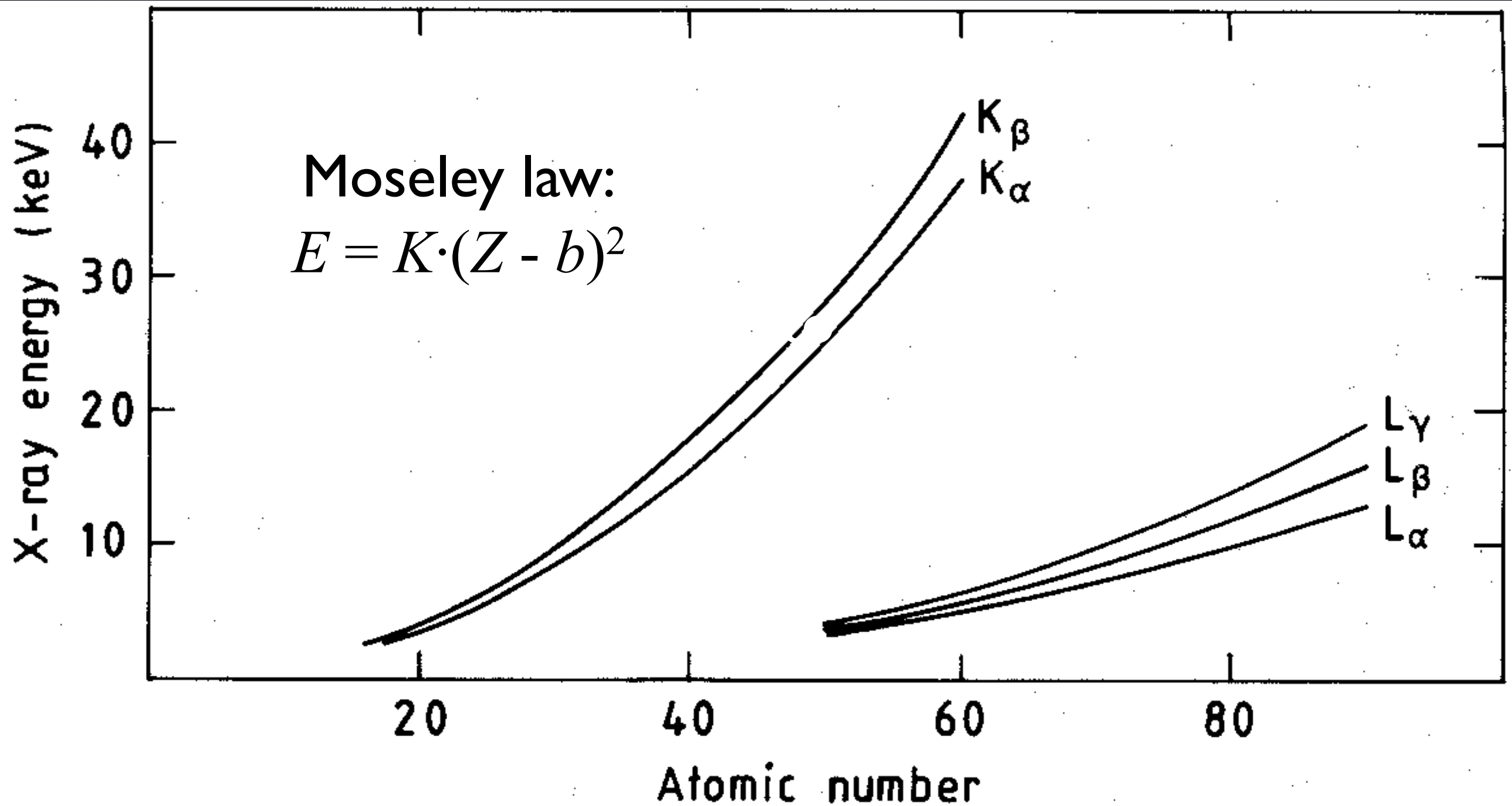


L lines: filling vacancies in the L shell

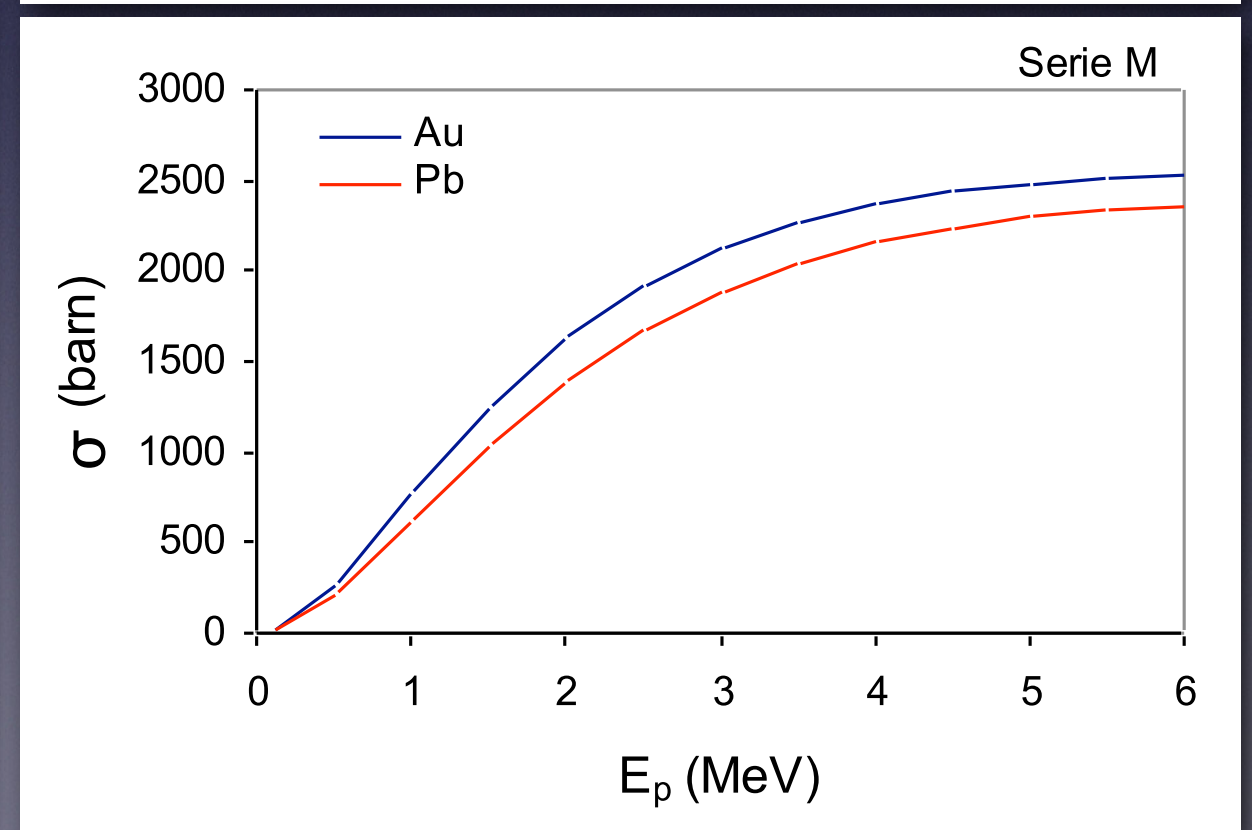
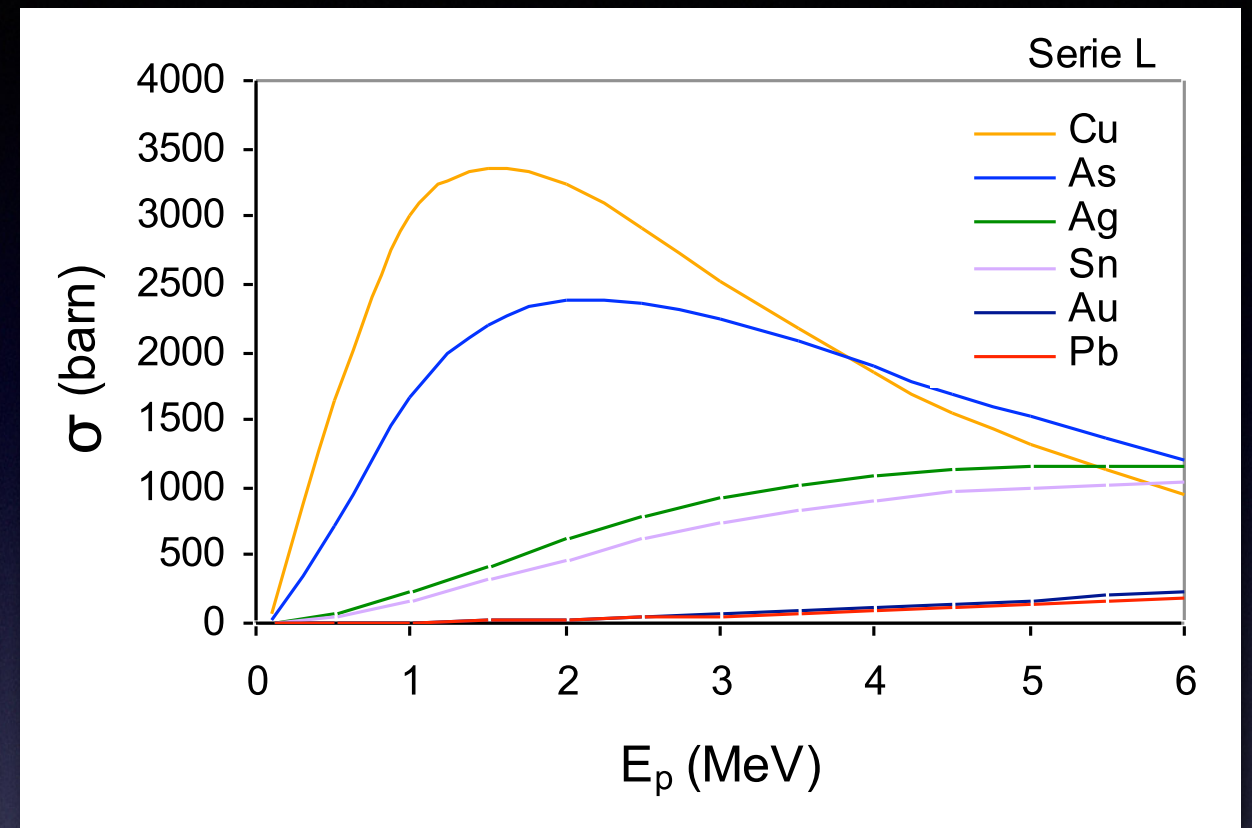
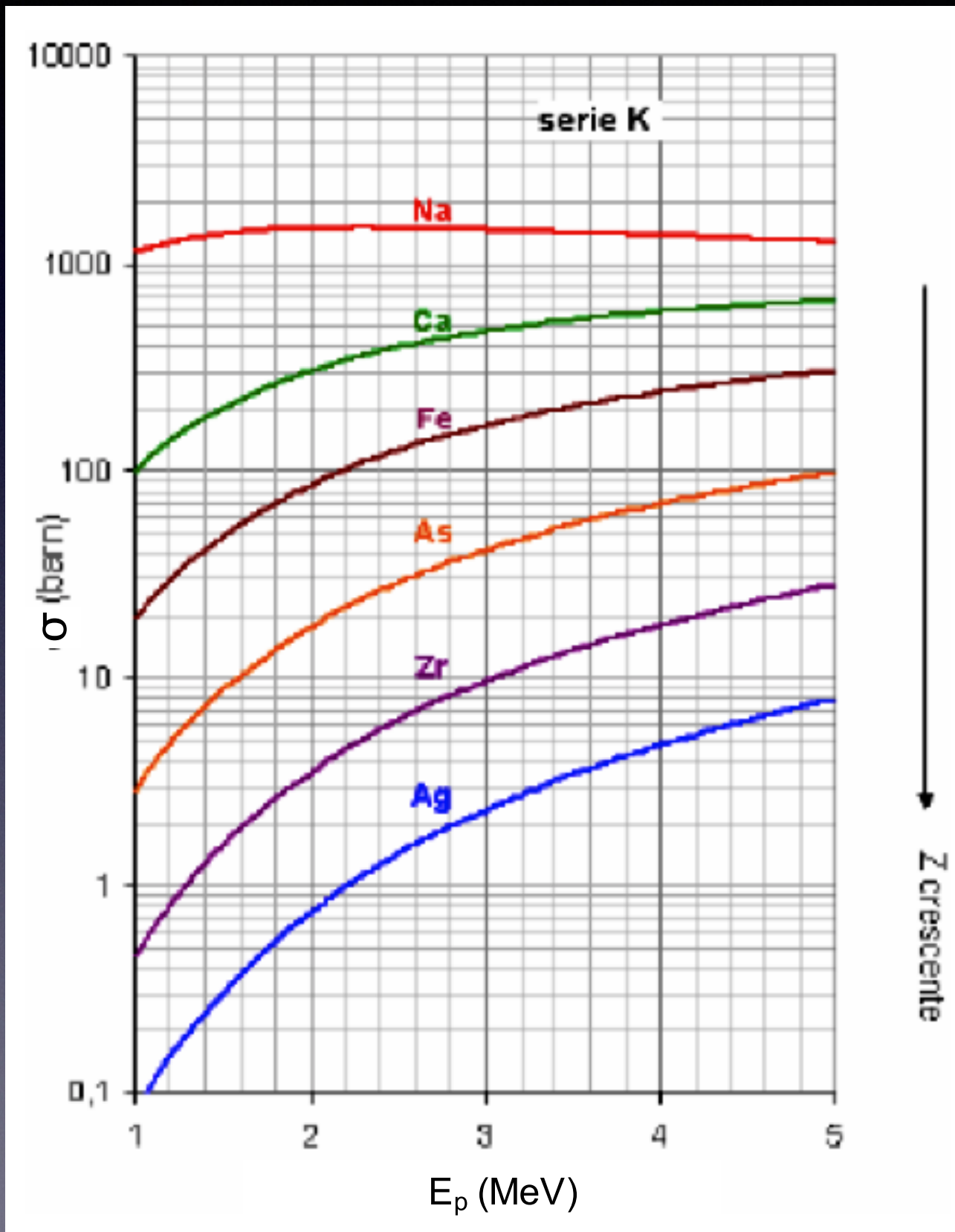
K lines: filling vacancies in the K shell



Energy of characteristic X-rays



X-ray production cross sections



Advantages of PIXE

Among IBA techniques, PIXE is a “killer application” for the non-destructive analysis of cultural heritage object since it is highly sensitive over a broad range of elements and it can be performed with external beams while maintaining the object in atmosphere, avoiding the need of picking up samples and greatly easing the object positioning, thus precious and big artefacts can be studied

- Very fast, high-sensitivity, non-destructive analysis
- Quantitative analysis
- Minimum energy of detected X-rays typically ~ 1 keV
 - ⇒ *all the elements with $Z \geq 11$ are quantifiable simultaneously*

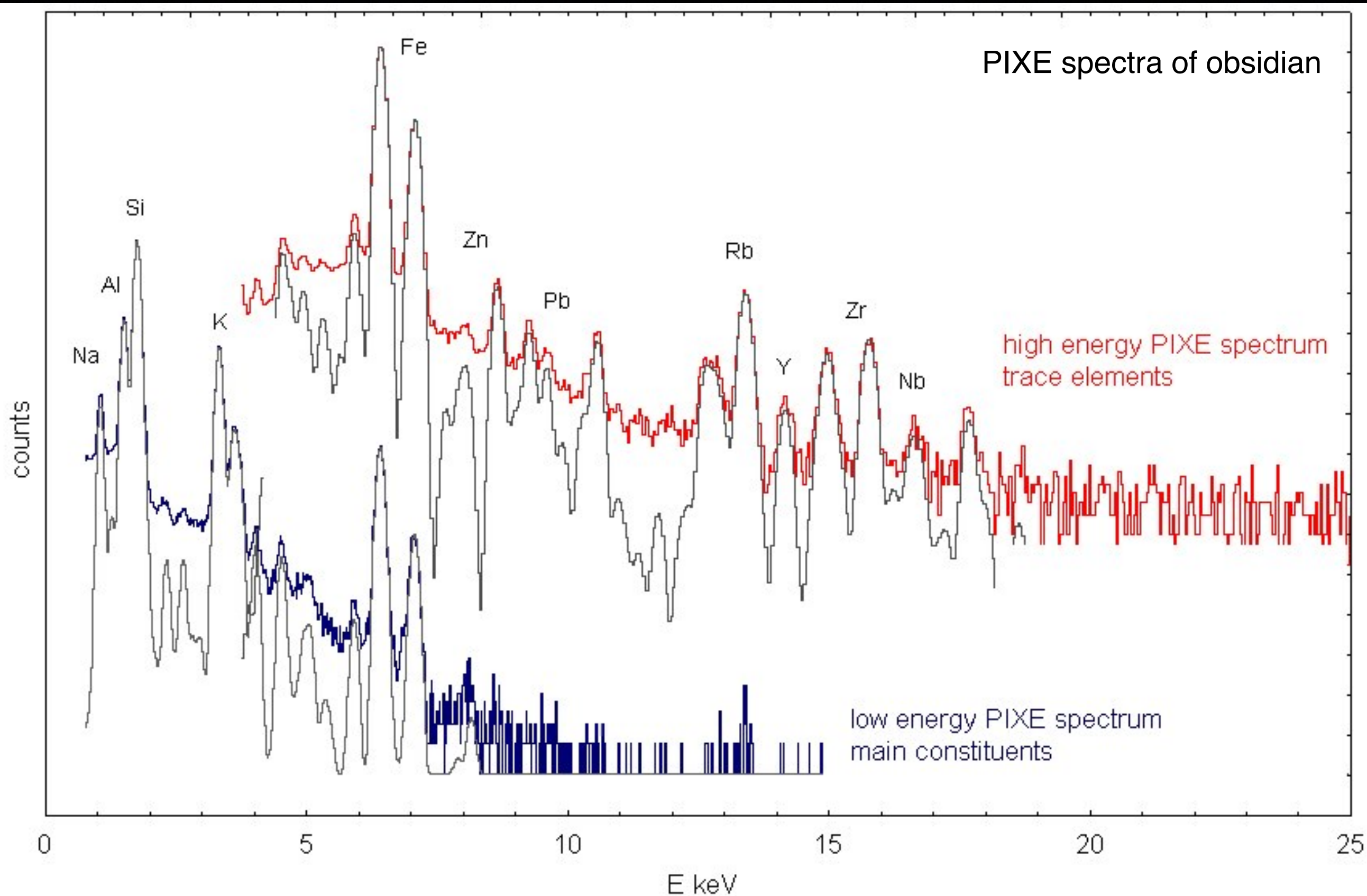
Limitations of PIXE

- No information on the organic components
- No information on chemical states
- No structural information
- Surface analysis (problems with altered objects)
- No direct information on the stratigraphy and the depth distribution of the elements

What PIXE can do for cultural heritage?

- Materials identification
 - ➔ *analysis of major elements by PIXE (and PIGE)*
- Materials provenance
(sources of raw materials and trade routes)
 - ➔ *analysis of trace elements by PIXE*
- Manufacture technology
 - ➔ *high spatial resolution: lateral by μ -PIXE (in-depth by RBS)*

Example of PIXE spectra



PIXE quantitative analysis (thin targets)

$$Y_0(Z) = N_P \cdot N_Z \cdot t \cdot \sigma_{Z,E_0} \cdot (\alpha_Z \cdot \epsilon_Z \cdot \Delta\Omega / 4\pi)$$

$$Y_0(Z) = (Q/e)(N_A/A)(\rho_Z t) \cdot \sigma_{Z,E_0} \cdot (\alpha_Z \cdot \epsilon_Z \cdot \Delta\Omega / 4\pi)$$

defining $\eta_Z = (1/e)(N_A/A) \cdot \sigma_{Z,E_0} \cdot (\alpha_Z \cdot \epsilon_Z \cdot \Delta\Omega / 4\pi)$

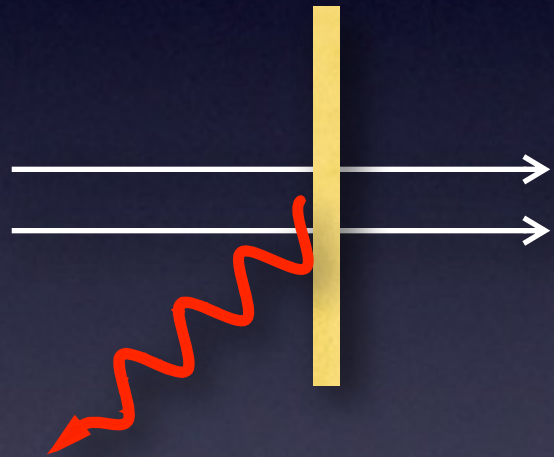
$$Y_0(Z) = \eta_Z \cdot Q \cdot (\rho_Z t)$$

Sensibility (counts/ $\mu\text{C}/(\mu\text{g}/\text{cm}^2)$)

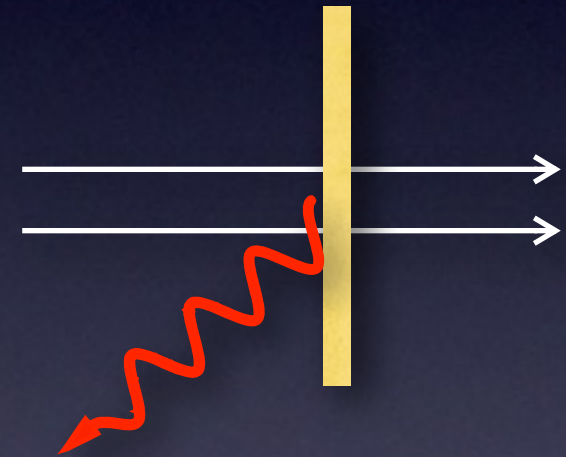

$$(\rho_Z t) = Y_0(Z) / (\eta_Z \cdot Q)$$

PIXE quantitative analysis by comparison with thin elemental standards

Sample



Standard

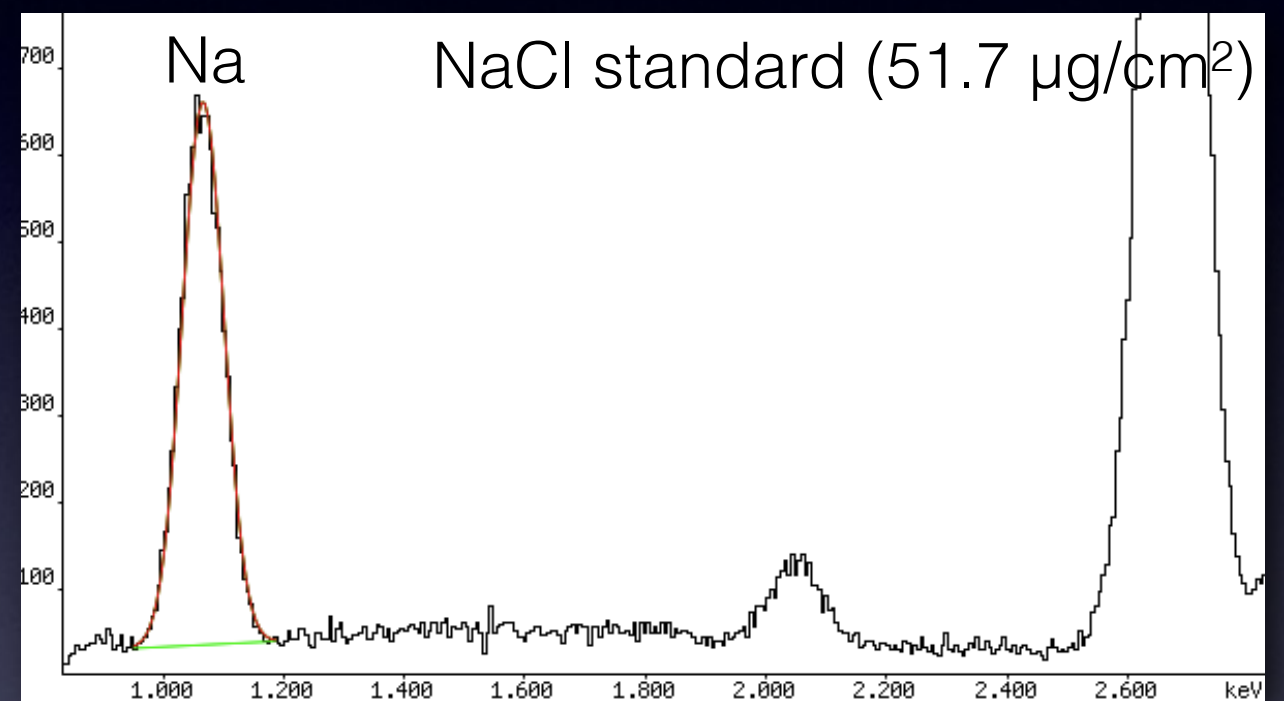
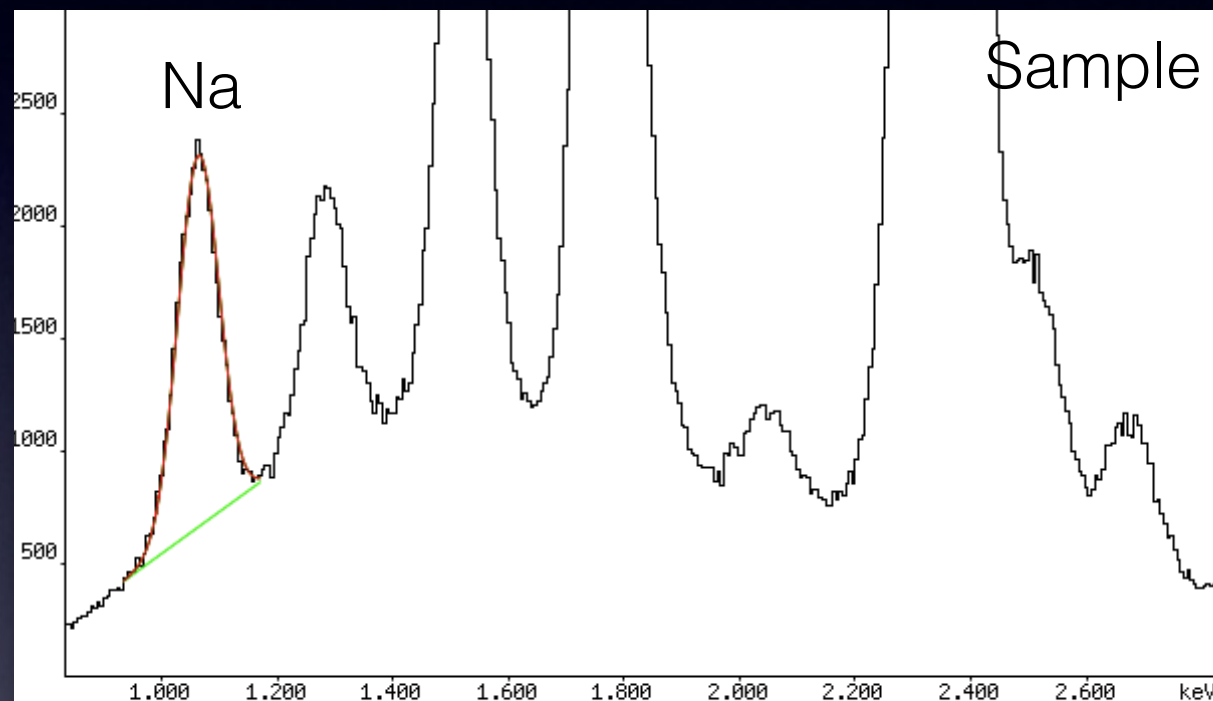


$$Y_0(Z)_{sample} = \eta_Z \cdot Q_{sample} \cdot (\rho_Z t)_{sample}$$

$$Y_0(Z)_{std} = \eta_Z \cdot Q_{std} \cdot (\rho_Z t)_{std}$$

$$(\rho_Z t)_{sample} = (\rho_Z t)_{std} \cdot [Y_0(Z)_{sample} / Y_0(Z)_{std}] \cdot (Q_{std} / Q_{sample})$$

Quantitative analysis by comparison with thin elemental standards



$$Y_0(Z)_{sample} = A_{Z,sample} \cdot 1/(1-DT_{sample}) \cdot 1/(1-PU_{sample})$$

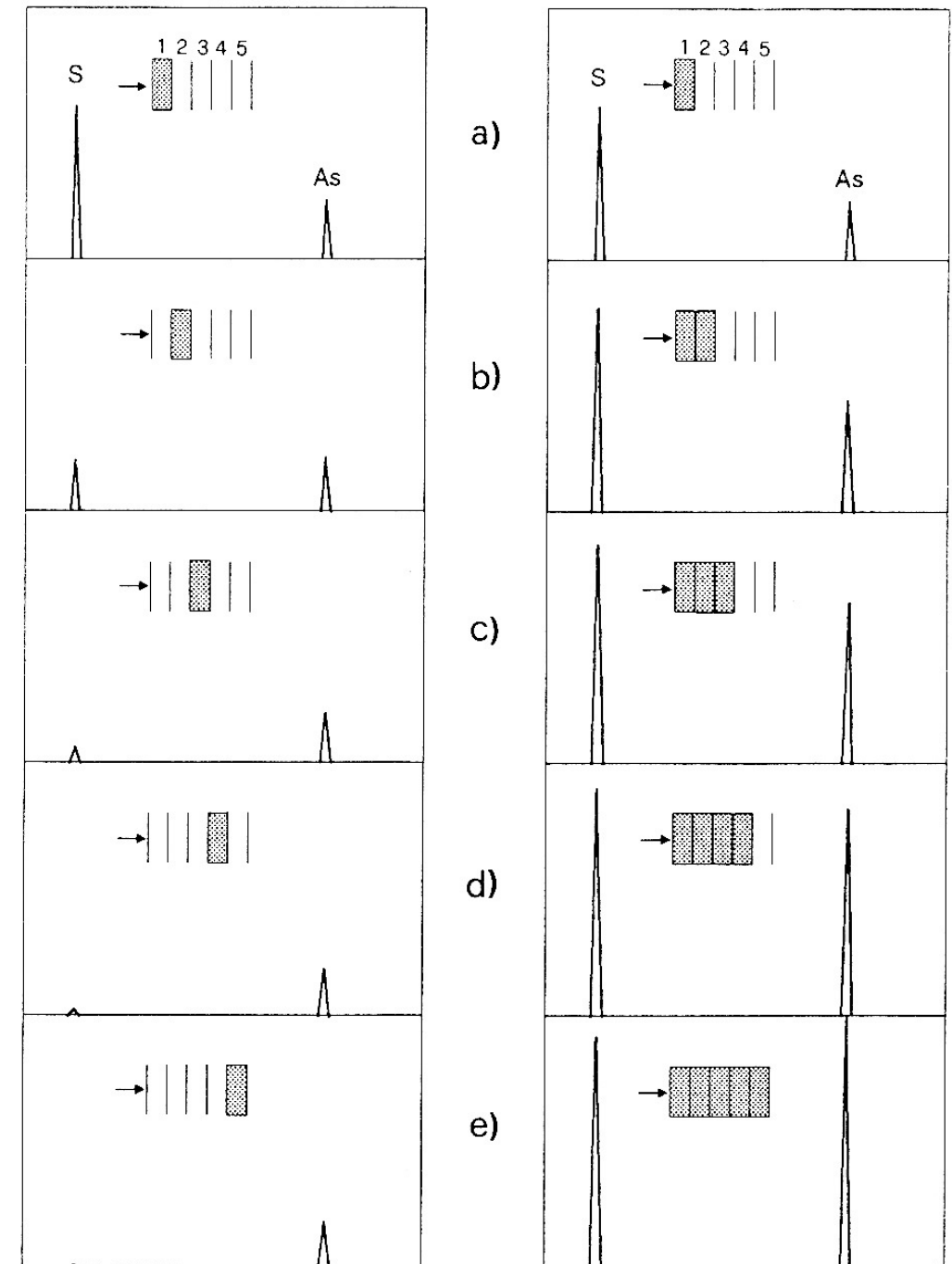
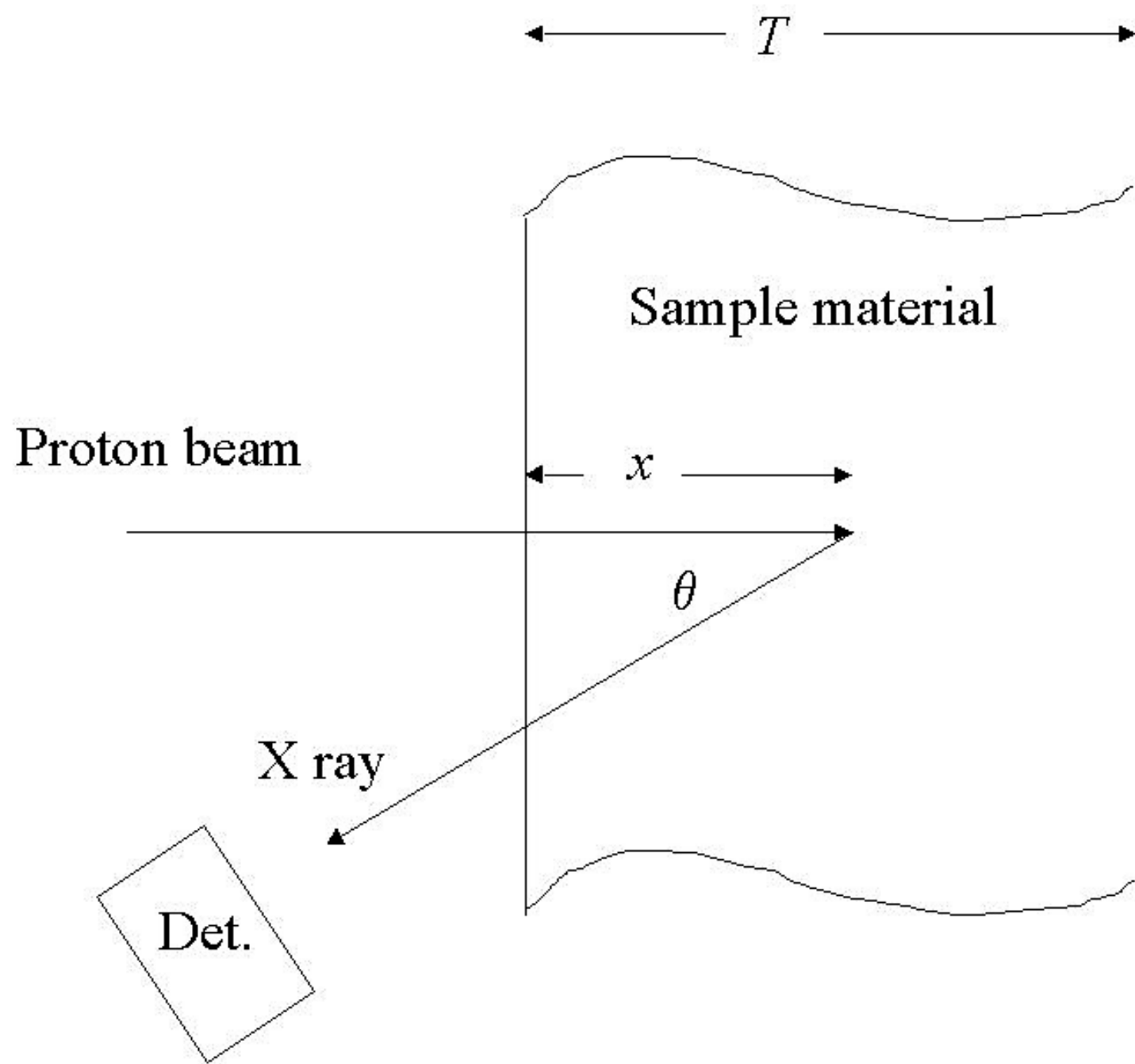
$$Y_0(Z)_{std} = A_{Z,std} \cdot 1/(1-DT_{std}) \cdot 1/(1-PU_{std})$$

X-ray peak area

Dead time fraction

Pile-up fraction

Thick targets



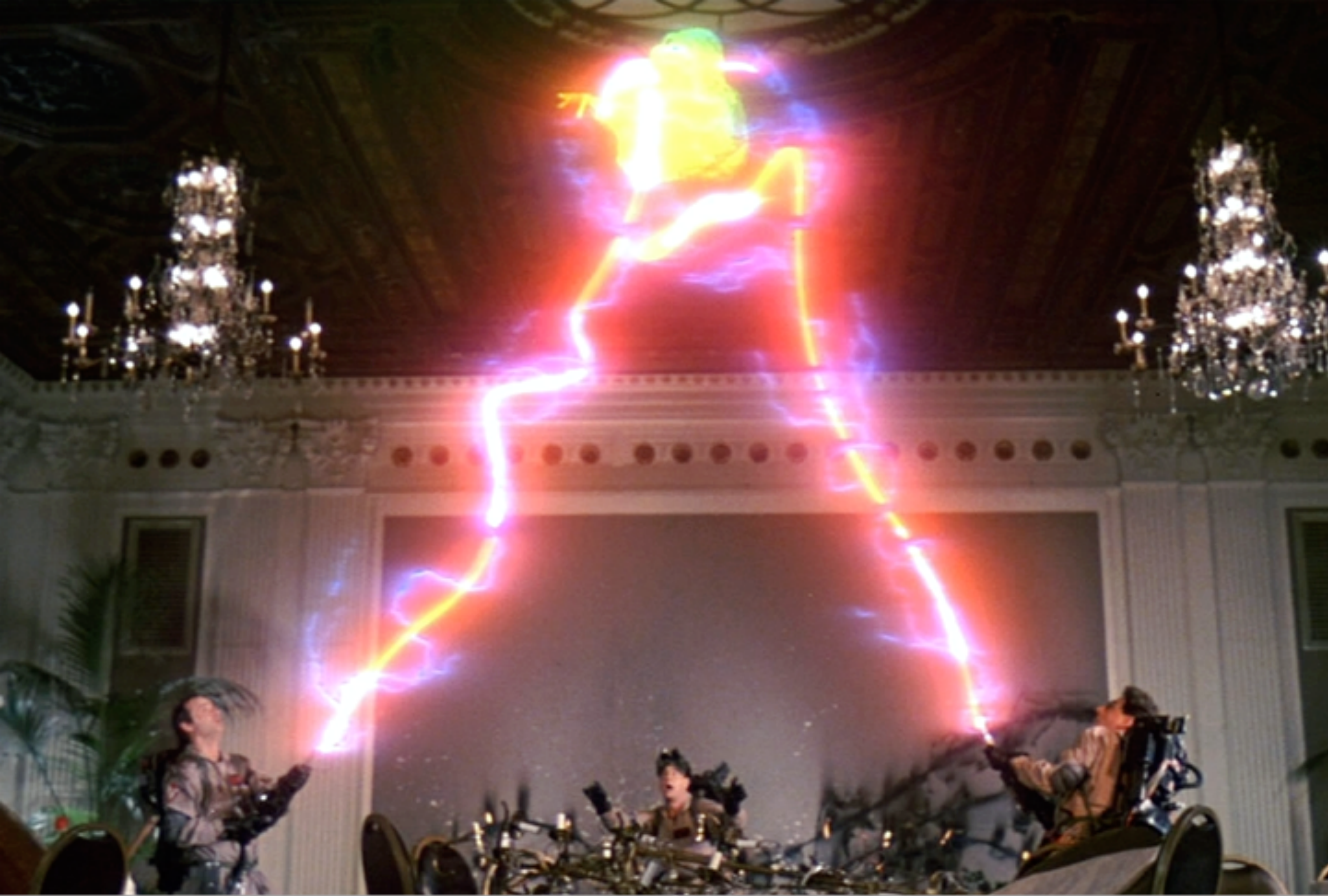
Quantitative analysis (thick targets)

$$Y(Z) = (Q/e)(N_A/A)(\alpha_Z \cdot \varepsilon_Z \cdot \Delta\Omega/4\pi) \cdot \rho_Z \int_0^T \sigma_{Z,E} \cdot \exp(-\mu \cdot x/\cos\theta) \cdot dx$$

$$Y(Z) = (Q/e)(N_A/A)(\alpha_Z \cdot \varepsilon_Z \cdot \Delta\Omega/4\pi) (\rho_Z/\rho) \int_{E_0}^{E_F} \sigma_{Z,E} \cdot \exp(-\mu \cdot x/\cos\theta) \cdot dE/S(E)$$

$$F(Z) = Y_0(Z)/Y(Z) = \frac{\rho \cdot T \cdot \sigma_{Z,E_0}}{\int_{E_0}^{E_F} \sigma_{Z,E} \cdot \exp(-\mu \cdot x/\cos\theta) \cdot dE/S(E)}$$

$$(\rho_Z t) = F(Z) \cdot Y(Z) / (\eta_Z \cdot Q)$$

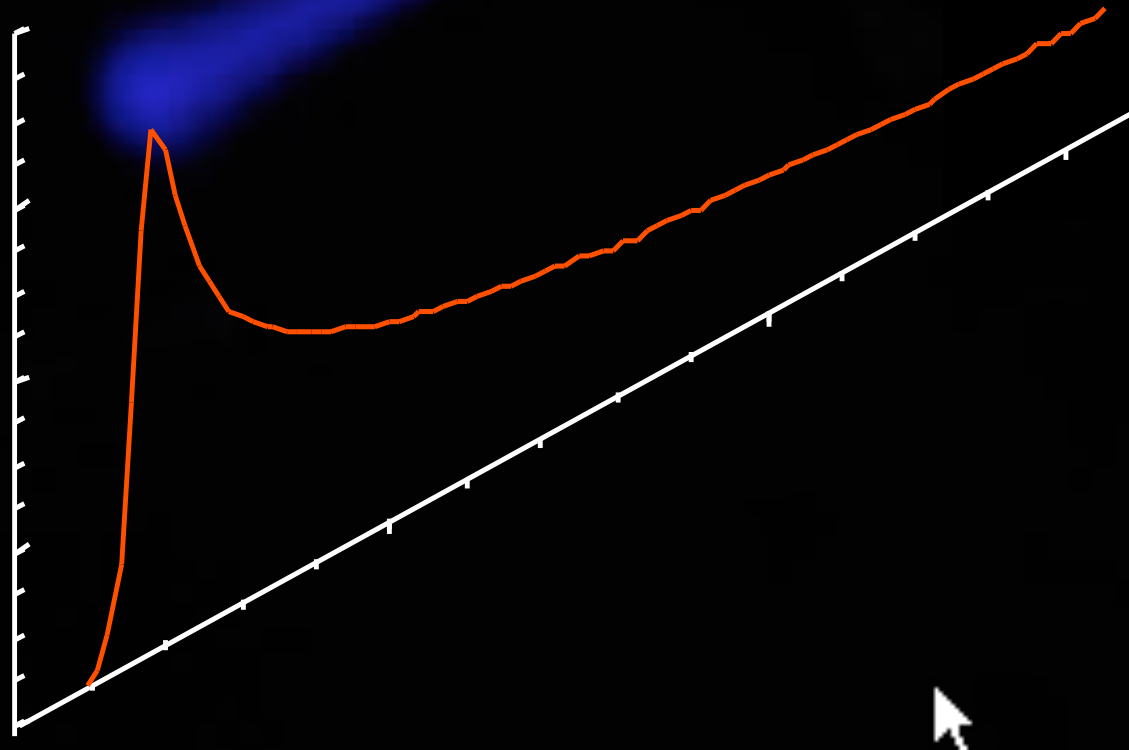


Do extracted ion beams look like these?

External ion beam

Advantages

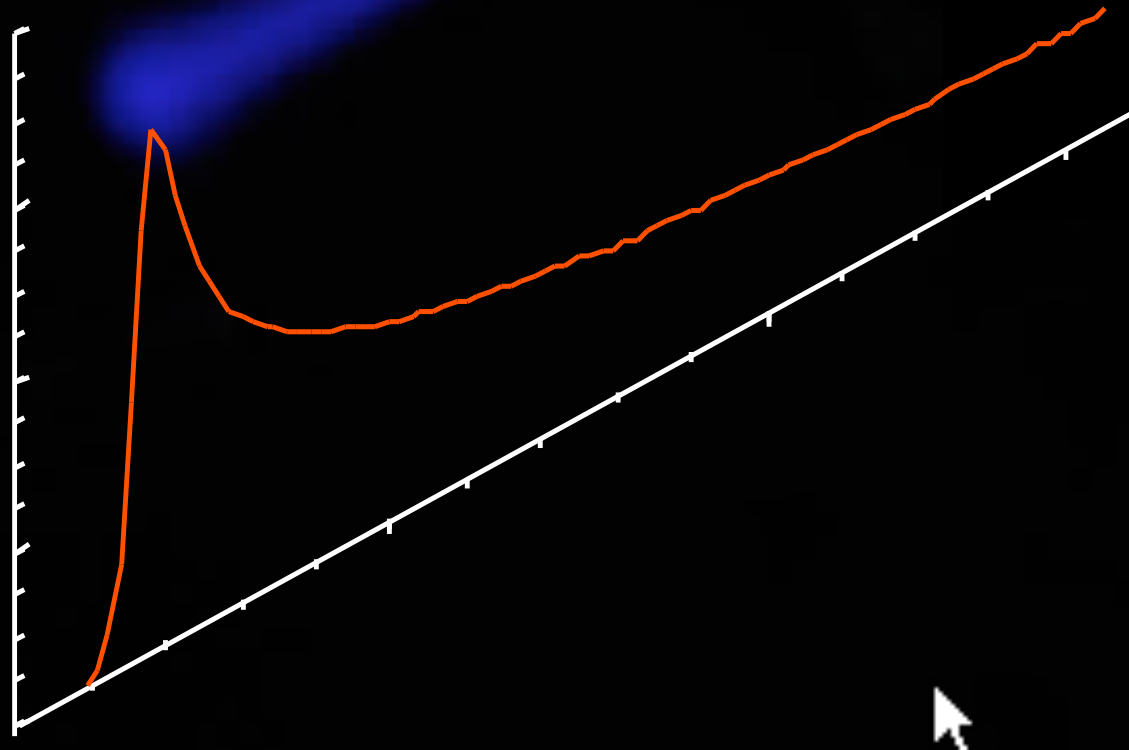
- direct analysis of artefacts having any shape and any size
- no sampling
- no charging, no preparation (conductive coating etc.)
- no heating, reduced damage risk
- easy sample positioning
- fast and efficient



External ion beam

Advantages

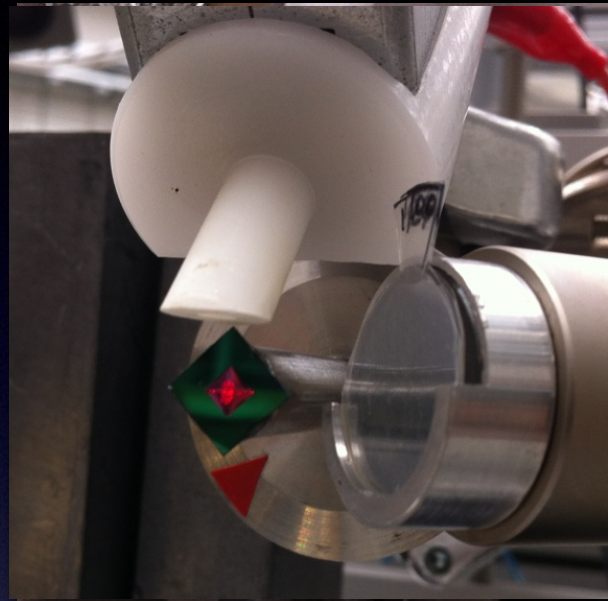
direct analysis of artefacts having any shape and any size
no sampling
no charging, no preparation (conductive coating etc.)
no heating, reduced damage risk
easy sample positioning
fast and efficient



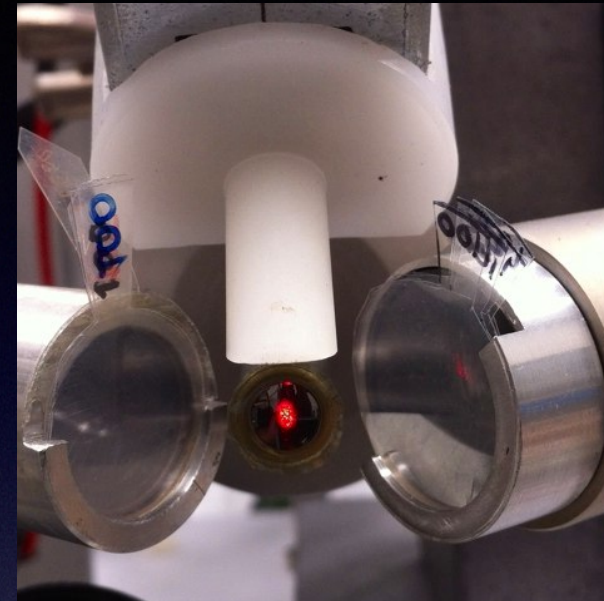
Disadvantages

energy loss
energy straggling
beam lateral spread
x-ray attenuation

Typical extraction windows



0.5 μm Si_3N_4



7.5 μm Upilex

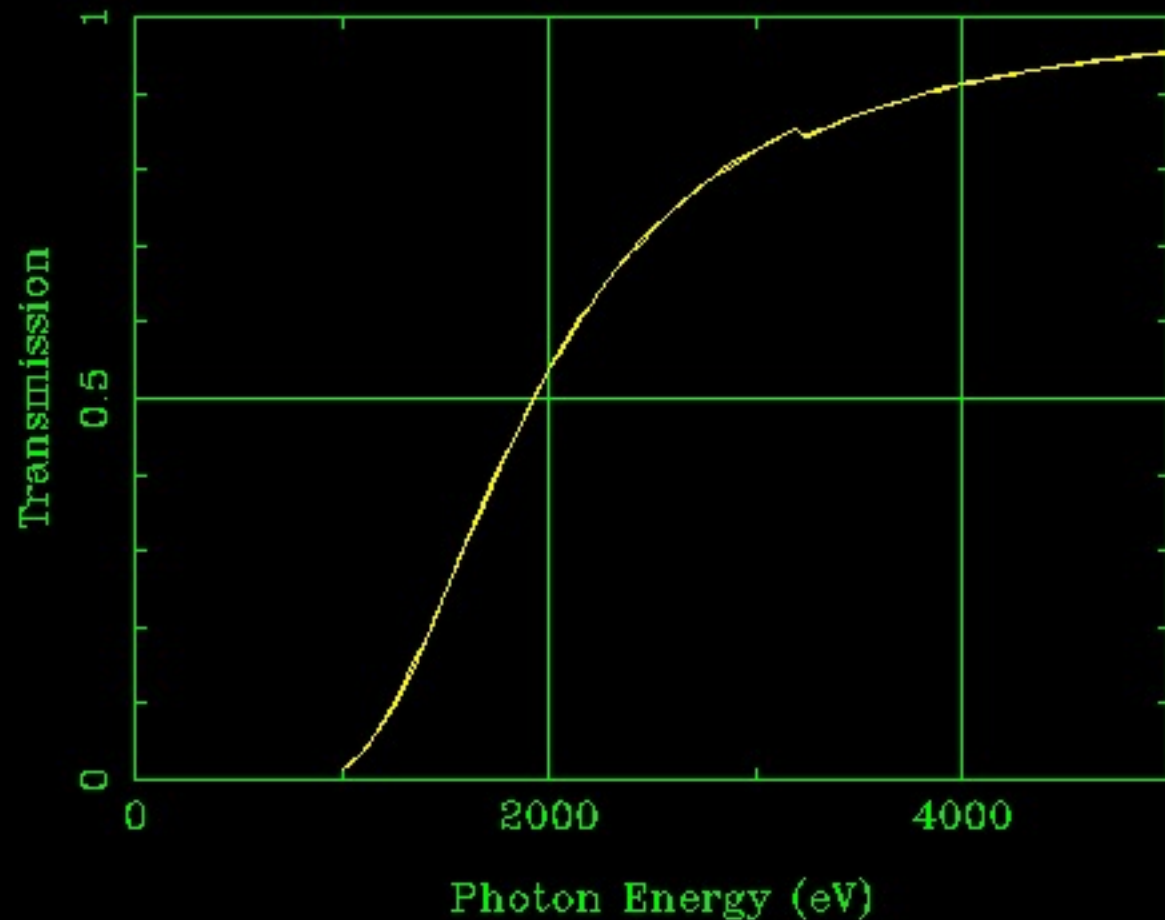
Material	Thickness (μm)	ΔE (keV)	σ_E (keV)	σ_θ ($\mu\text{m}/\text{mm}$)
Al	10	235	16	14
Kapton	8	130	9	6
Zr	2	75	7,3	15
Si	0.1	8	5	<1
	0.5	40	9	<2

Choice of external atmosphere

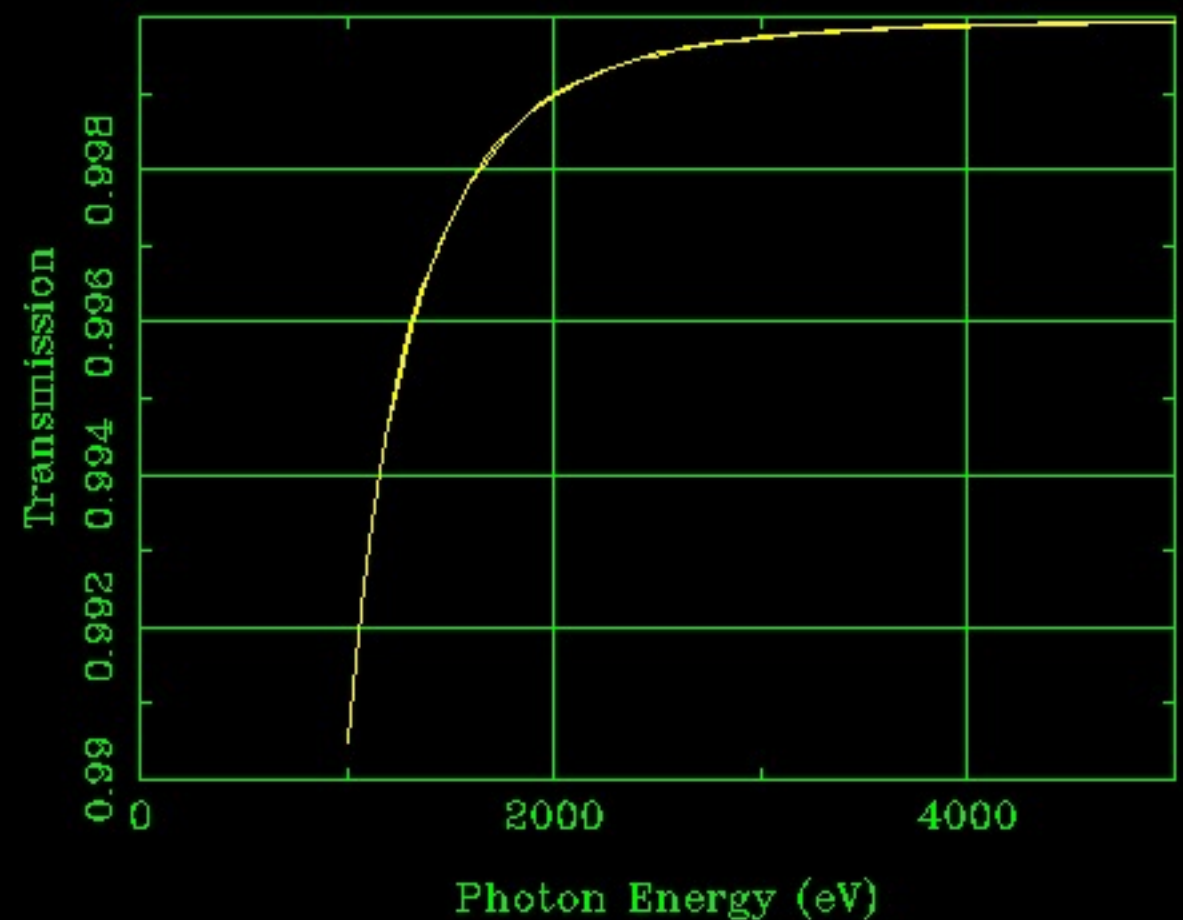
Air

Helium

N1.5620.42C.0003Ar.0094 Pressure=760. Path=1. cm

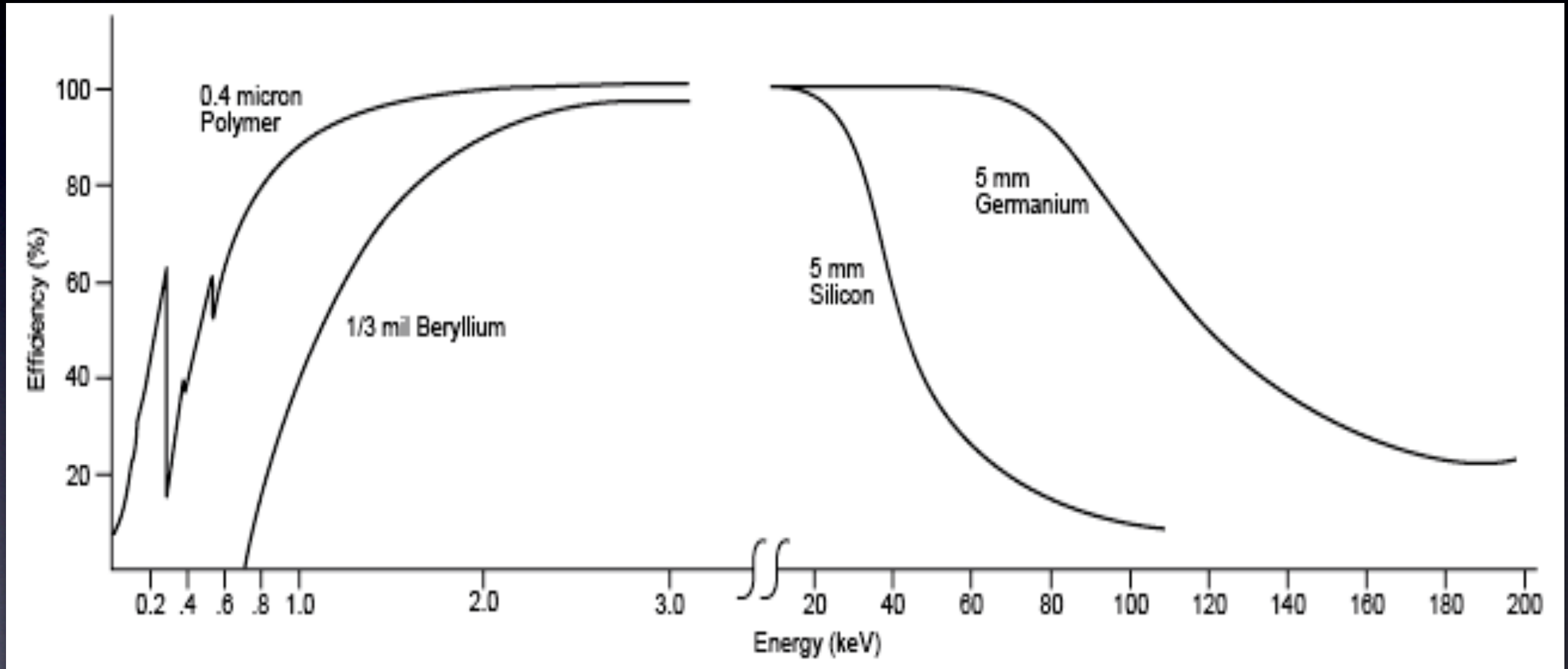


He Pressure=760. Path=1. cm



The use of an helium-saturated atmosphere in front of the X-ray detector is mandatory

X-ray detector efficiency



Low energy:

$$\varepsilon \approx \exp[-\mu(Z, E_X) \cdot t_{\text{window}}]$$

High energy:

$$\varepsilon \approx 1 - \exp[-\mu(Z, E_X) \cdot L_{\text{detector}}]$$

Typical PIXE detectors



Silicon Drift Detector (SDD)

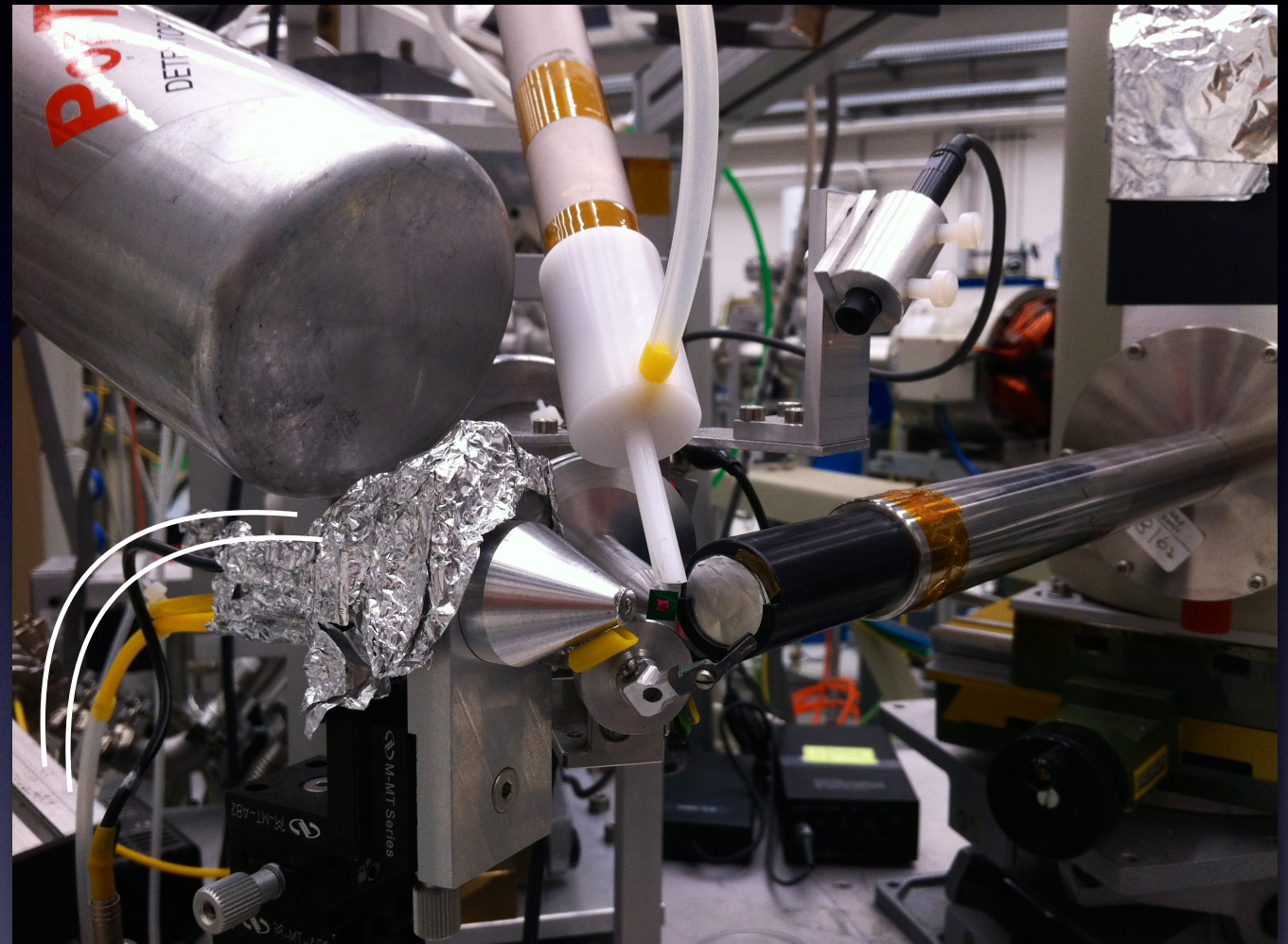
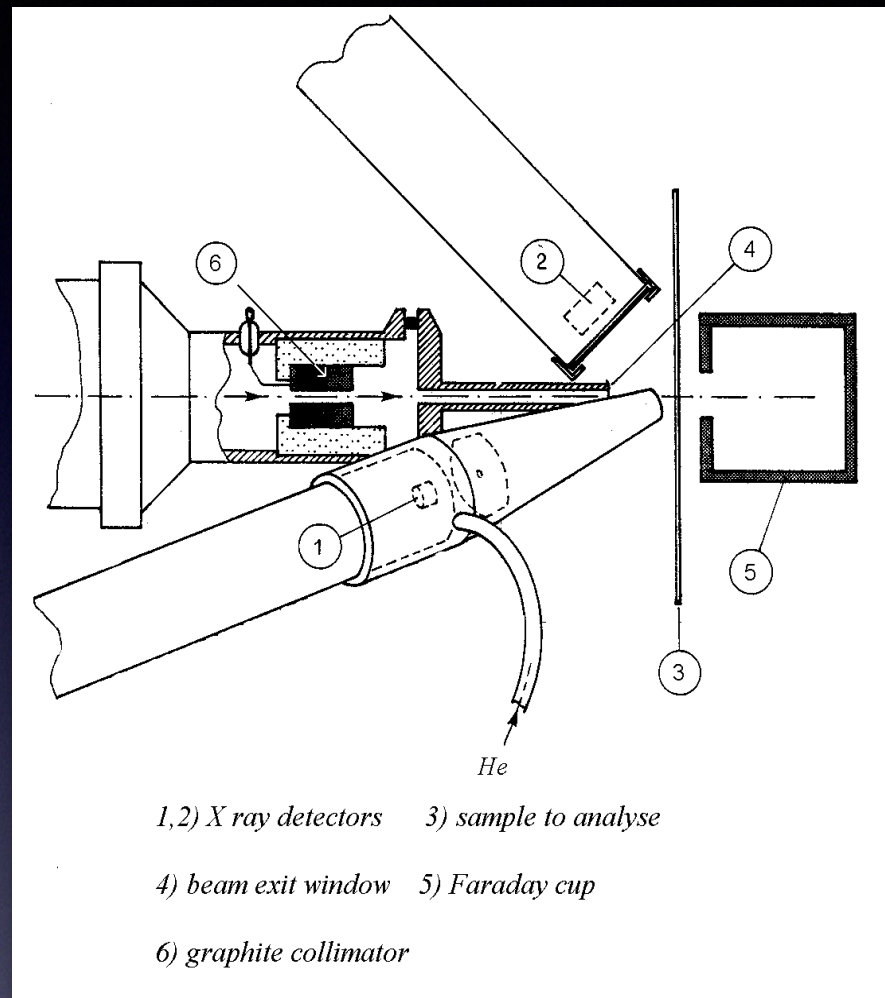
- Active area: 7 - 100 mm²
- Thickness: 300 - 450 μm
- Energy resolution < 140 eV
- High count-rate (100 kHz)
- Peltier cooling (-10, -20 °C)

Lithium-drifted Si / Ge, Si(Li) / Ge(Li)

- Active area: 10 - 100 mm²
- Thickness: 3 - 5 mm
- Energy resolution < 180 eV
- Liquid N₂ cooling (77 K)
- Ge(Li): high-Z material, but “escape peak”

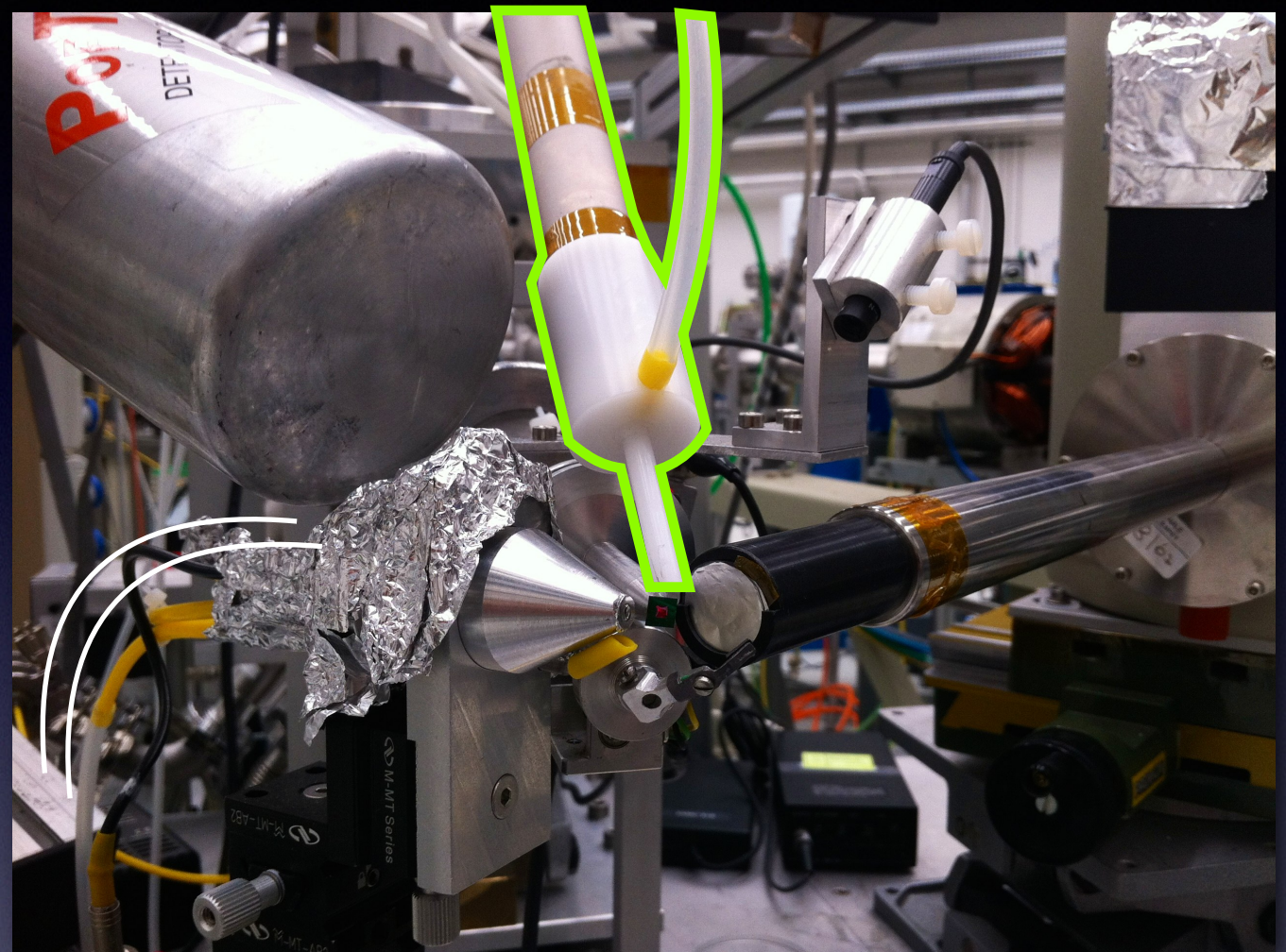
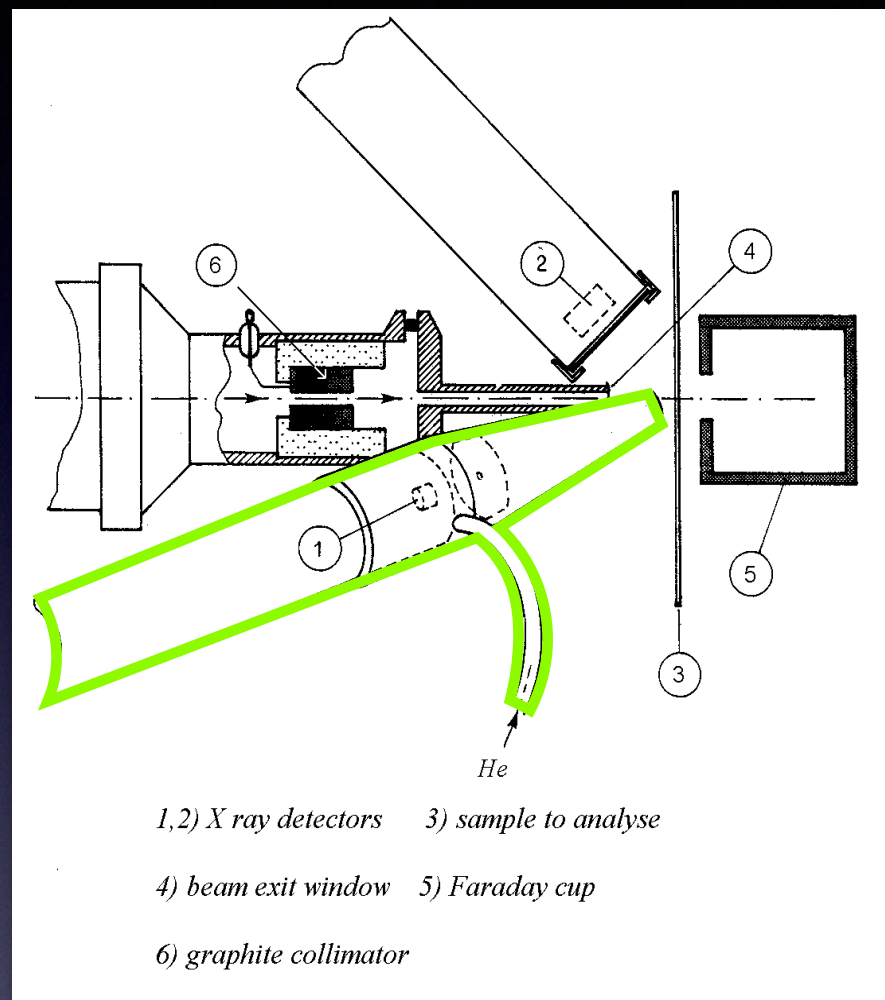


2-detectors PIXE set-up



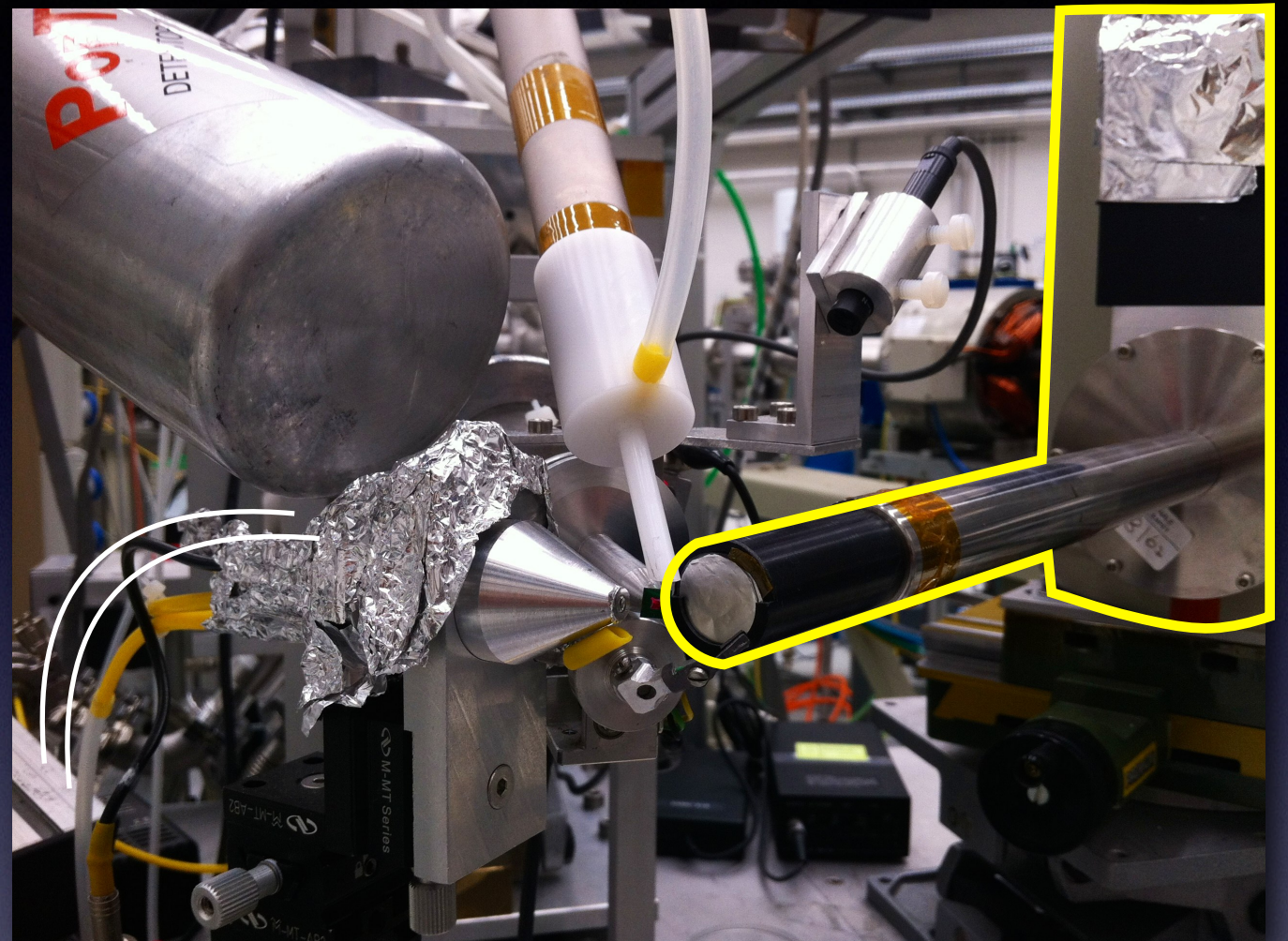
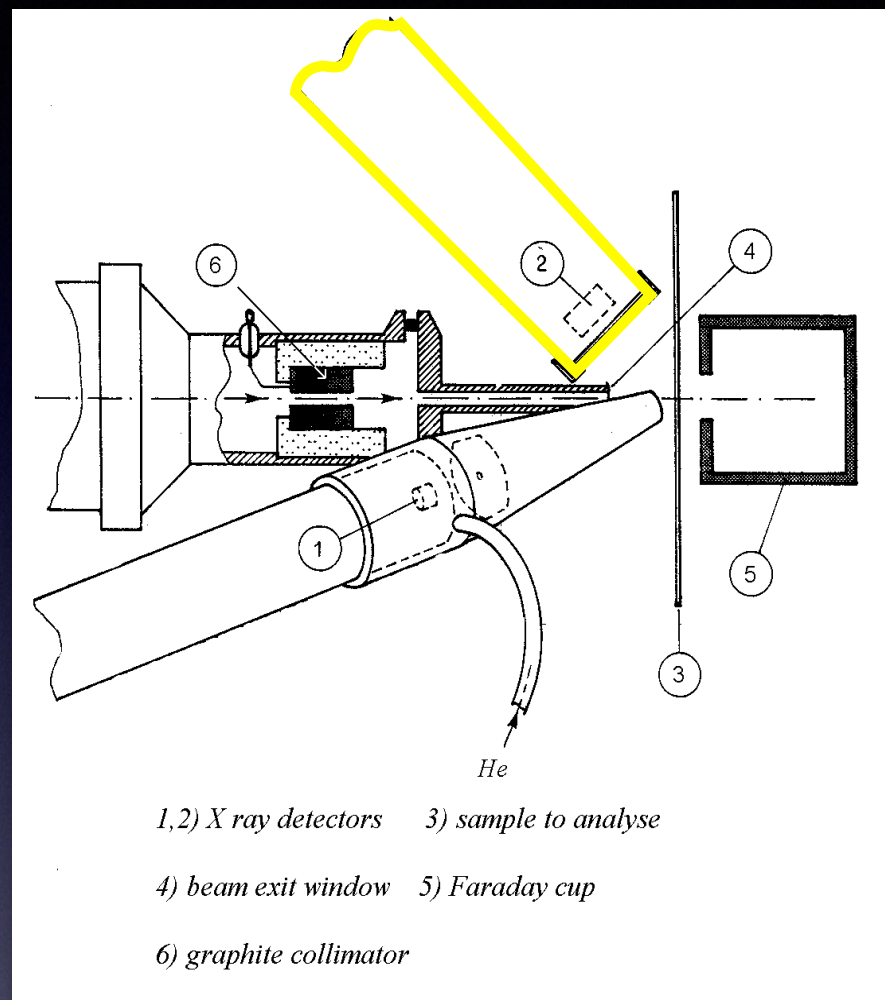
Target	X-rays	What is needed	Detector features
Low-Z elements	Low energy High cross sections	Minimum dead layers Small solid angles	Thin entrance window Small active area
Medium-high-Z elements	High energy Low cross sections	Large solid angles Efficiency	Large active area Large active thickness

2-detectors PIXE set-up



Target	X-rays	What is needed	Detector features
Low-Z elements	Low energy High cross sections	Minimum dead layers Small solid angles	Thin entrance window Small active area
Medium-high-Z elements	High energy Low cross sections	Large solid angles Efficiency	Large active area Large active thickness

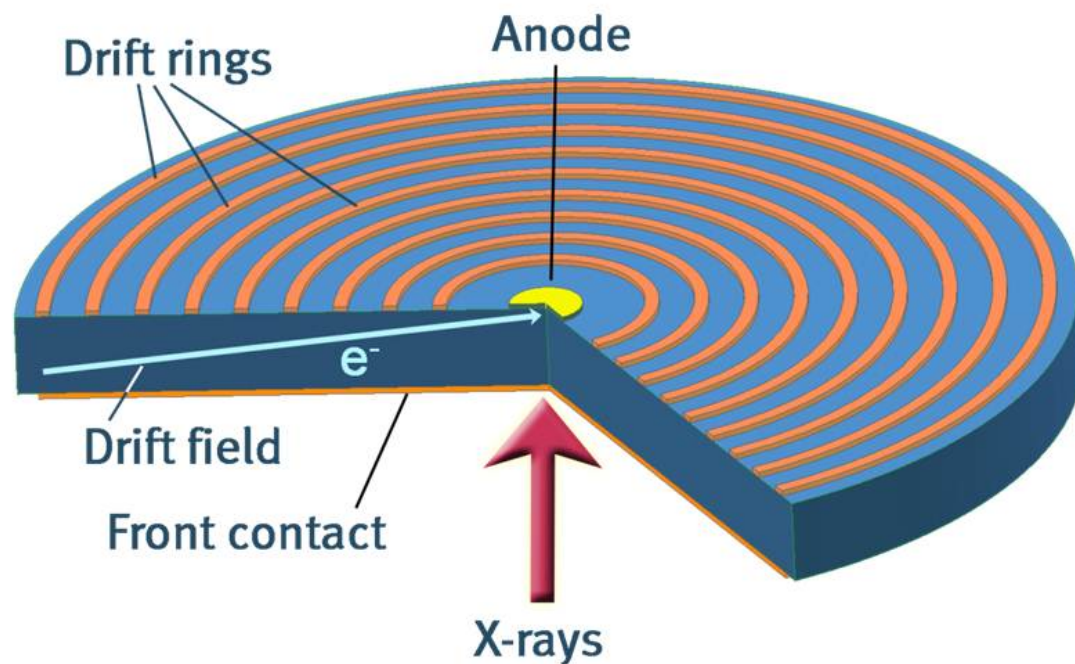
2-detectors PIXE set-up



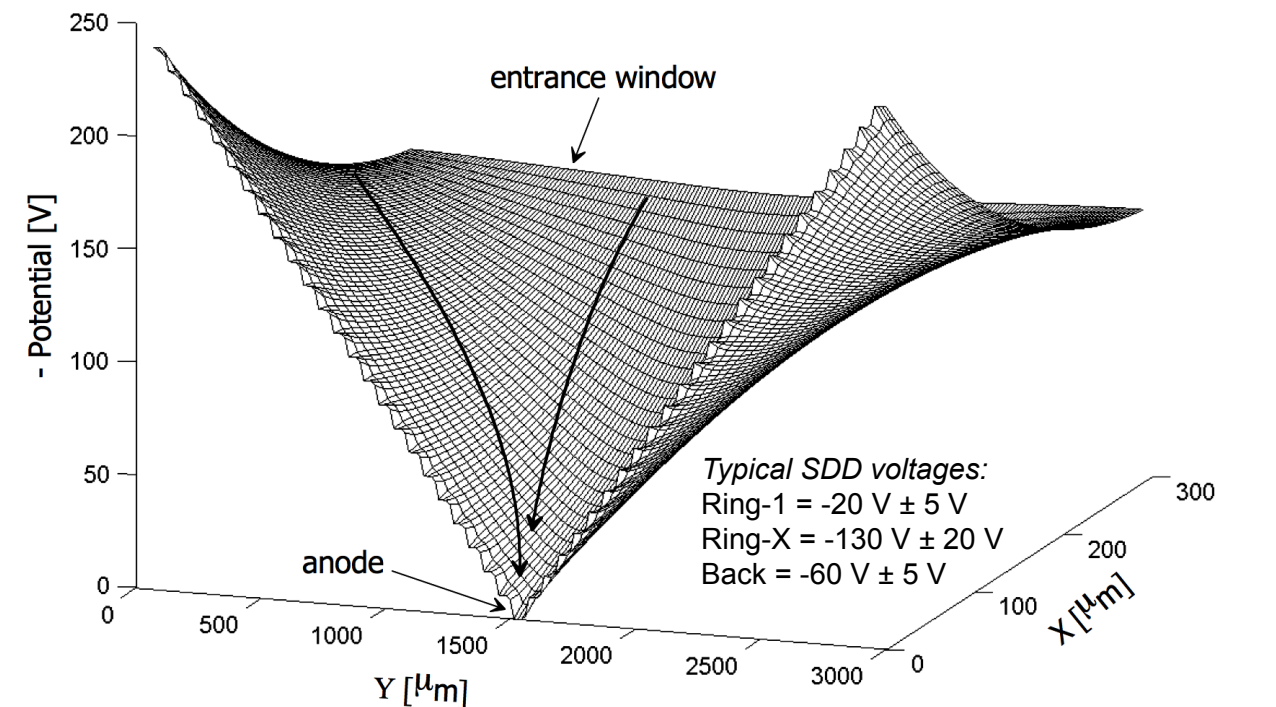
Target	X-rays	What is needed	Detector features
Low-Z elements	Low energy High cross sections	Minimum dead layers Small solid angles	Thin entrance window Small active area
Medium-high-Z elements	High energy Low cross sections	Large solid angles Efficiency	Large active area Large active thickness

The working principle of Silicon Drift Detectors

- The Silicon Drift Detector (SDD) was first proposed in the early '80s by Emilio Gatti and Pavel Rehak [Gatti & Rehak, NIM 225 (1983) 608] as a position sensitive semiconductor detector for high energy charged particles, based on a novel charge transport scheme where the field responsible for the charge transport is independent of the depletion field



Schematic diagram of the Silicon Drift Detector for X-ray spectroscopy with radiation entrance window of the detector consisting of a continuous shallow p+ implant

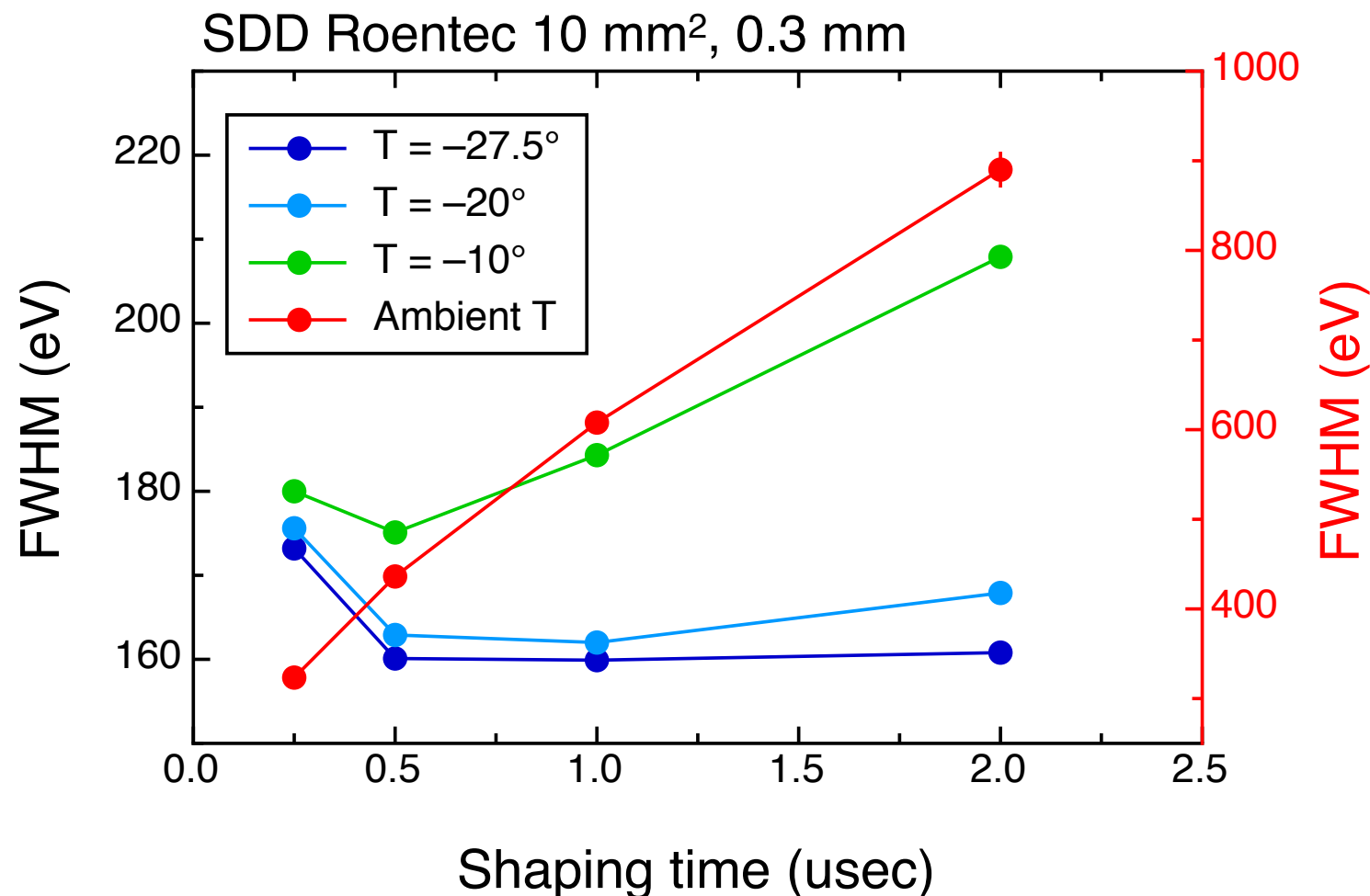


Energy potential for electrons inside a SDD with homogeneous entrance window.

The SSD for X-ray spectroscopy

- The SSD is employed in high-resolution X-ray spectroscopy because of the low capacitance of the collecting electrode (0.5-1 pF/cm²) and the low leakage current (1-2 nA/cm² at room temperature) resulting in improved energy resolution

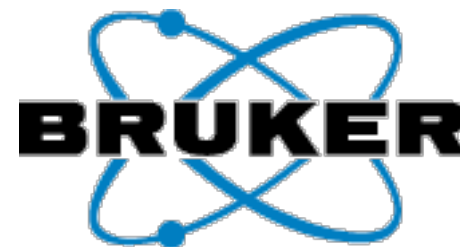
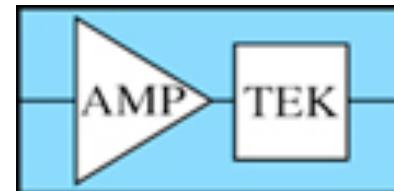
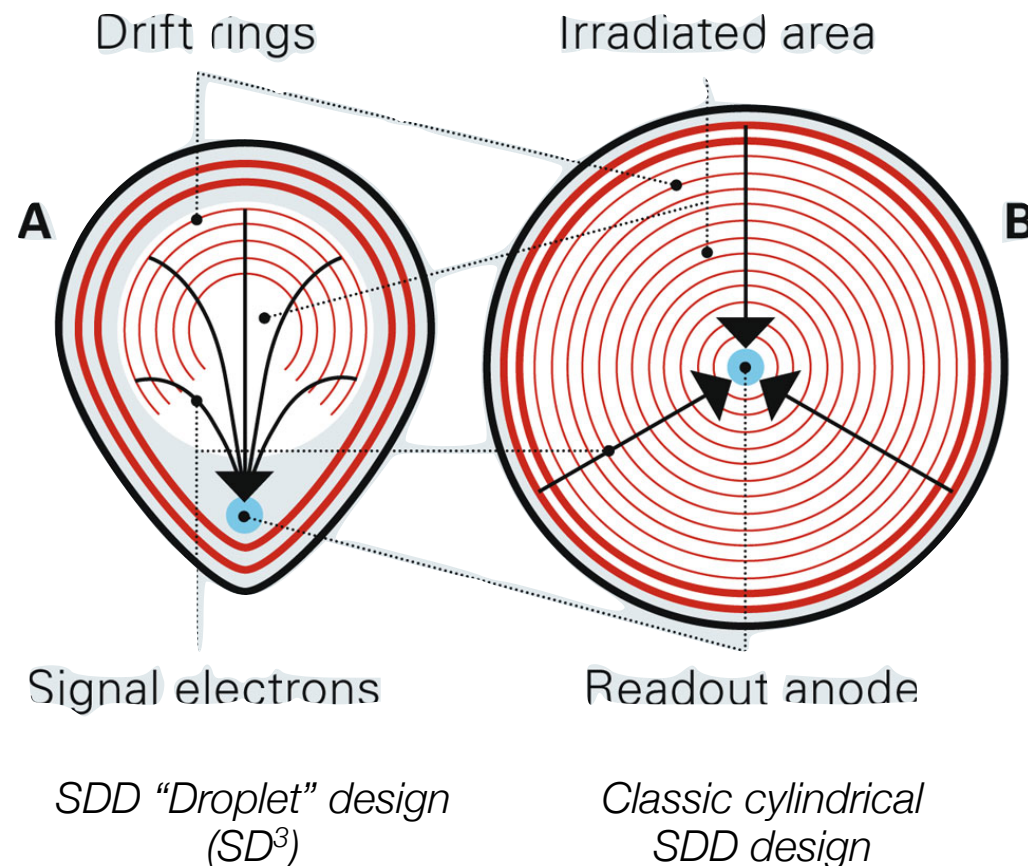
$$\text{ENC} = \left[\frac{k_1 \cdot \langle e_w^2 \rangle \cdot (C_d + C_i + C_p)^2}{\tau} + k_3 A_{1/f} (C_d + C_i + C_p)^2 + 2k_2 q I_l \tau \right]^{1/2}$$



	SDD	Si(Li)
Energy resolution	140-160 eV	180-200 eV
Shaping time	1 μs	6 μs
Sustainable count-rate	50 kHz	5 kHz
Cooling	-10/-20 °C	-195 °C

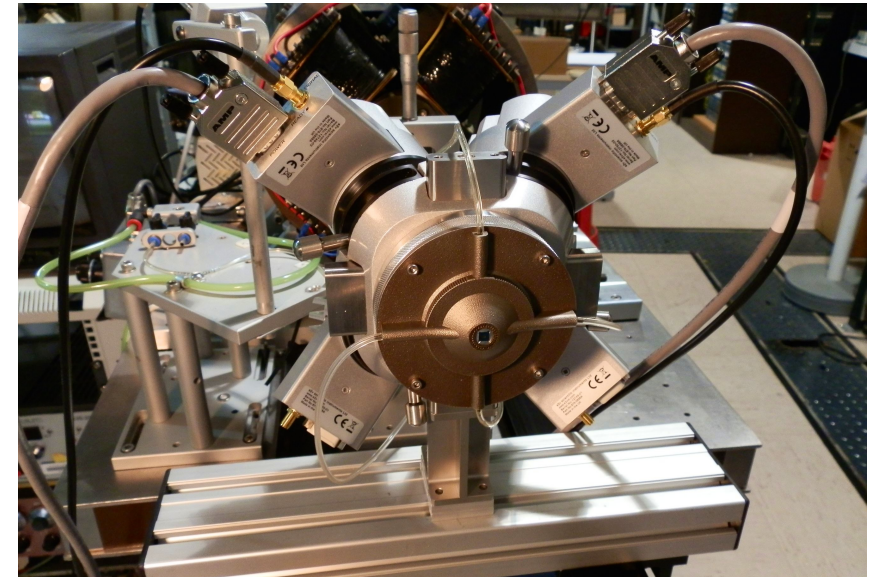
Commercial SDD

- Starting from the first SDDs, 5 or 10 mm² area, 0.3 mm thick, now several companies are selling SDDs with a wide range of characteristics and designs, and competitive prices

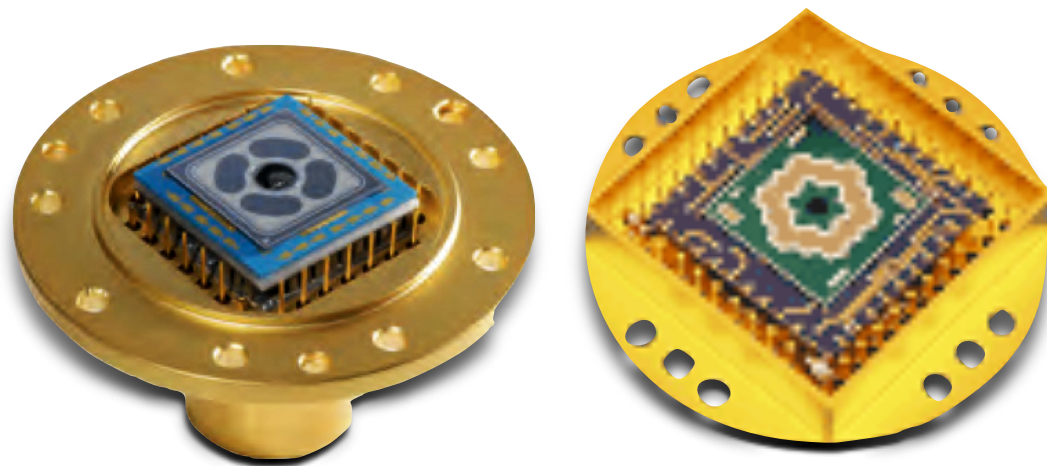


Large area SDD

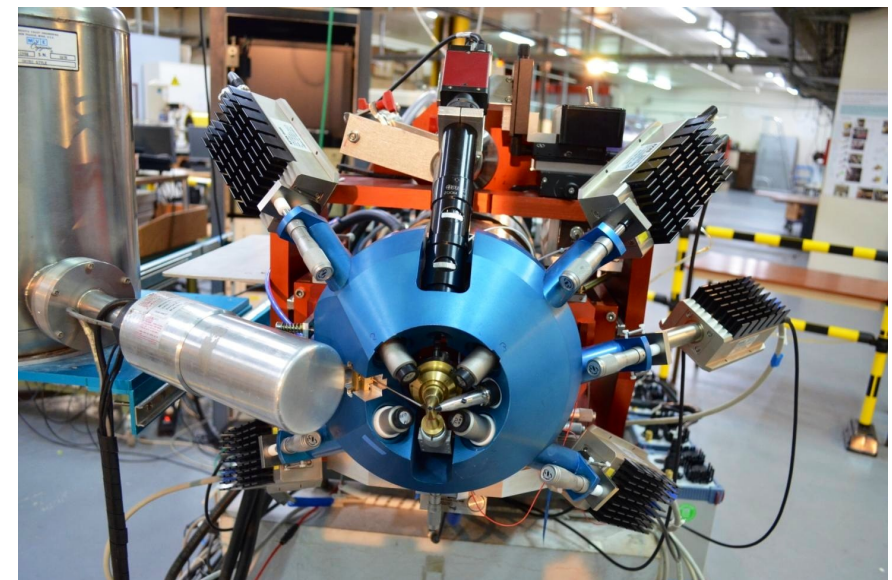
- A single SDD with active area up to 150 mm² is now commercially available (Ketek GmbH)
- Larger areas can be obtained using arrays of individual systems or integrated multi-channel SDDs



4-channel SDD (30 mm² each) PIXE system at Surrey Ion Beam Centre (SGX Sensortech, UK)



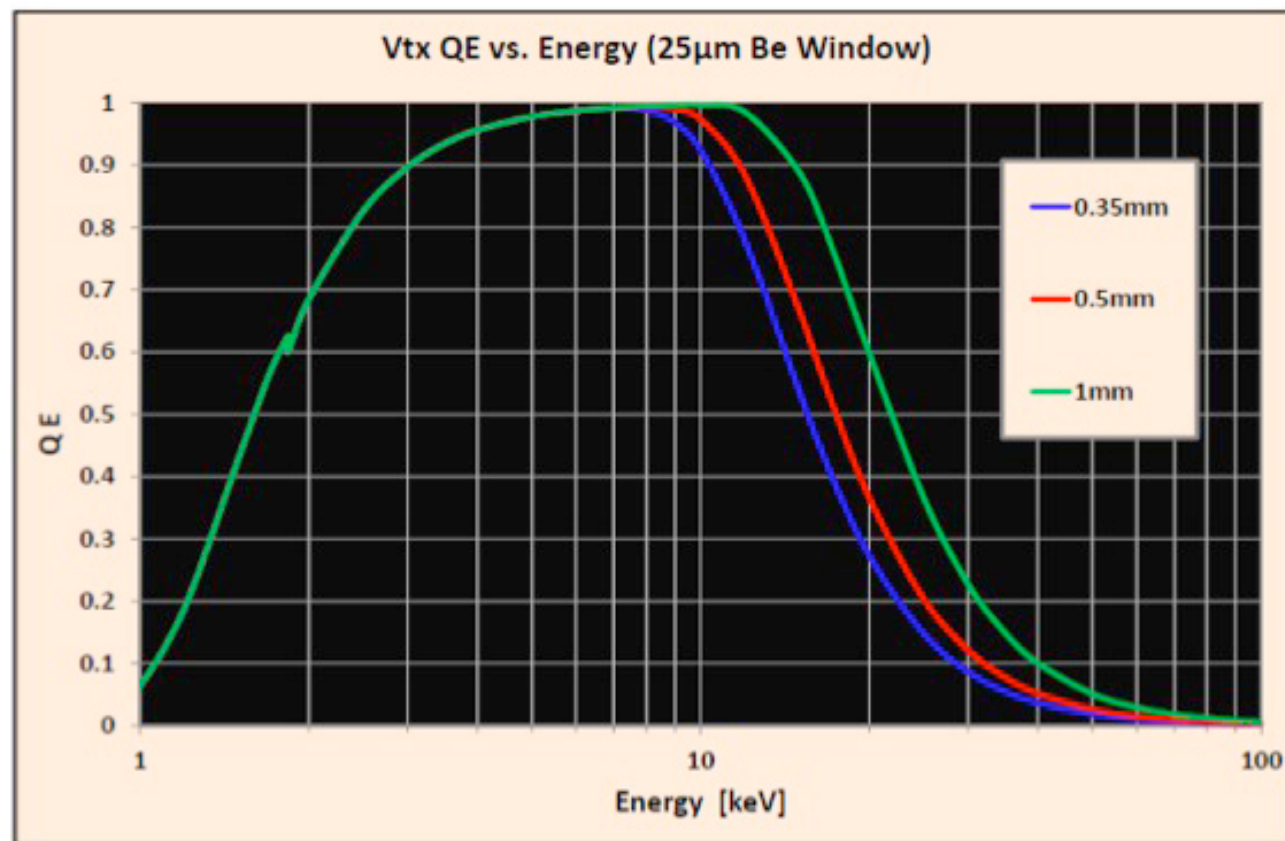
Ring-shaped multi cell SDD with 12 x 5 mm² hexagonal cells (PN Detectors, Germany)



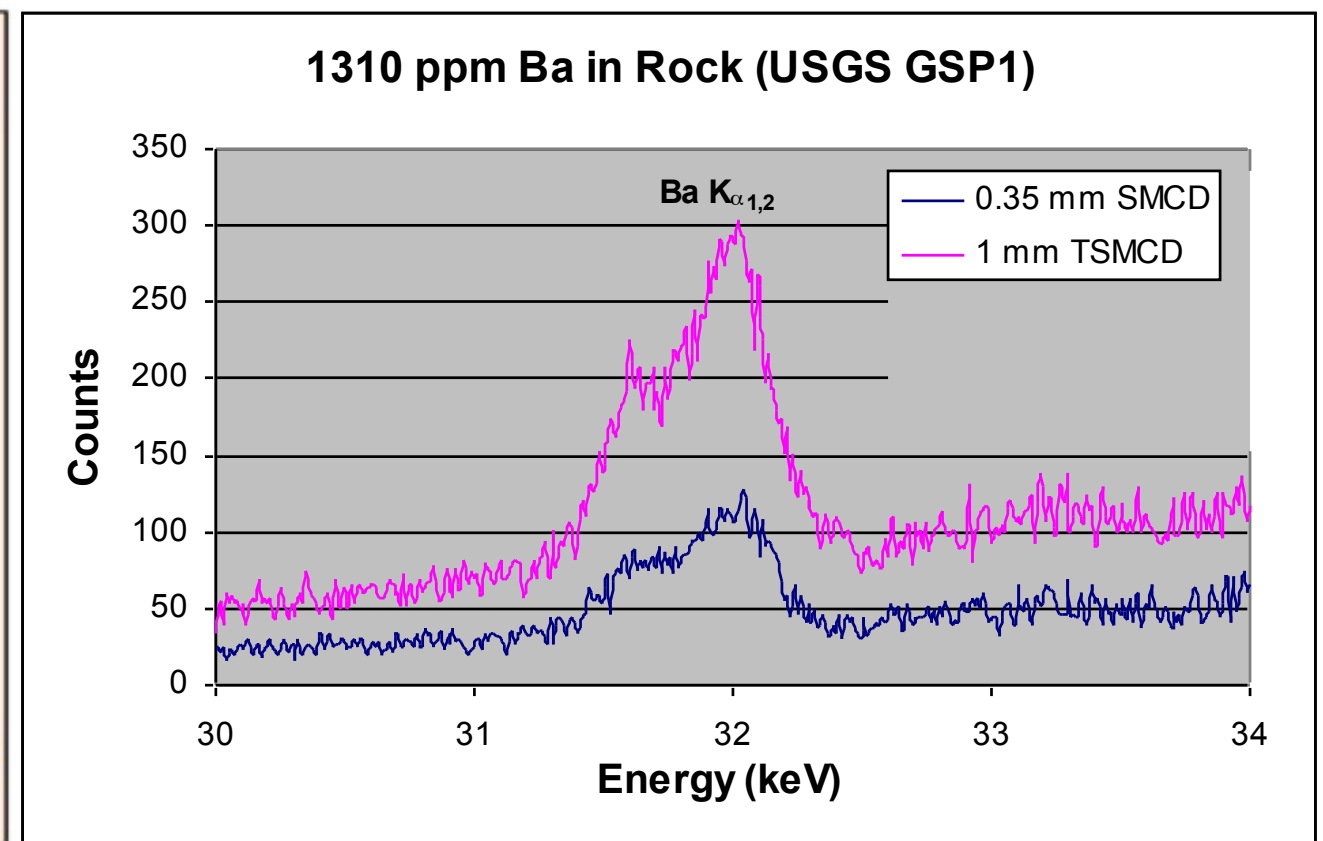
Multi SDD PIXE system (1 low and 4 high energy), total solid angle 500 msr, at AGLAE, Paris (Ketek GmbH, Germany)

Increased thickness SDD

- Single SDD with active thickness of 0.7 mm (Ketek GmbH) or 1 mm (Hitachi High-Technologies Science America, Inc) are now commercially available

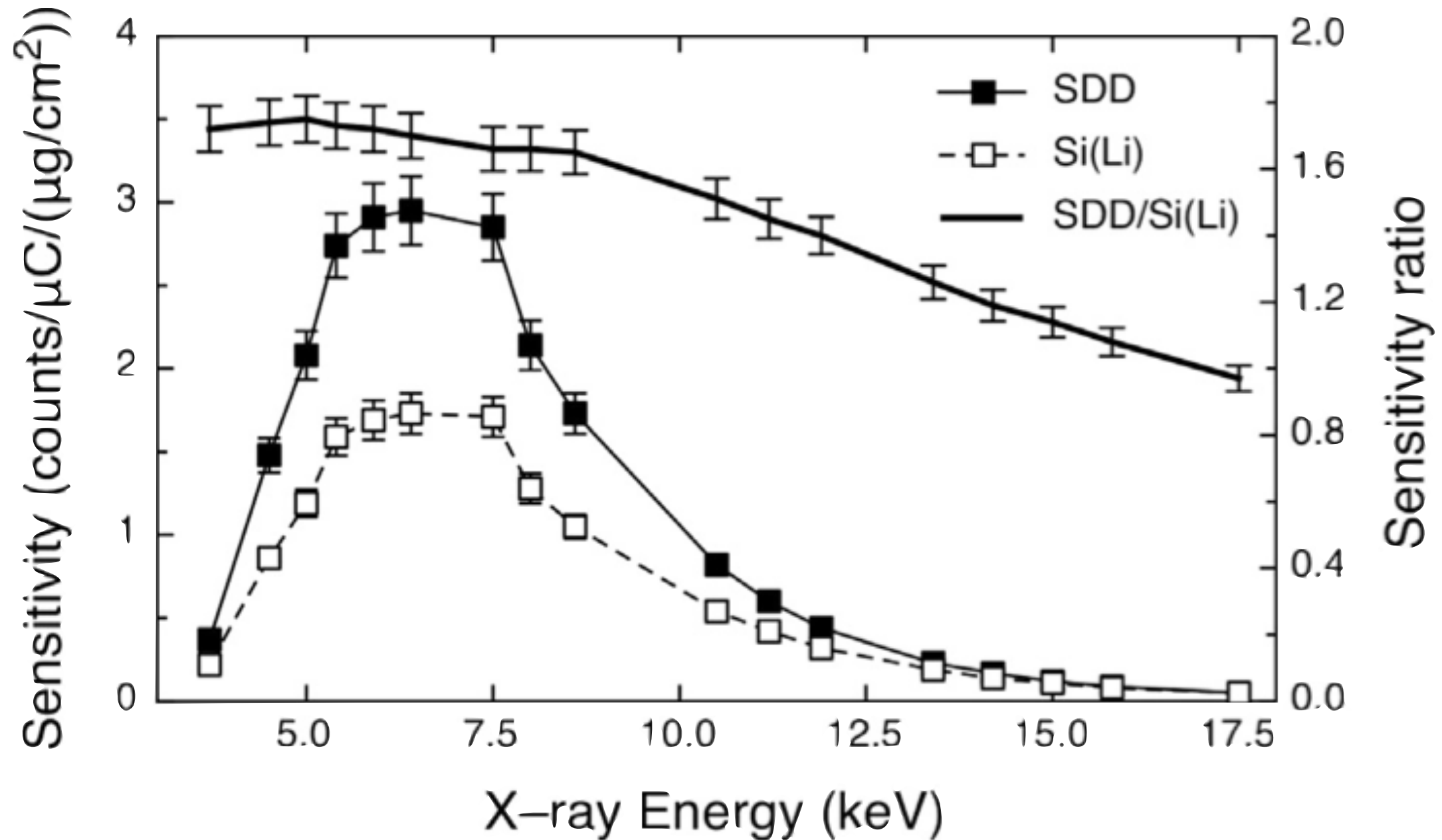


QE (0.3 mm) = 90% @10 keV; 25% @20 keV
QE (0.5 mm) = 100% @10 keV; 40% @20 keV
QE (1.0 mm) = 100% @10 keV; 60% @20 keV



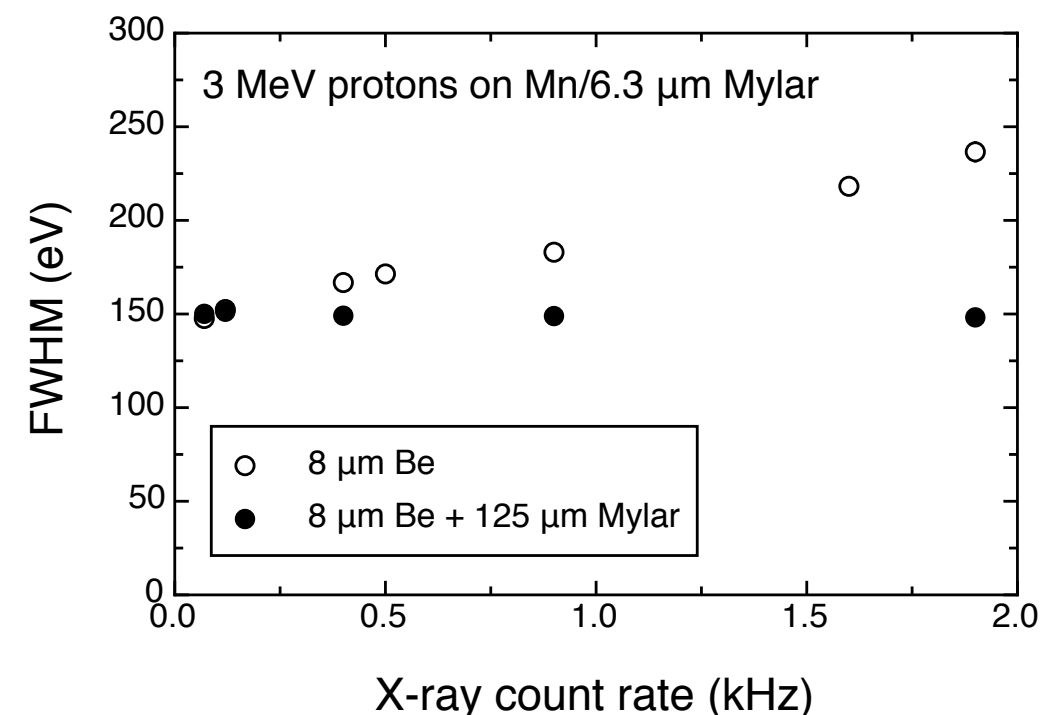
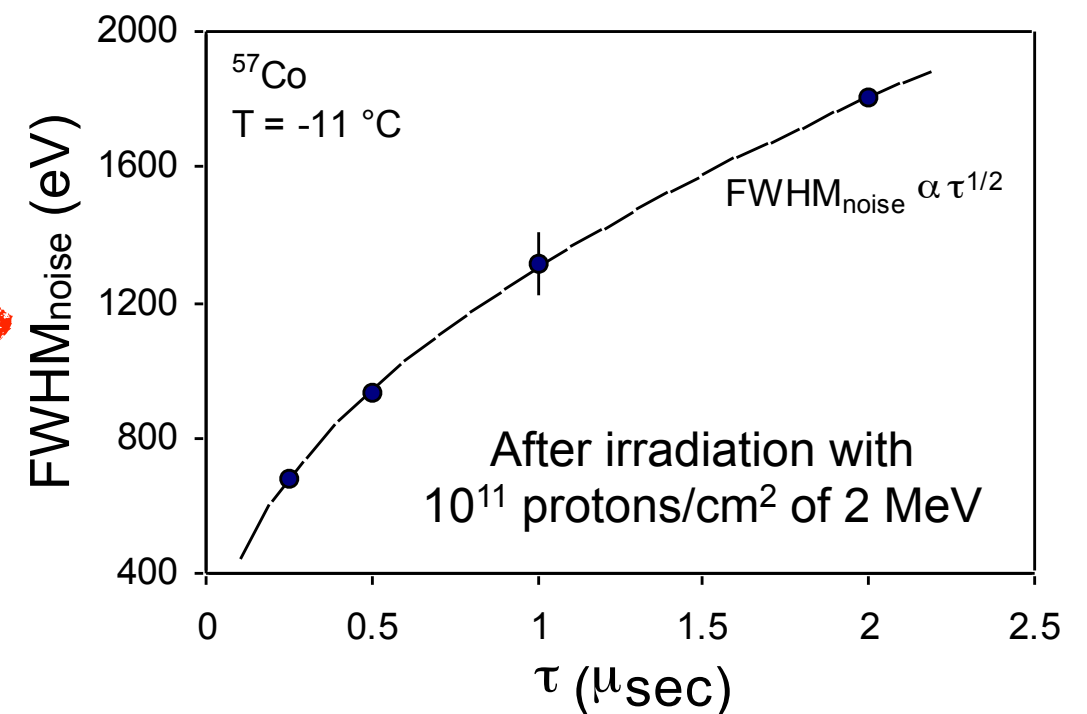
32 keV Ba spectra from USGS GSP1 – Rh tube,
50 kV, 1 mA, 0.5 mm Cu + 6 mm Al Filter,
0.5 µs peaking time, 300 sec. livetime.
(Gordon Myers, Hitachi High-Technologies Science America, Inc.)

Sensitivity curve for large area SDD and Si(Li)



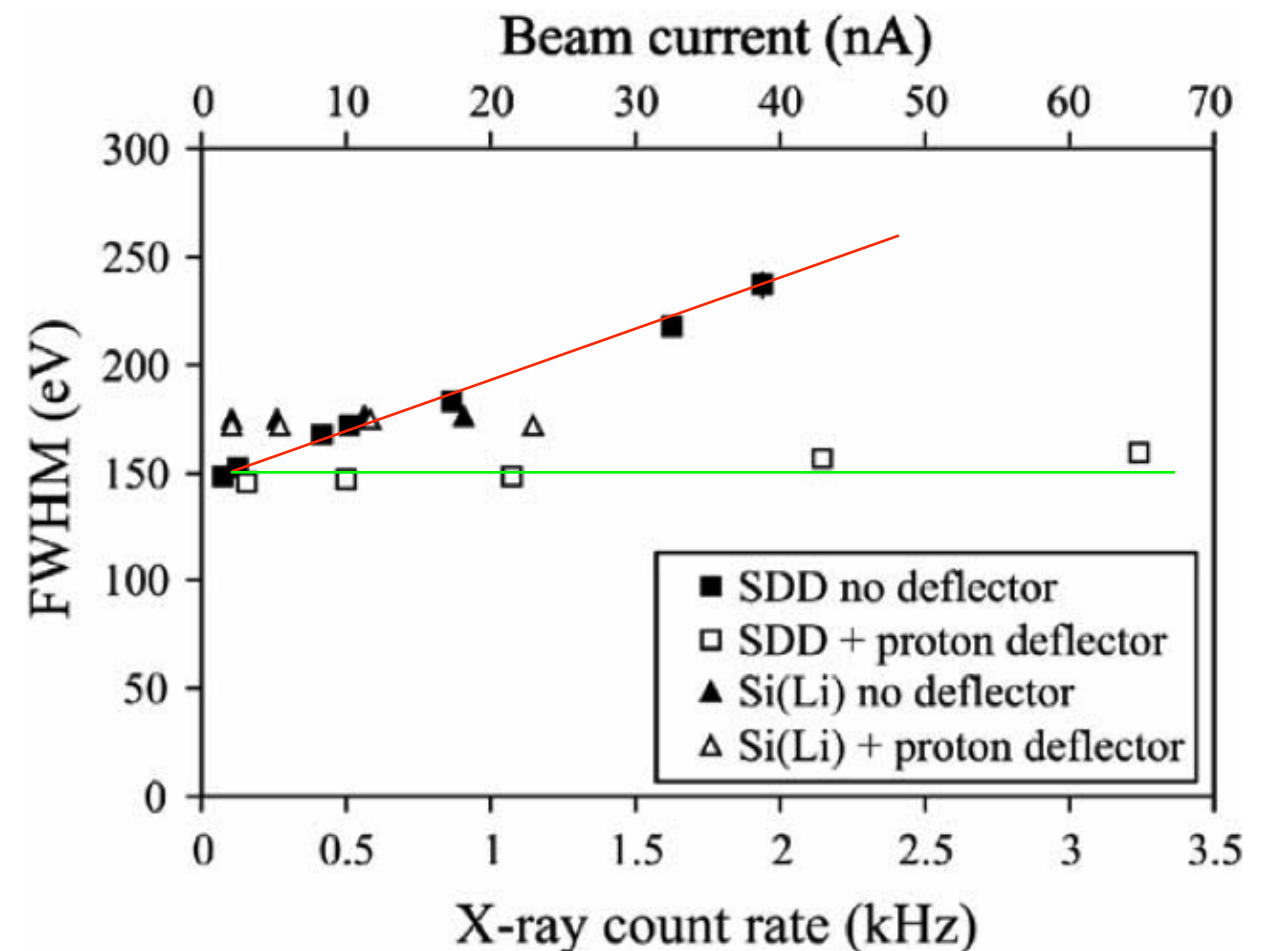
Backscattered protons effects on SDD

- PIXE detectors with thin entrance window used in presence of a large backscattered protons flux from the sample can suffer unrecoverable damages (**long-term effects**) and worsening of the energy resolution under beam irradiation (**short-term effects**)

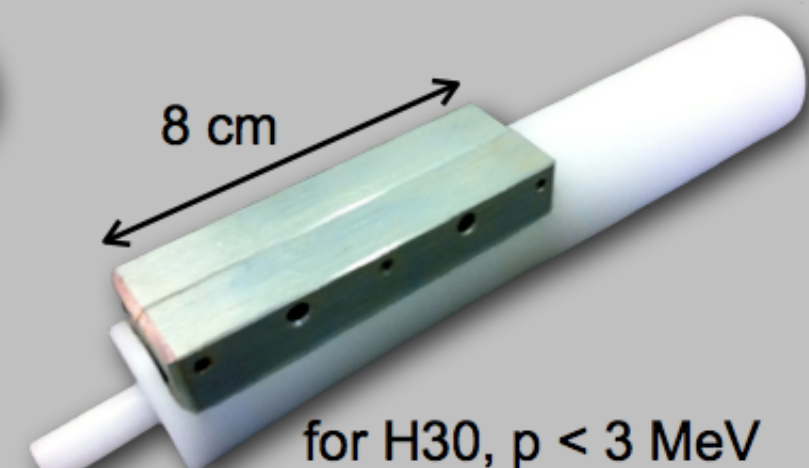
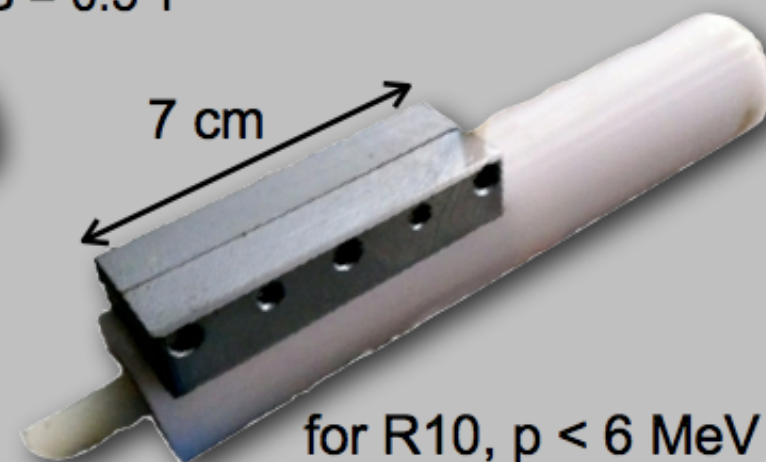
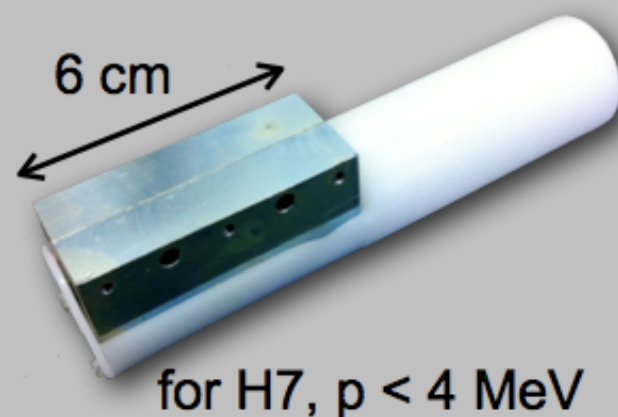


Magnetic proton deflector

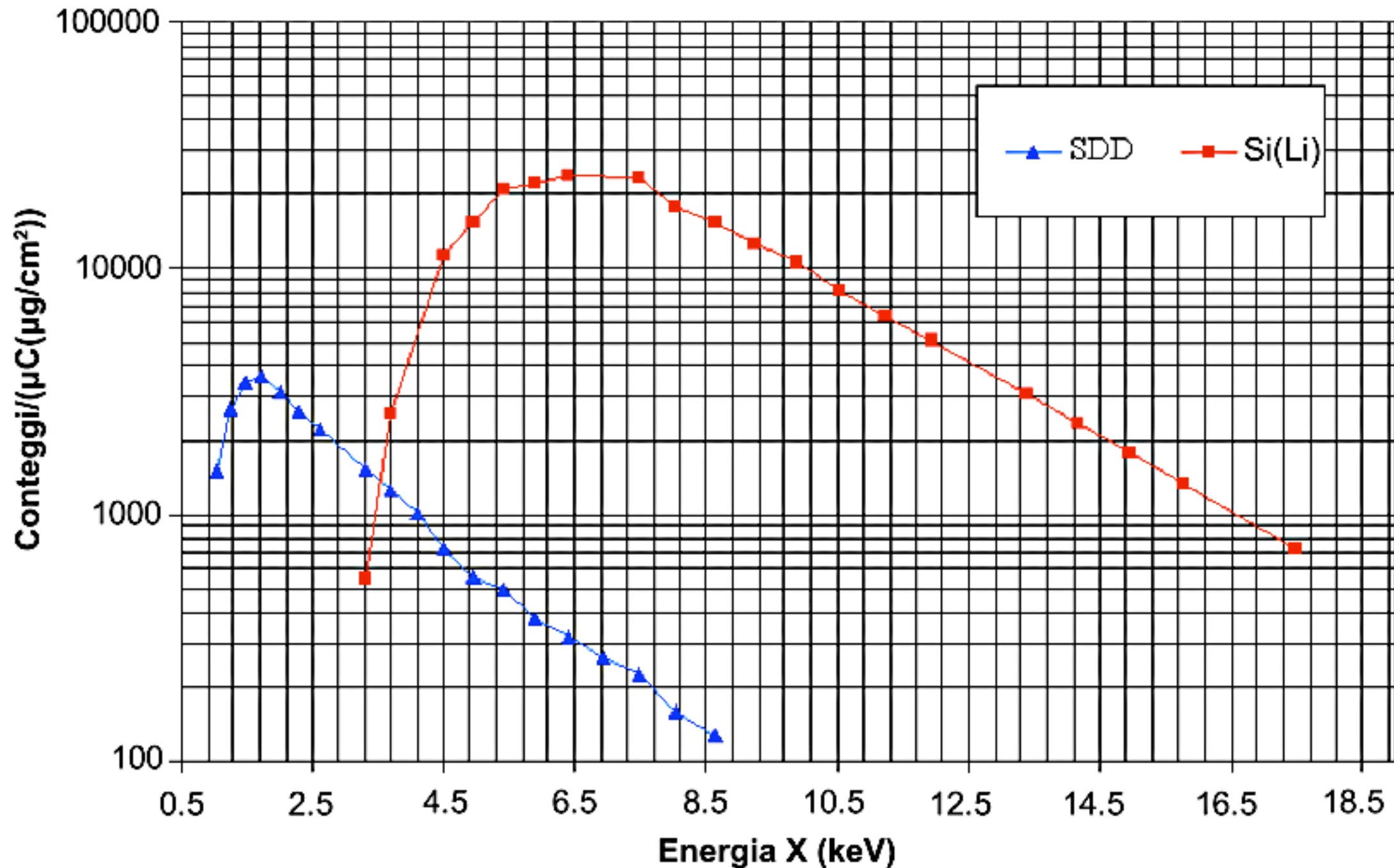
- The use of a properly designed magnetic deflector to filter out the backscattered protons without substantial limitations to the SDD intrinsic efficiency at low X-ray energies is mandatory to prevent any long-term damages and to avoid the worsening of the energy resolution



NdFeB permanent magnets, $B = 0.5$ T

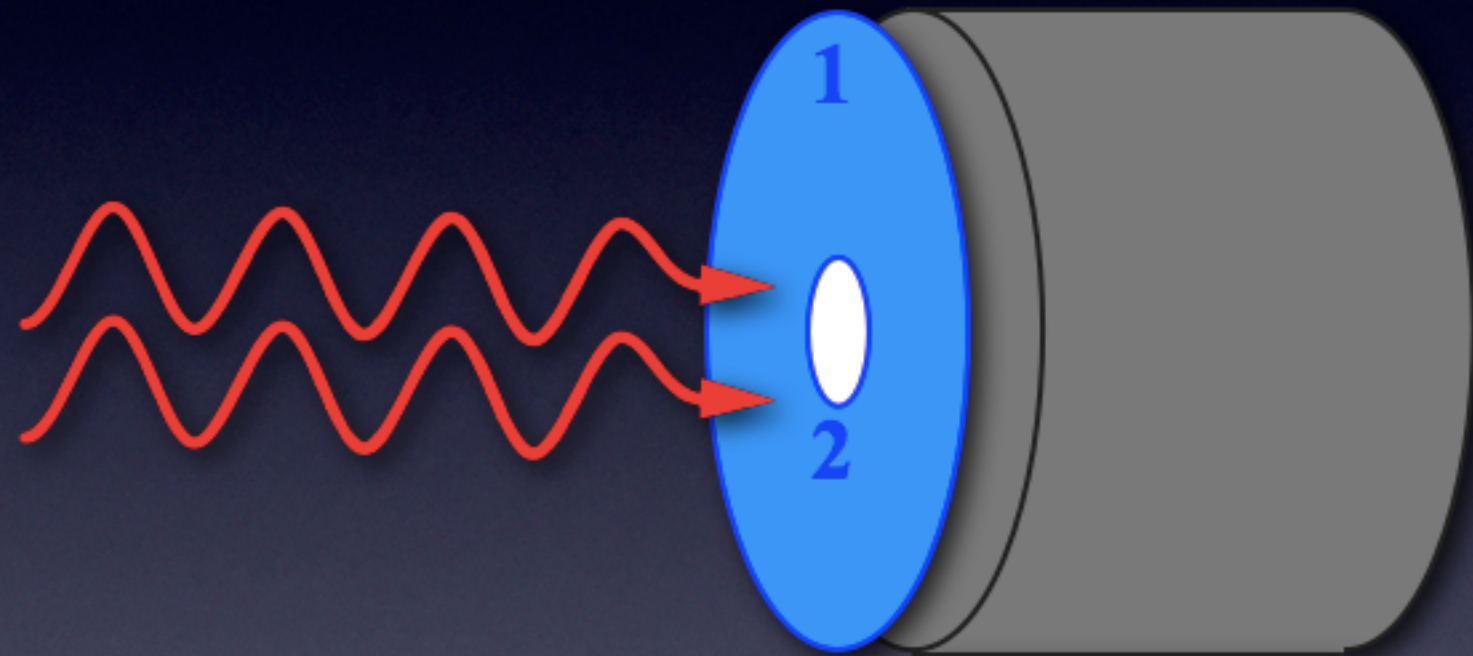


Detection efficiency for a 2-detectors PIXE set-up



“Funny filter”

The “funny filter” concept was introduced by Harrison and Eldred in 1973, when PIXE was starting to develop as an analytical technique



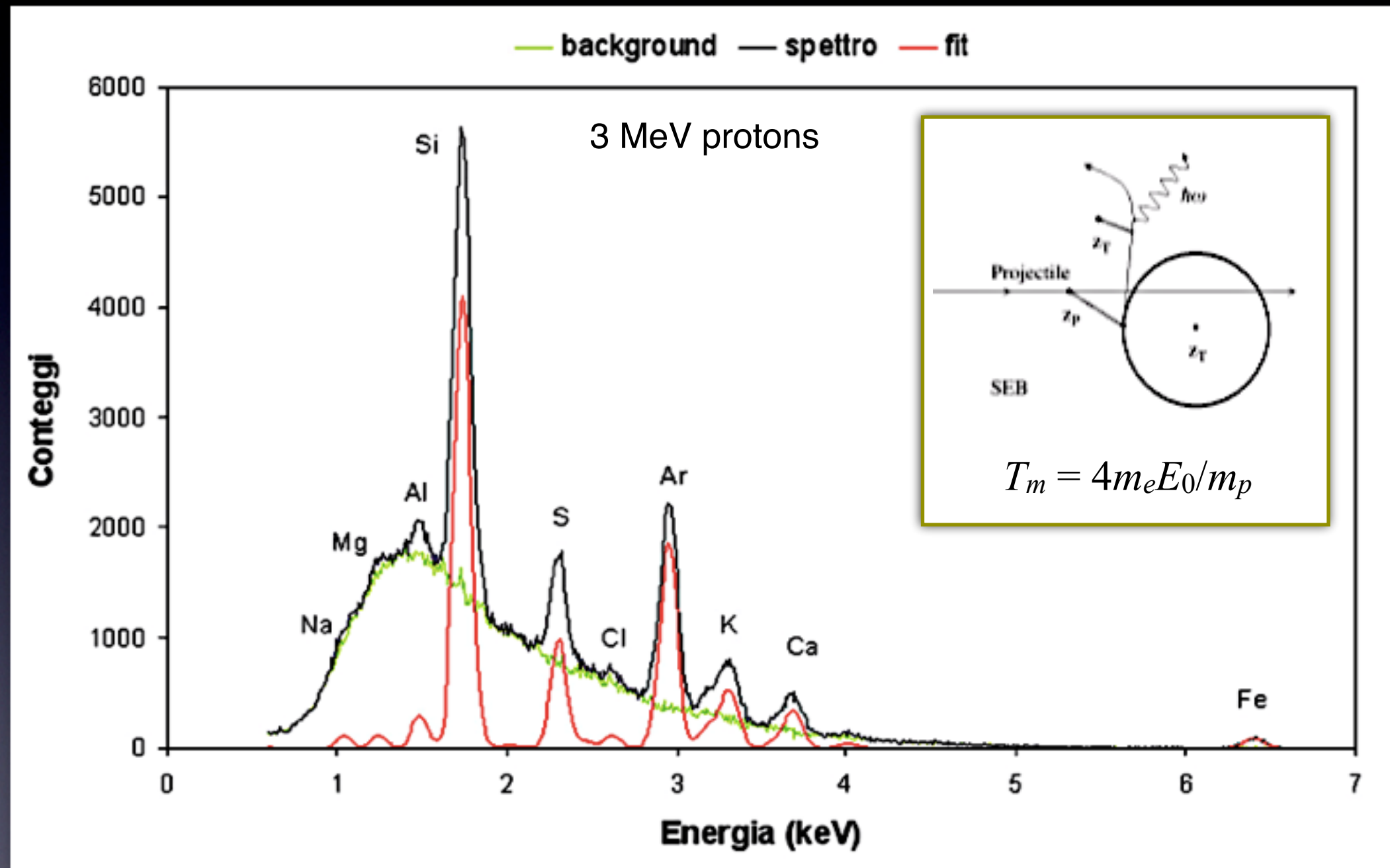
$\alpha_1(Z)$, transmission coefficient of absorber 1

$\alpha_2(Z)$, transmission coefficient of absorber 2

R , ration between absorber 2 area and detector area

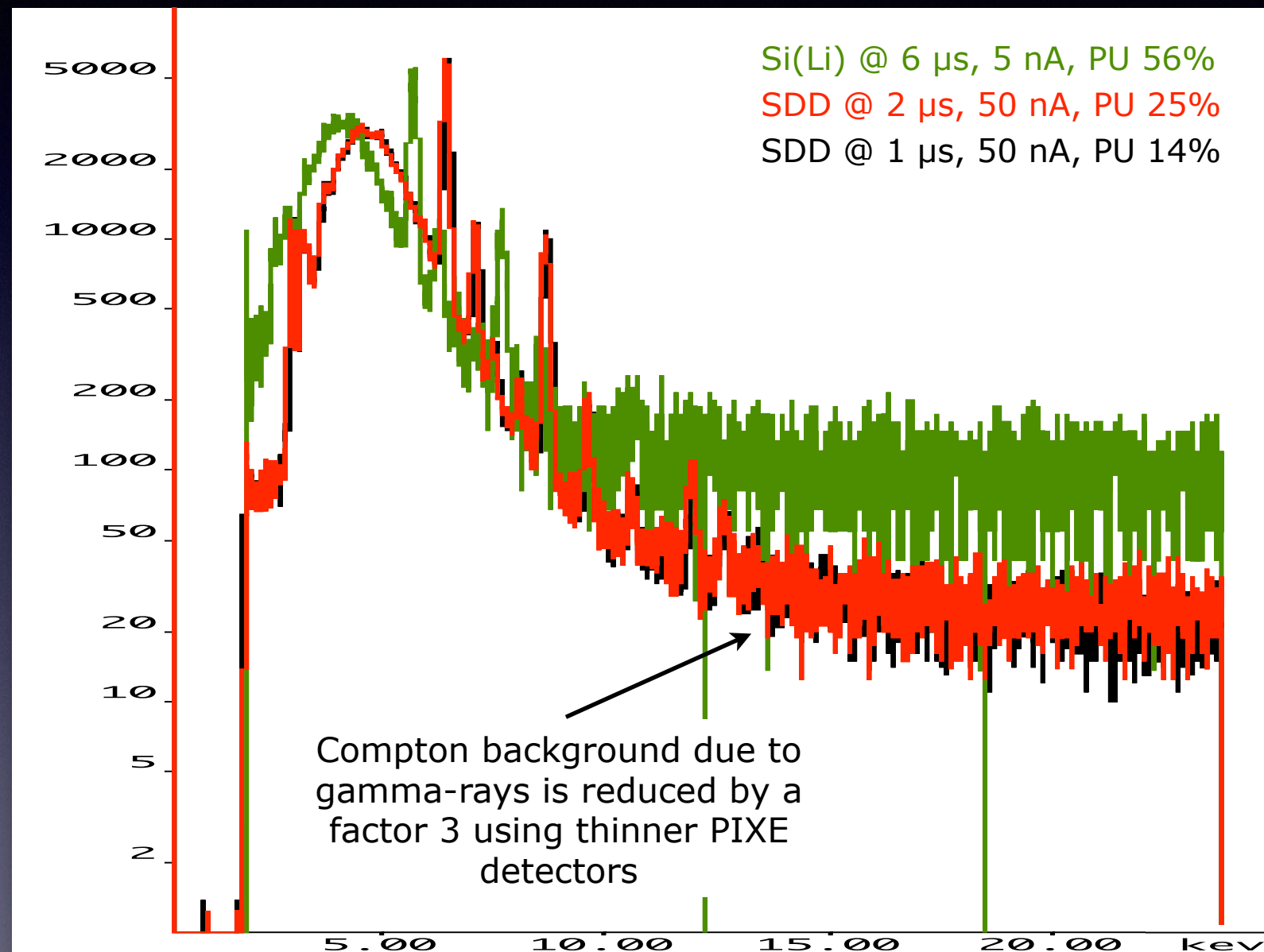
$$\alpha_Z = \alpha(Z) = \alpha_1(Z) \cdot [R + (1 - R) \cdot \alpha_2(Z)]$$

PIXE spectrum background



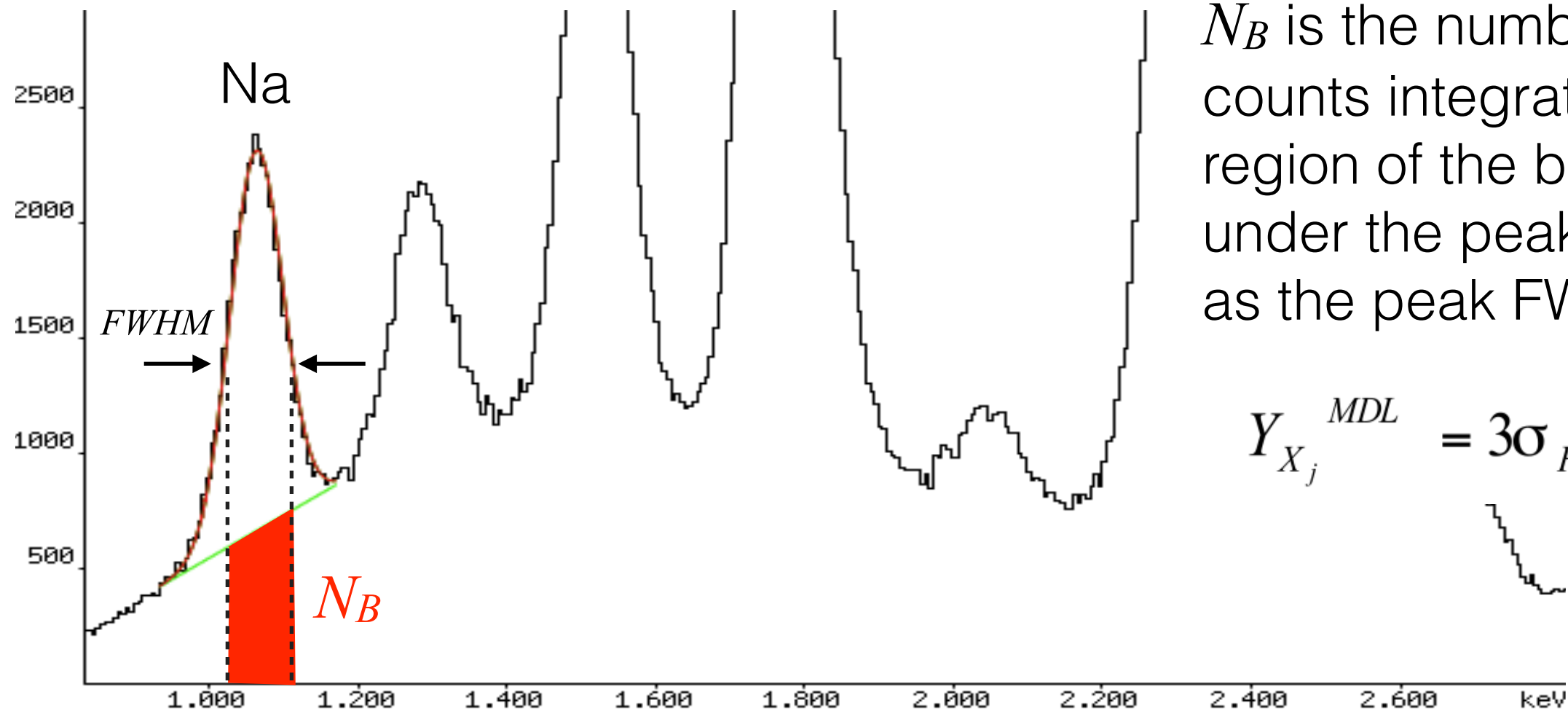
Mainly due to *Secondary Electron Bremsstrahlung* radiation
(for $E < 10$ keV)

PIXE spectrum background



Possible contribution from Compton interaction of gamma-rays in the detector active volume (for $E > 10$ keV)

Minimum Detection Limit (MDL)



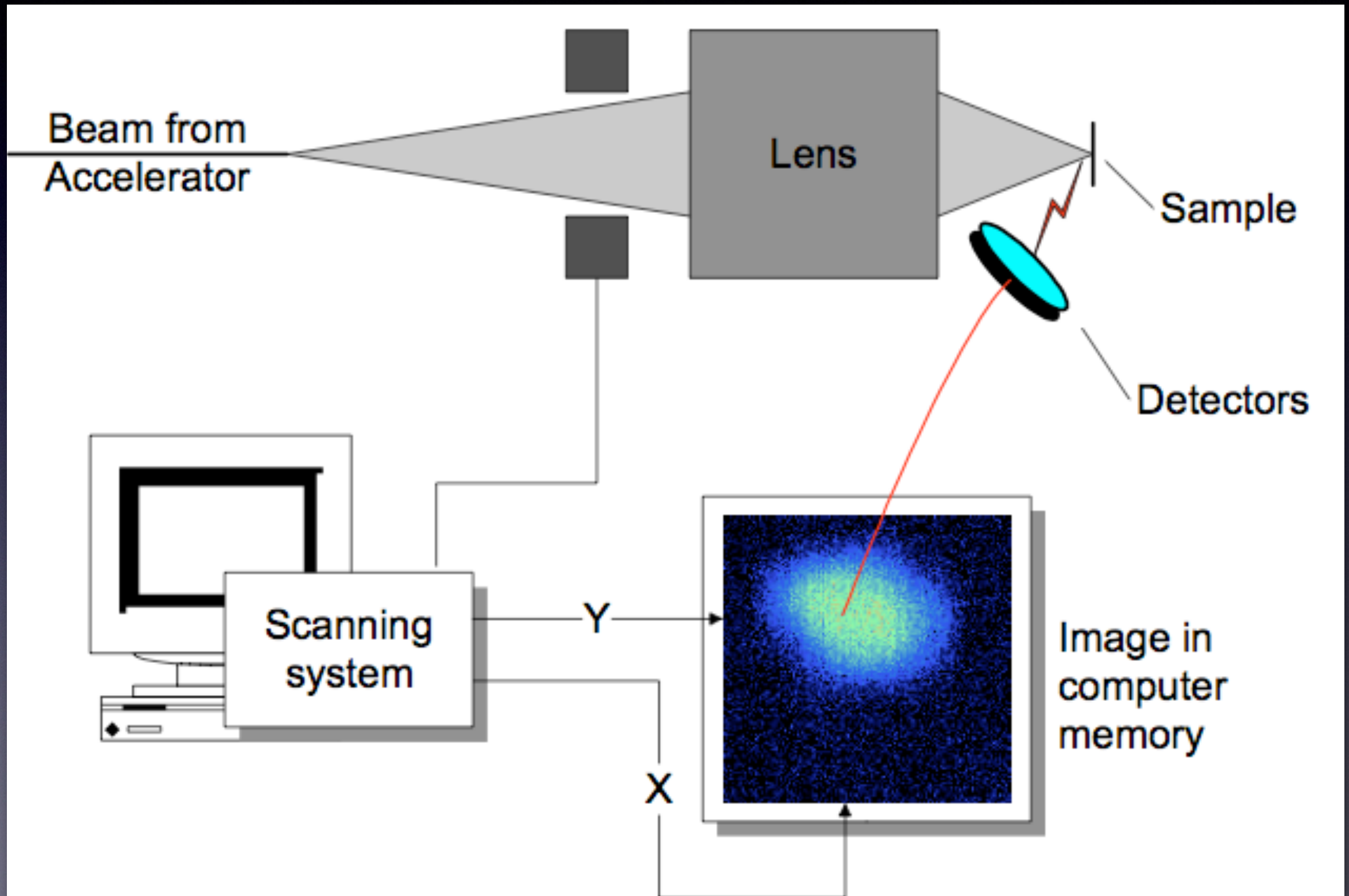
N_B is the number of counts integrated in a region of the background under the peak as wide as the peak FWHM

$$Y_{X_j}^{MDL} = 3\sigma_F = 3\sqrt{N_B}$$

In terms of areal density (i.e. $\mu\text{g}/\text{cm}^2$) the PIXE MDL can be calculated as:

$$MDL_Z = \frac{3 \cdot \sqrt{N_B}}{\eta_Z \cdot Q}$$

Nuclear microscopy

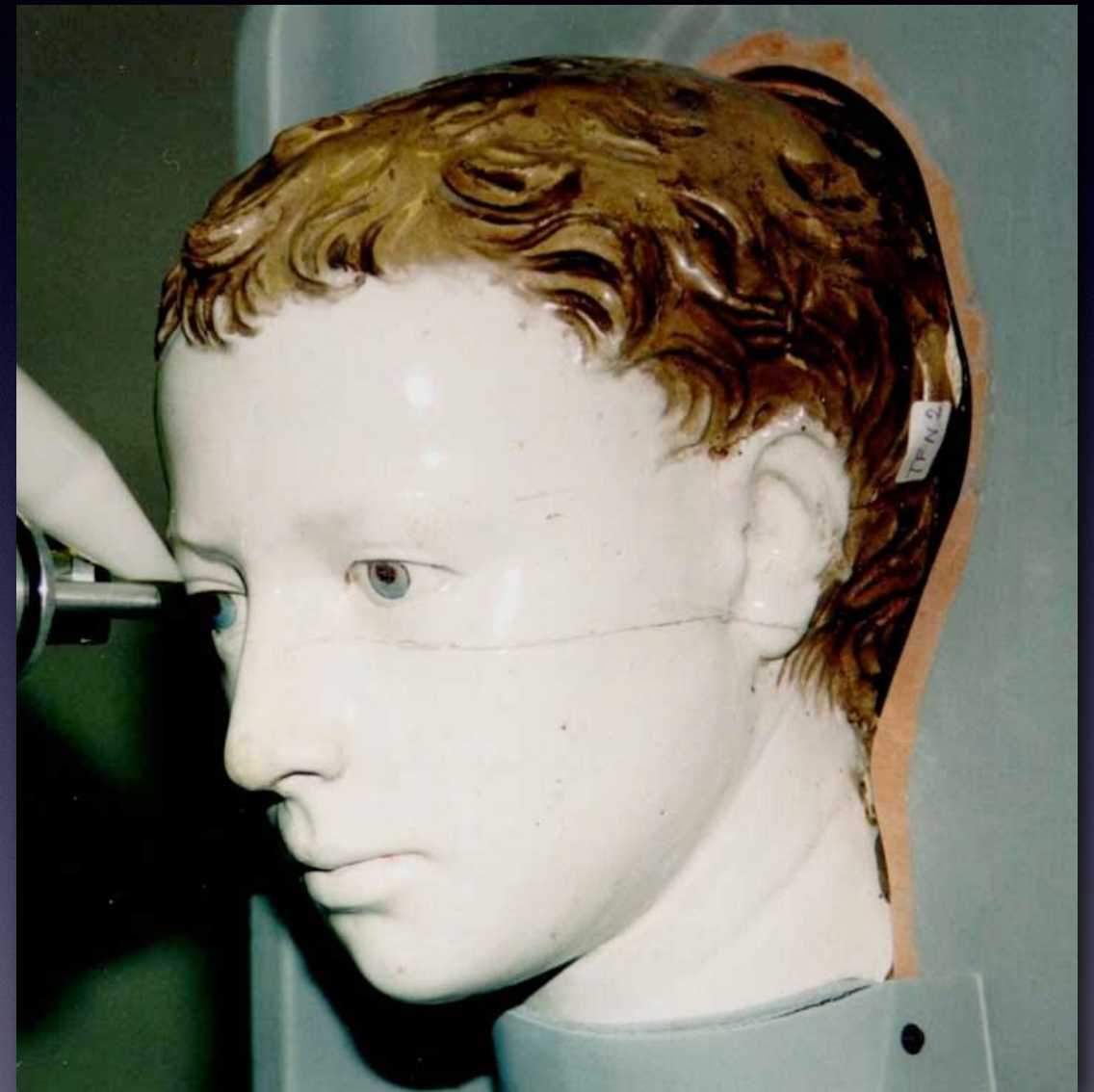


External beam PIXE of
ancient manuscripts,

...ceramics,



PIXE analysis of the frontispiece of
PI.16,22, from Biblioteca
Laurenziana in Florence



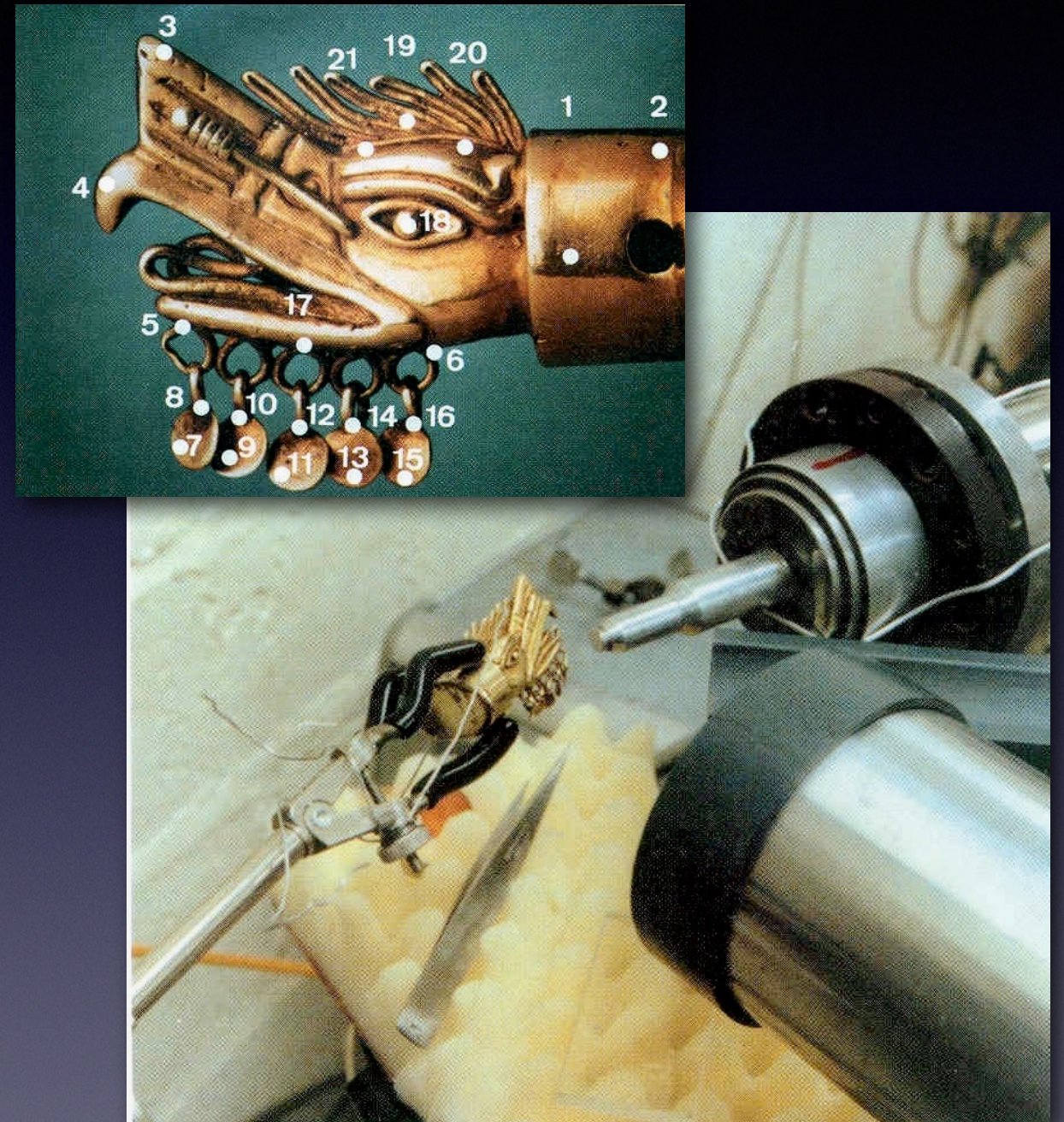
Analysis of the Ritratto di fanciullo
by Luca Della Robbia – before
restoration at the Opificio delle
Pietre Dure in Florence

... drawings,



Micro-PIXE measurements of
Portrait of Lucas de Leyde by
Alfred Dürer
A.Duval et al., (Louvre laboratory)

... jewels,



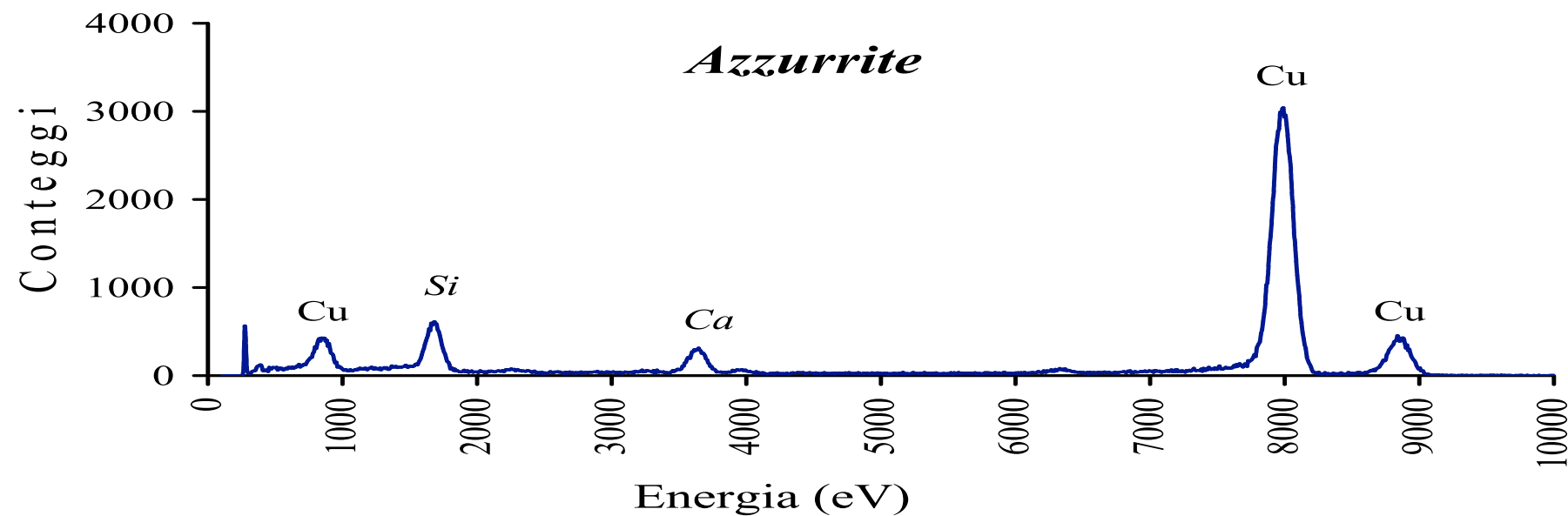
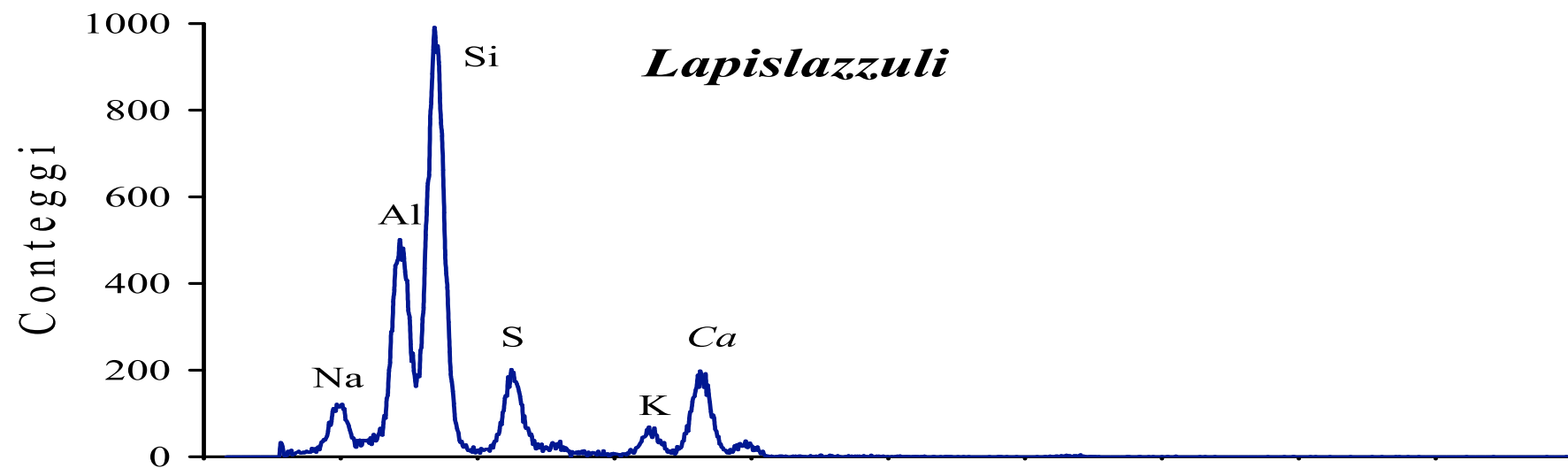
Micro-PIXE measurements of a
Mexican gold alloy ornament
G.Demortier and J.L.Ruvalcaba Sil
(Namur)

...paintings



PIXE analysis of a painting by
Lucas Cranach the Elder
C. Neelmeijer et al.
(Rossendorf Forschungszentrum, Dresden)

Blue Temperas



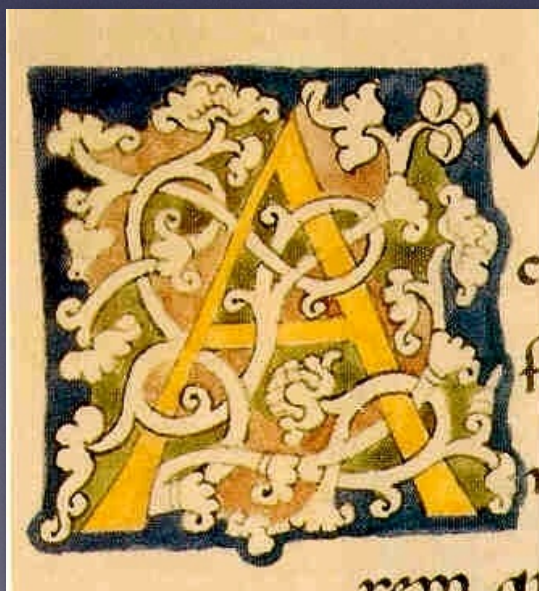
Example of
PIXE spectra
of two blue
pigments

Blue Temperas

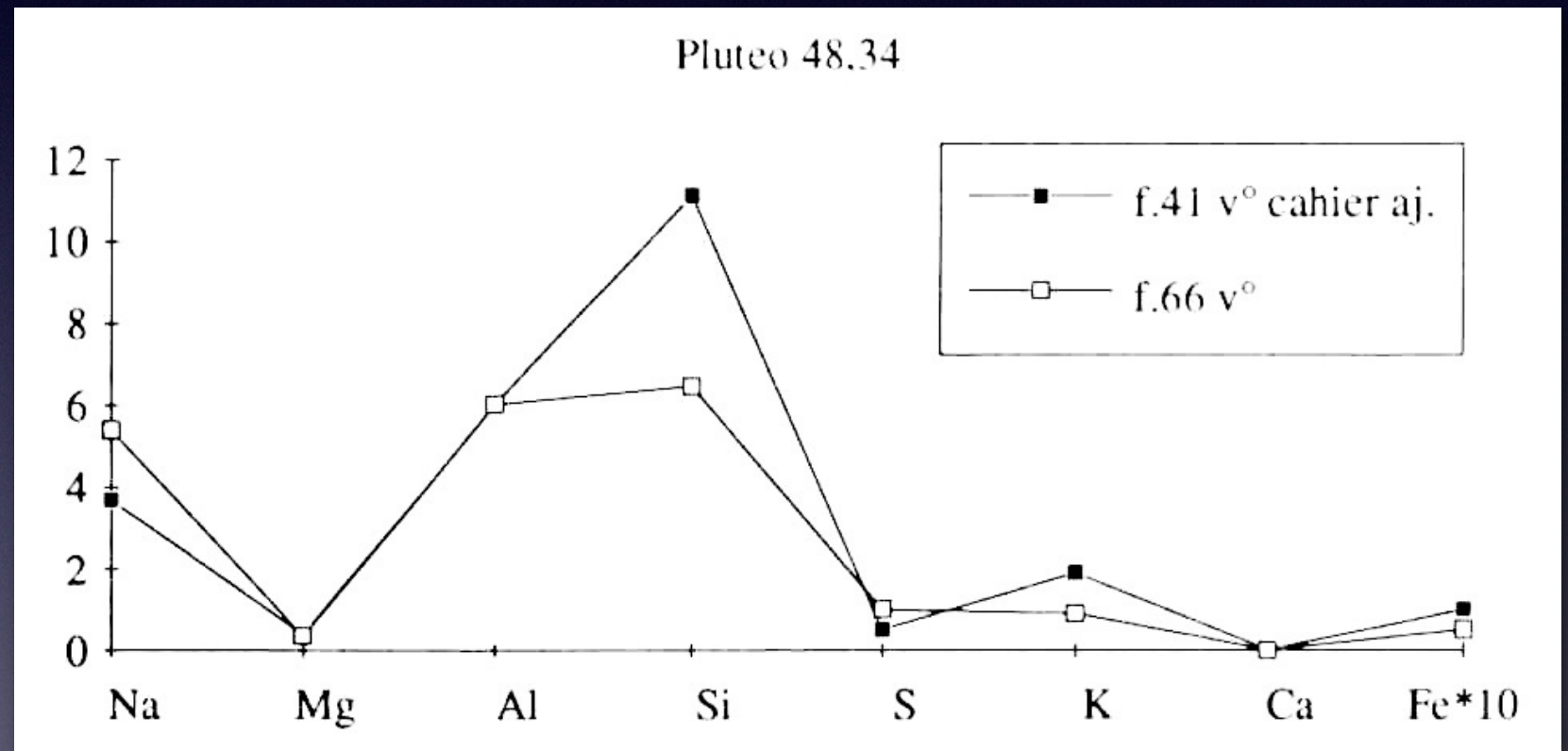
Extensive use of lapislazuli starting from XI century



Pluteo 48, 34, f. 66 v°



Pluteo 48, 34, f. 41 v°



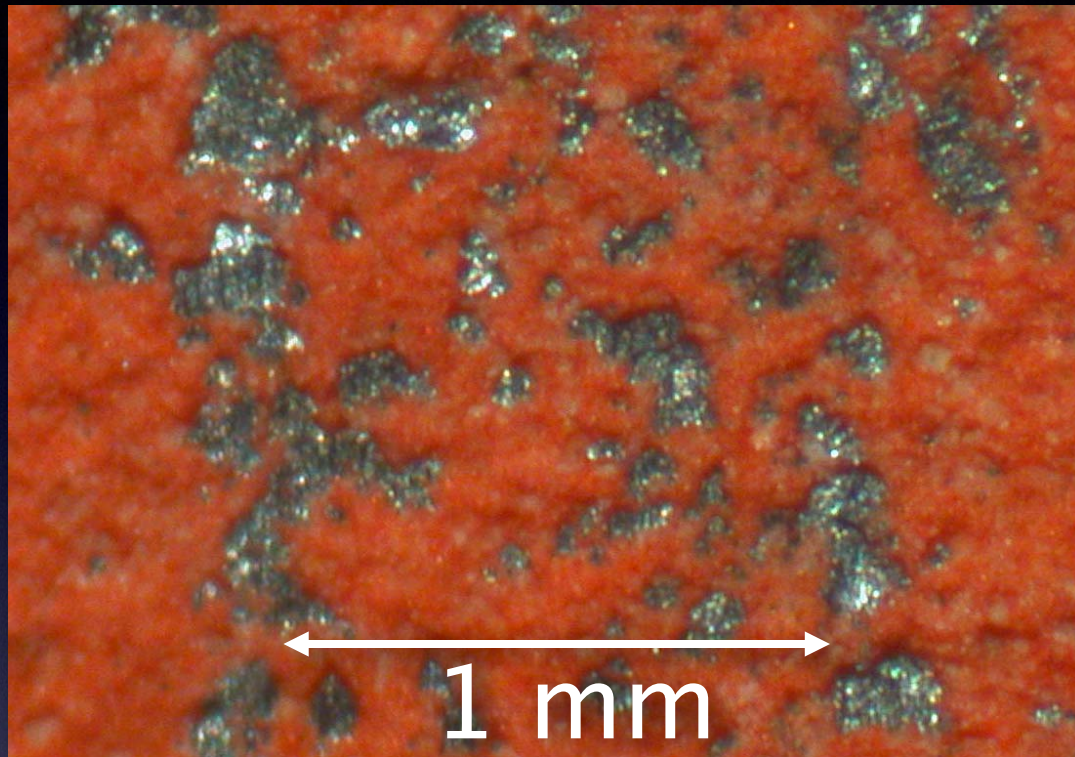
Metal point drawings

LEONARDO DA VINCI
STUDY OF A DRAPERY
Roma, Istituto Nazionale
per la Grafica

metal point, lead white
red prepared paper



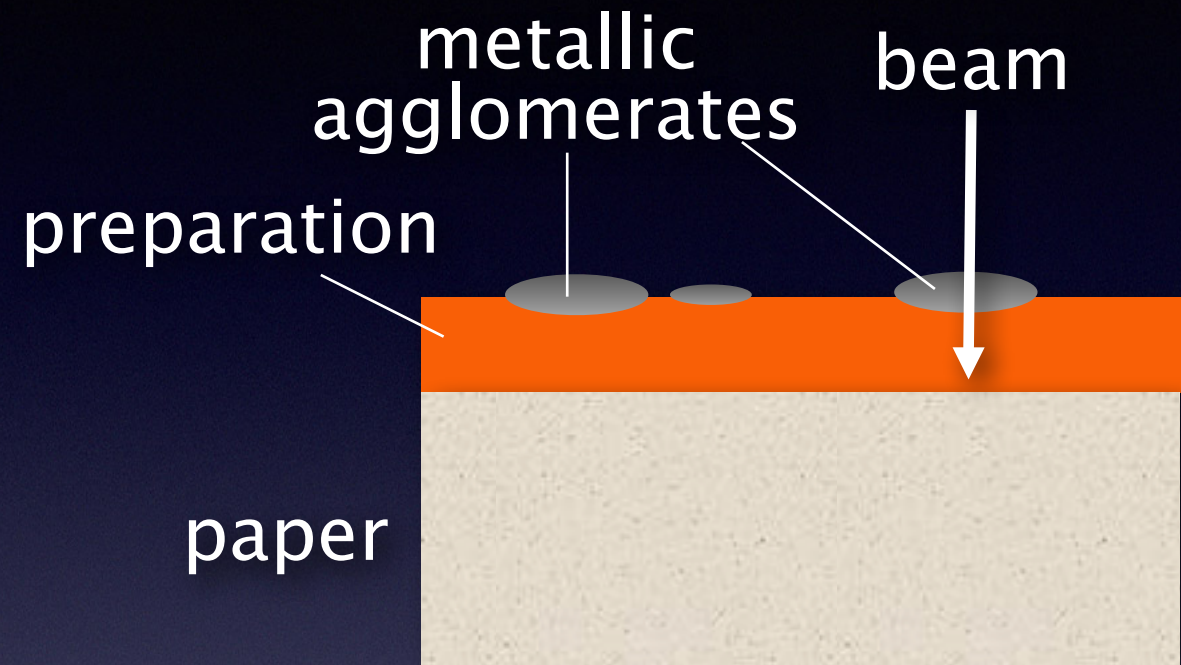
Characteristics of metal point drawings



The extension of the metallic agglomerates on the surface is some tens of μm



The beam size does not allow a detailed analysis



The beam can pass through the trace and hit the preparation



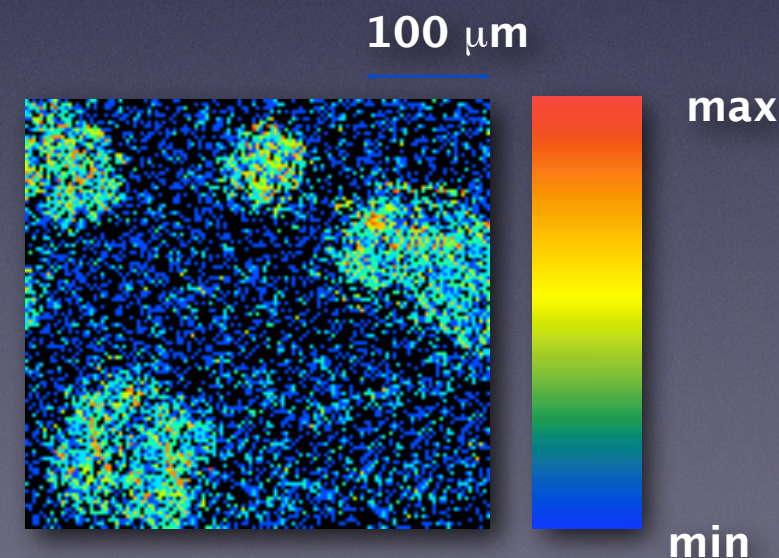
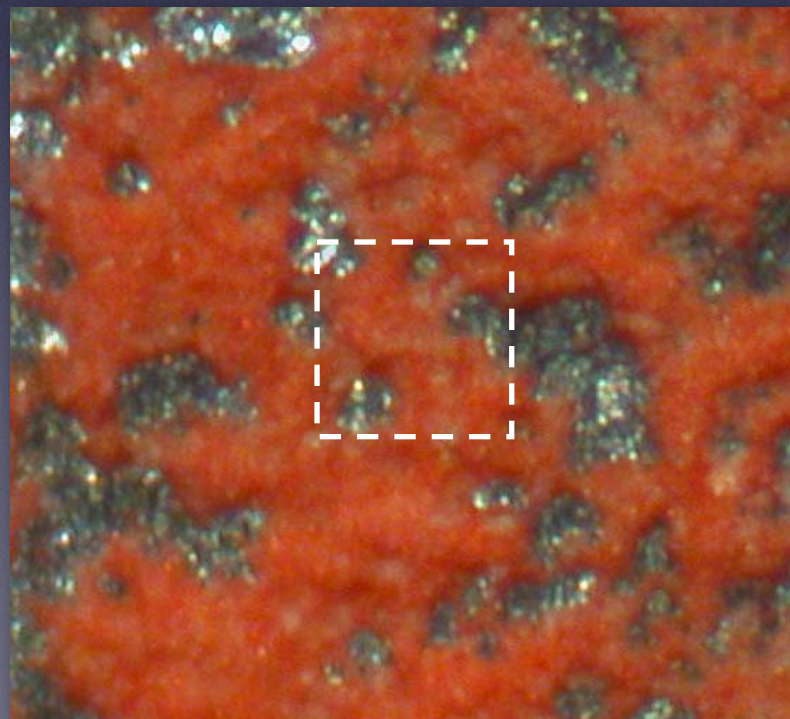
The contribution of the preparation must be taken into account

MicroPIXE analysis of metal point drawings

Four metallic points:
silver, lead, gold, copper

Red preparation:
cinnabar, yellow ochre,
lead white, bone white

Au Cu Pb

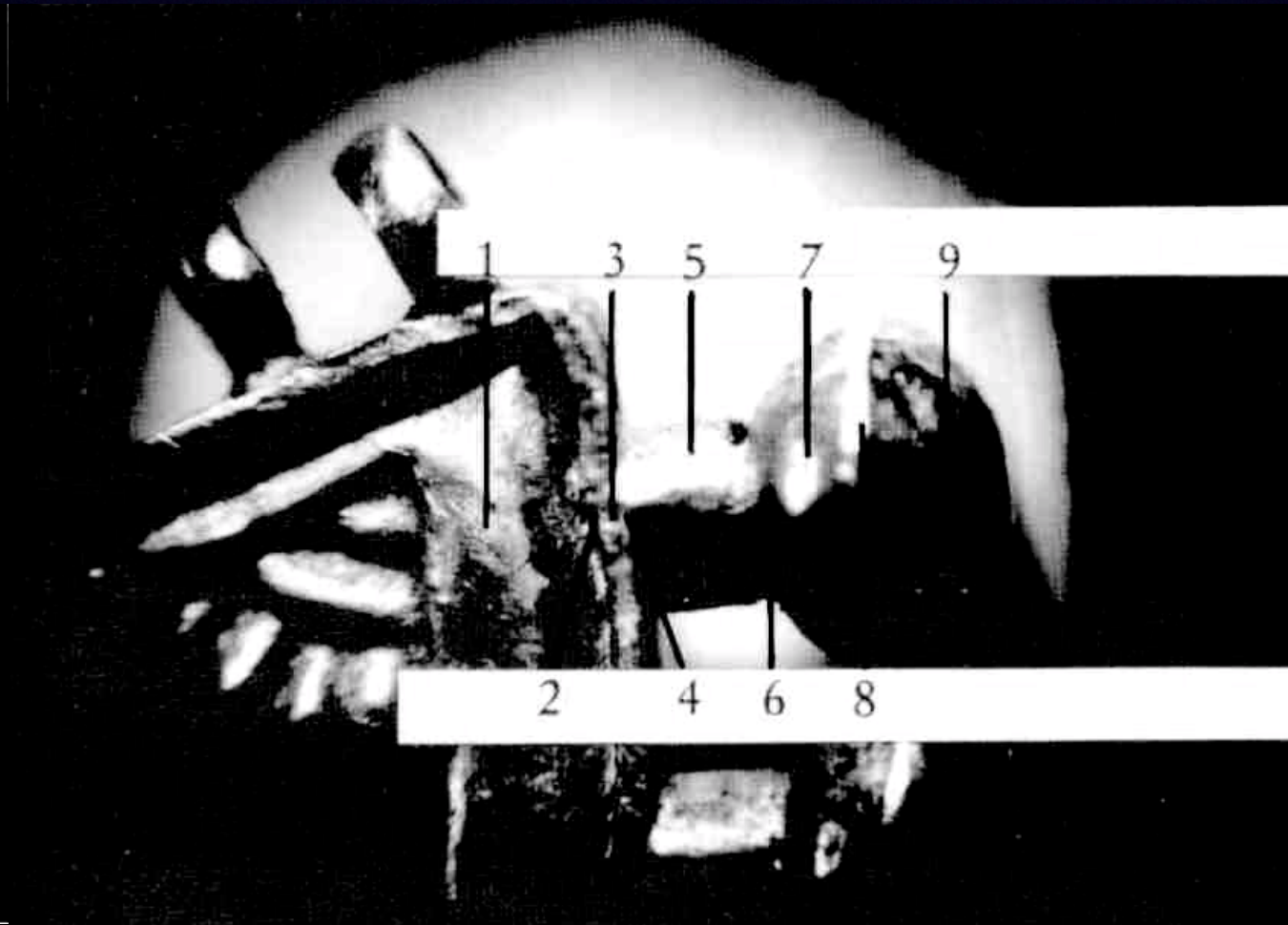
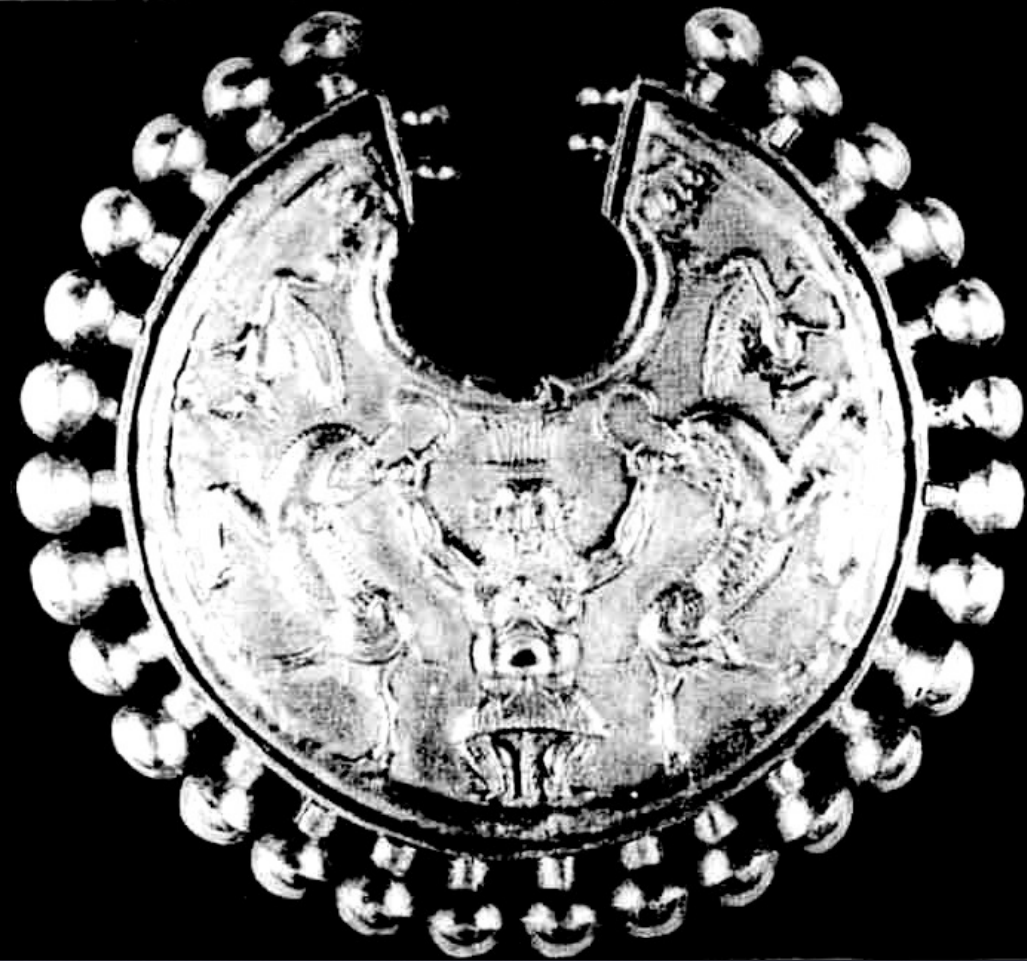


Elemental map on
0.4x0.4 mm²

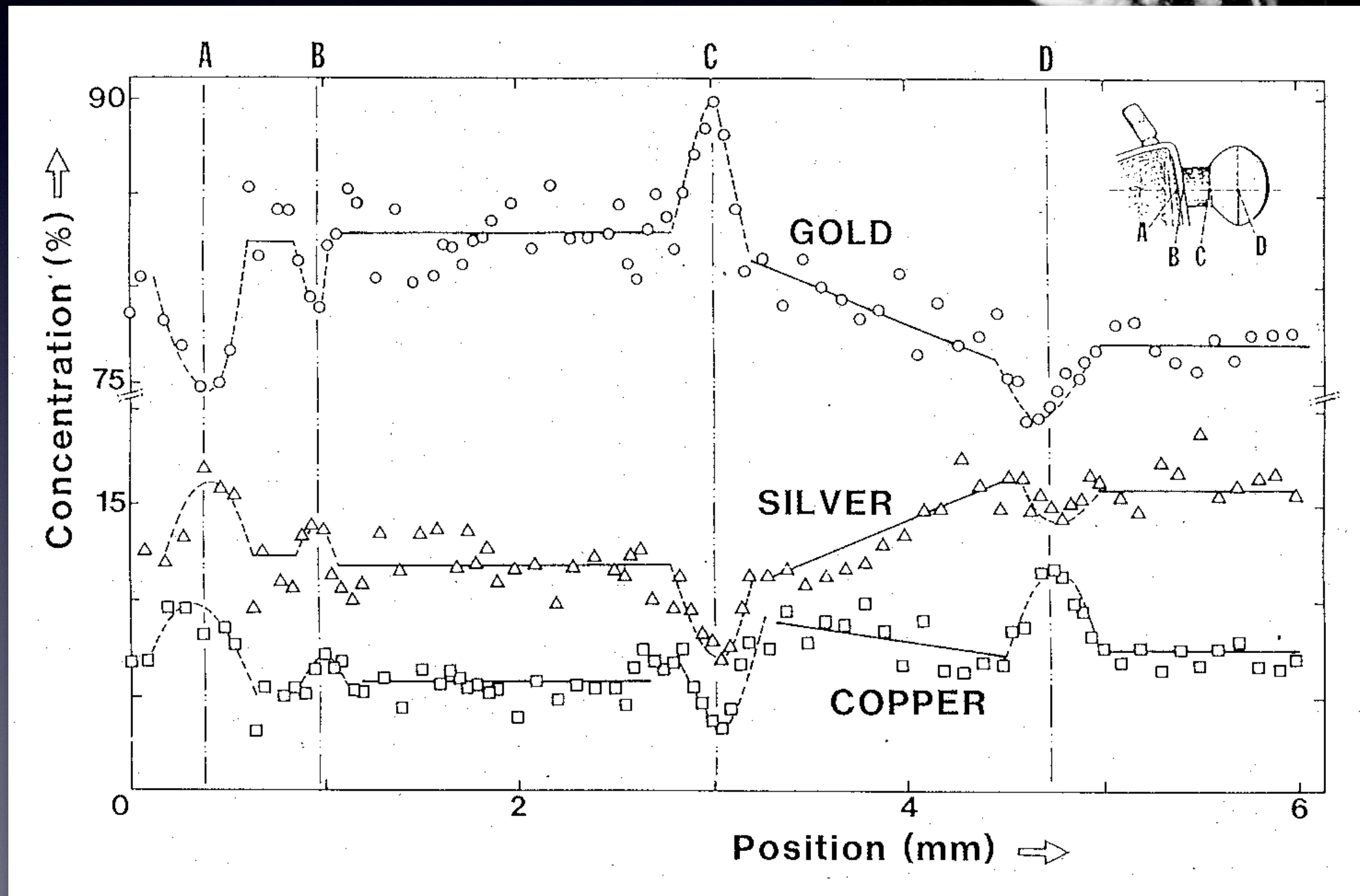
Lead stylus
(Pb, trace of Sn)

Red preparation
(S, Hg, Pb, Fe, P, Ca)

Micro-PIXE measurements of an Achemenide pendant (IV century BC)



Micro-PIXE measurements of an Achemenide pendant (IV century BC)

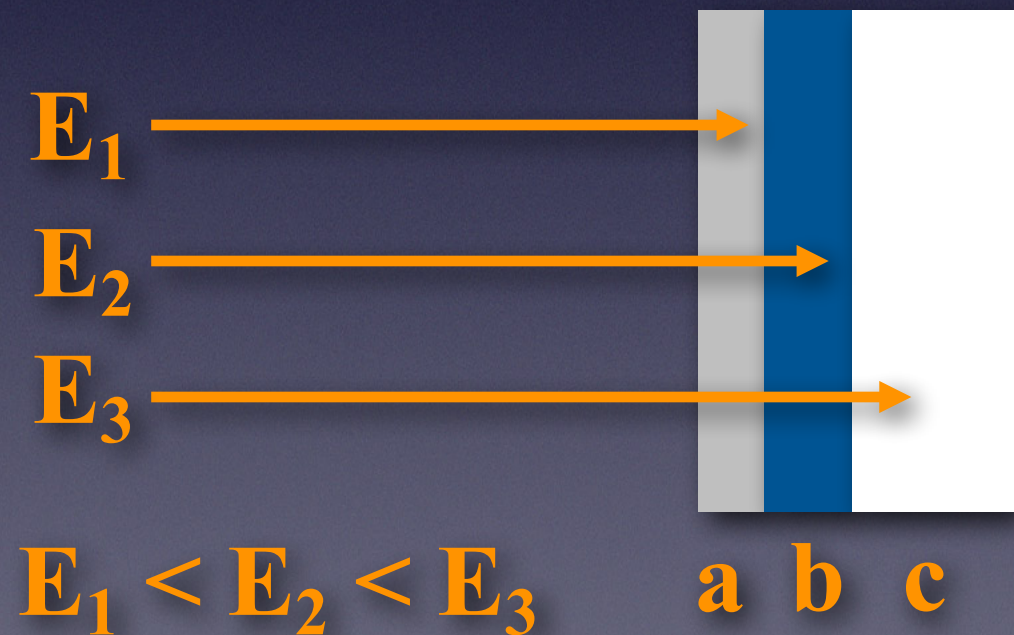


Differential PIXE

Whereas PIXE does not provide elemental depth profiles, “Differential PIXE” measurements can provide semi-quantitative stratigraphical information on cultural heritage objects (works mainly by the groups in Florence, Ljubljana and Namur).

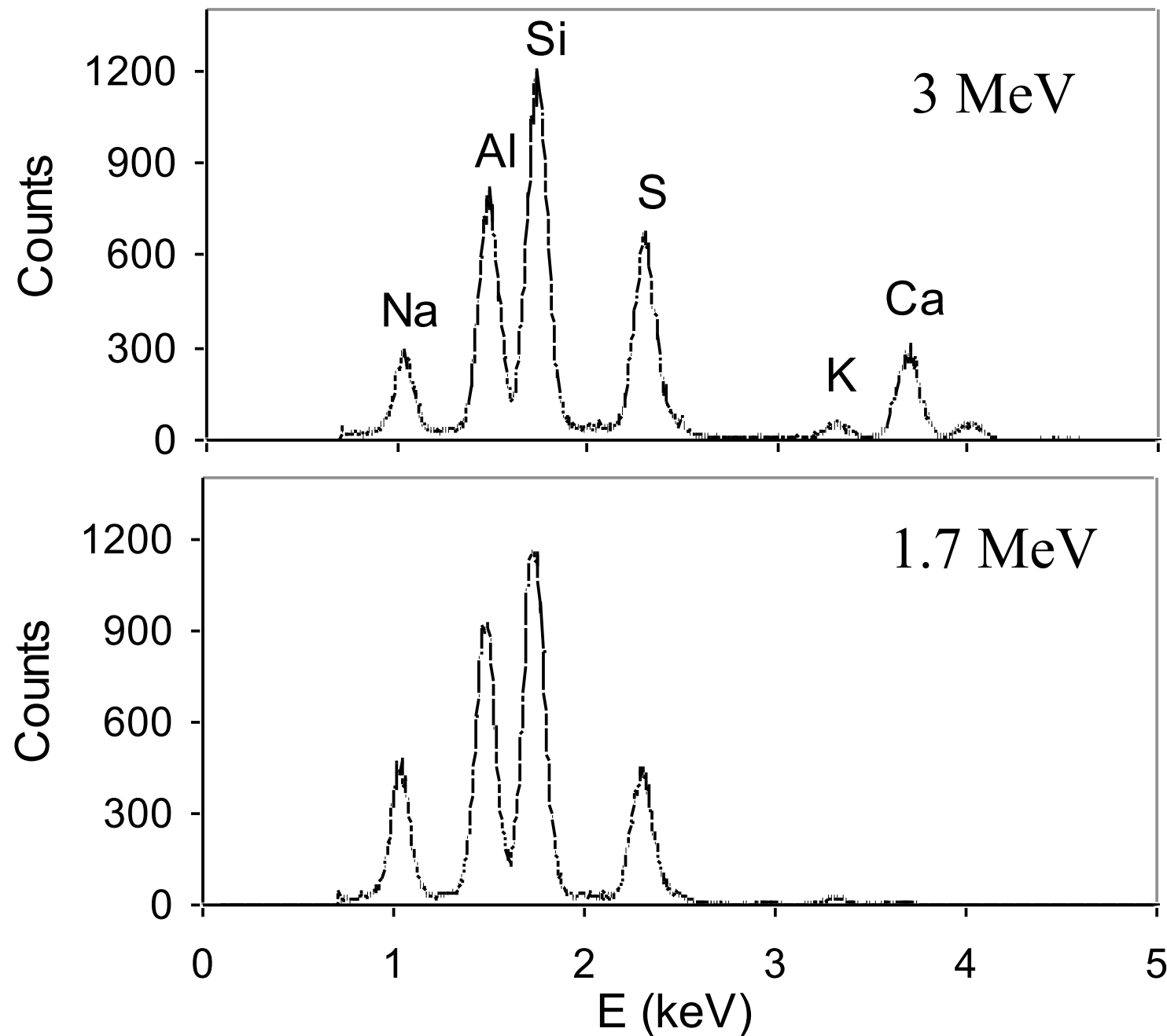
“Differential PIXE” consists in performing measurements on the same area with beams of different energies

*At different energies
proton beam ranges are
different*

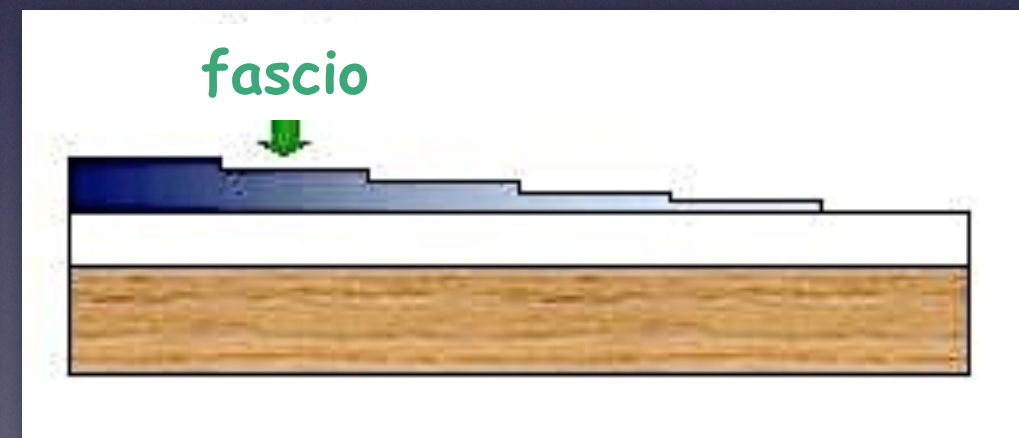


By comparing X-ray spectra taken at different energies, stratigraphic information can be obtained

PIXE spectra at different energies

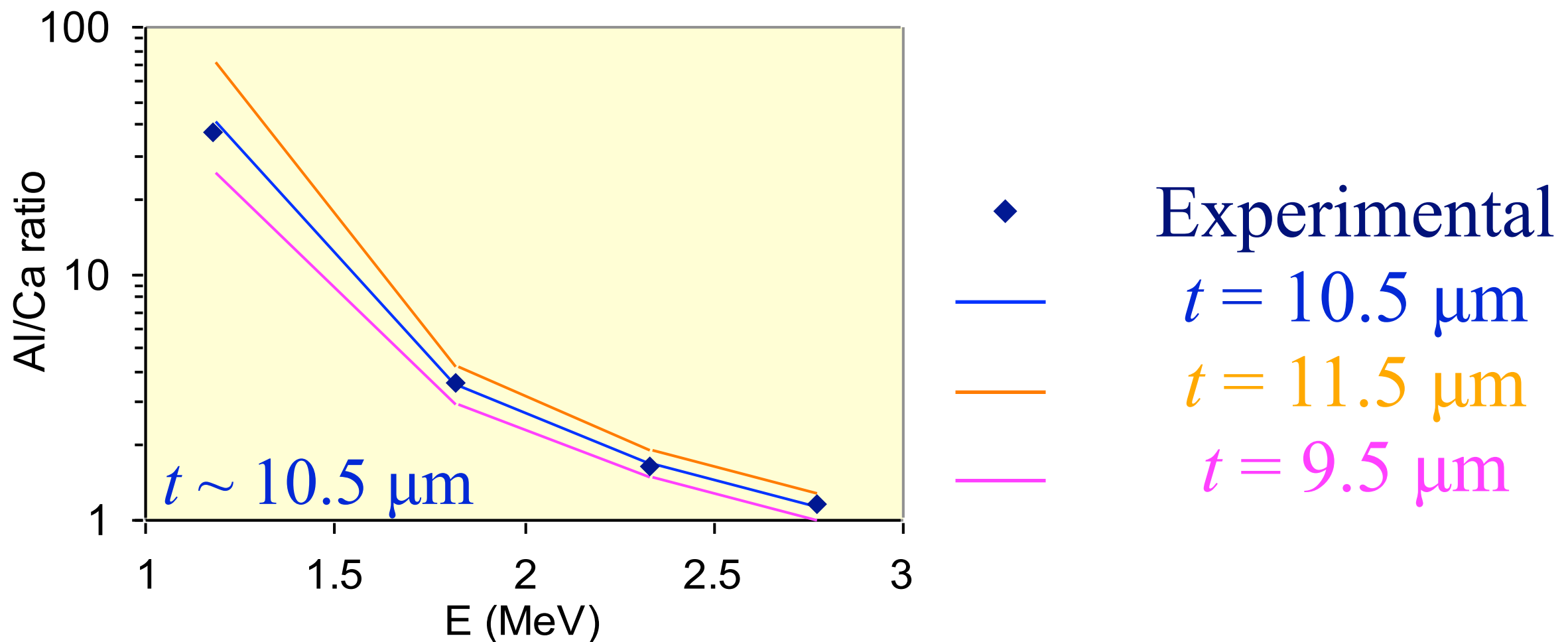


Blue paint layer
(lapislazuli) on a substrate
of calcium sulphate

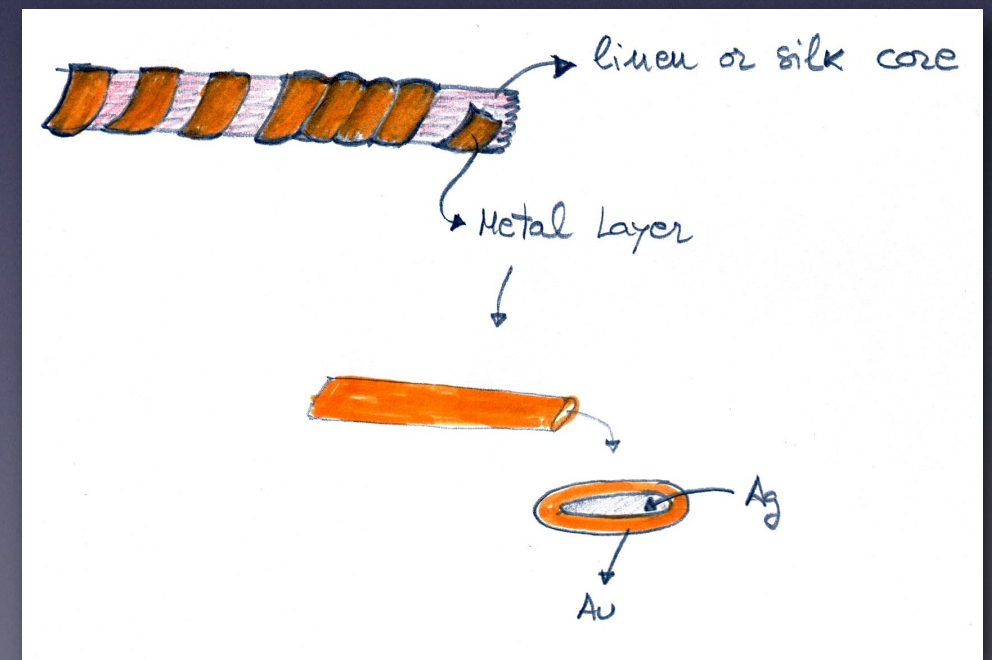
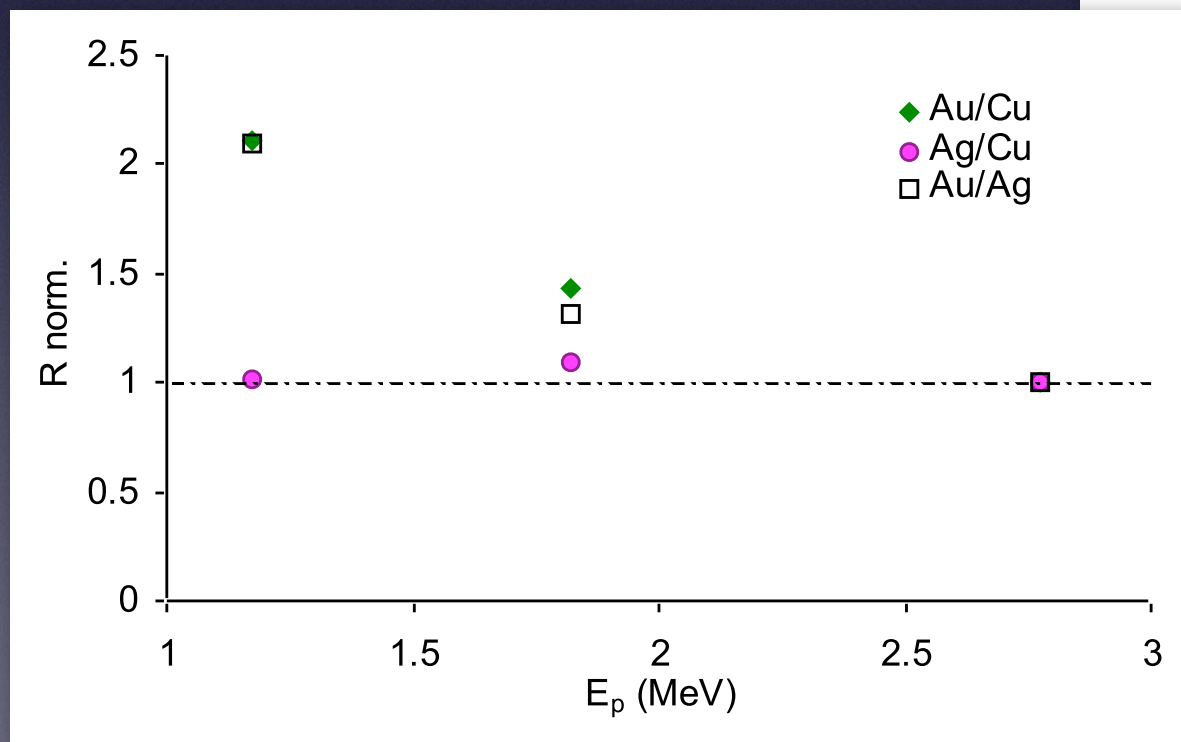
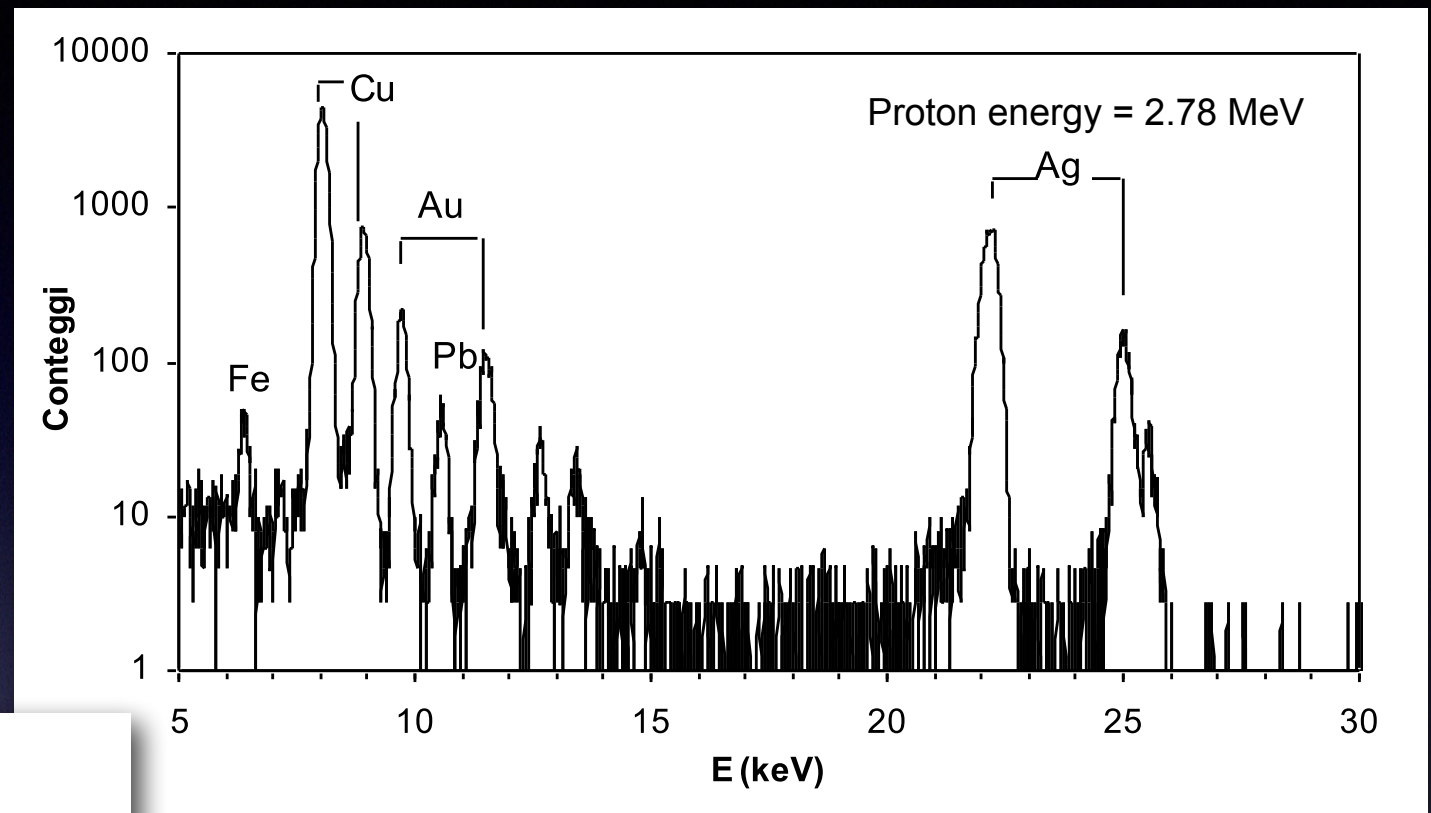
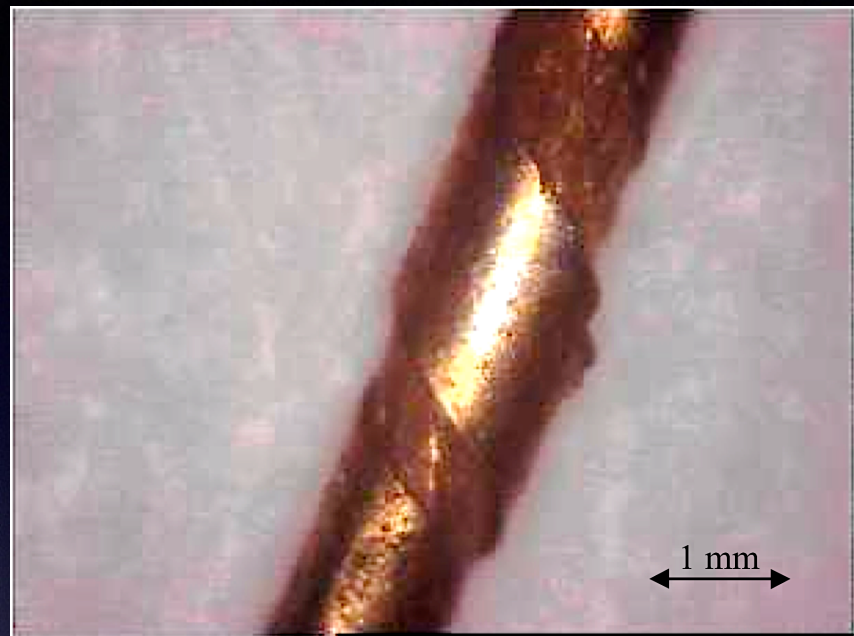


Estimate of the paint layer thickness

$$\frac{Y_{Al}}{Y_{Ca}} = \frac{C_{Al}}{C_{Ca}} \frac{\int_{E_p}^{E_p - \Delta E_{lap}(t)} \sigma_X^{(Al)}(E) e^{-\mu_{lap}^{(Al)} \frac{x(E)}{\cos \theta}} \frac{dE}{S_{lap}(E)}}{e^{-\mu_{lap}^{(Ca)} \frac{t}{\cos \theta}} \int_{E_p}^0 \sigma_X^{(Ca)}(E) e^{-\mu_{white}^{(Ca)} \frac{x'(E)}{\cos \theta}} \frac{dE}{S_{white}(E)}}$$

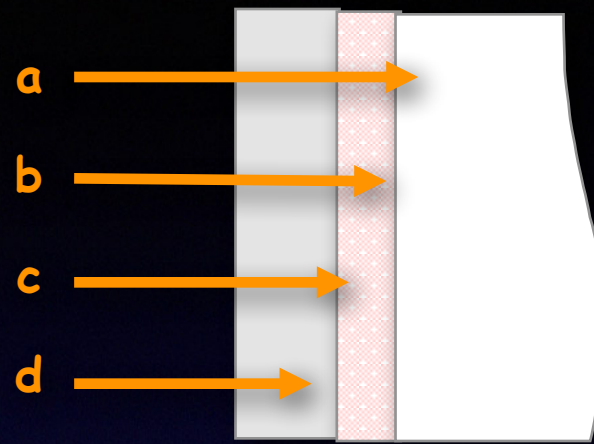
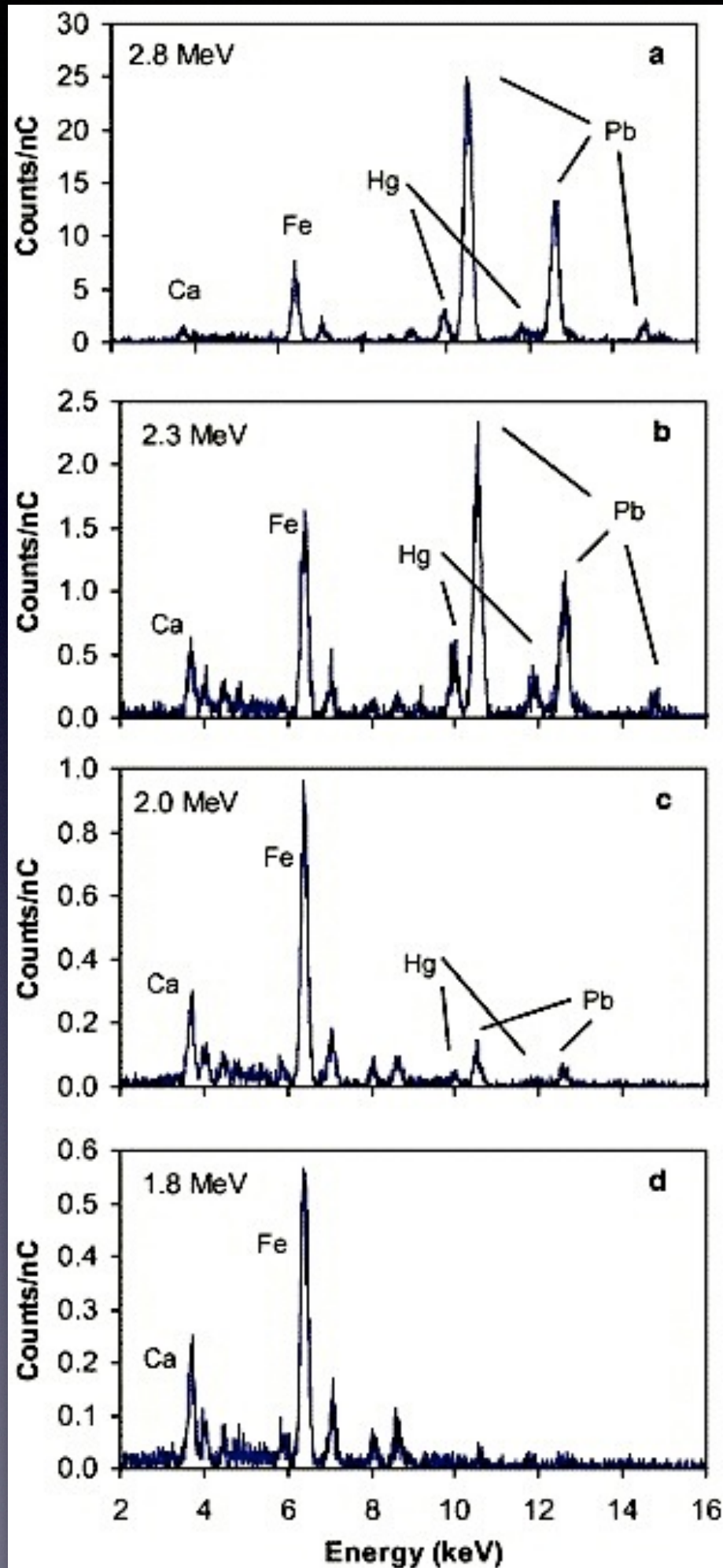


Metal threads (Alhambra, Granada)



Enrichment of gold on the surface

“Incarnato”



paint layer:

cinnabar (HgS, red pigment)+lead white

preparation:

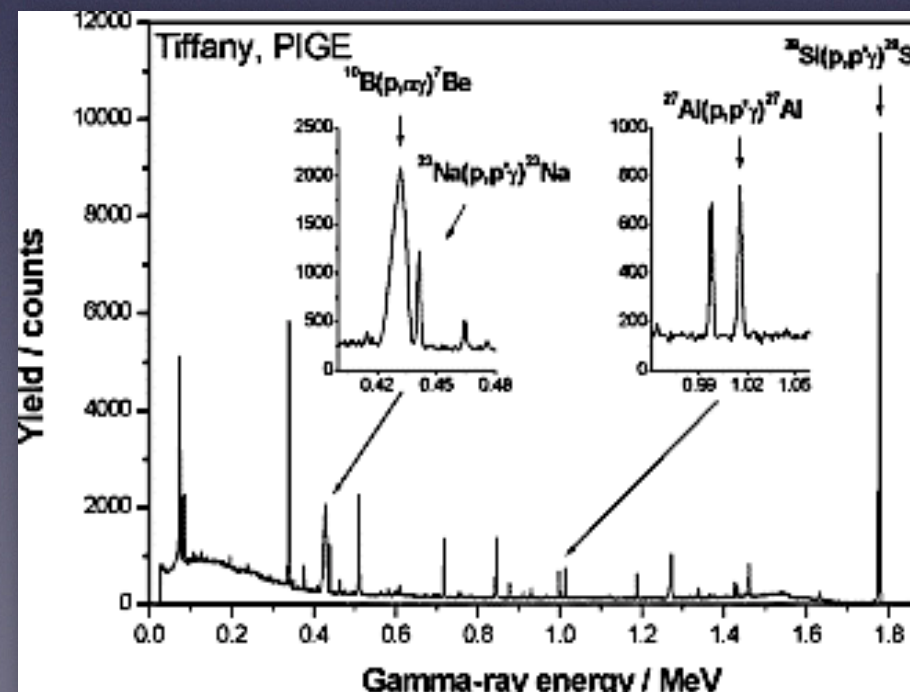
lead white

Ca and Fe are in the varnish

Complementary PIXE/PIGE

Particle Induced Gamma-ray Emission (PIGE) technique is an invaluable tool, complementary to PIXE, to quantify low-Z elements (Li, B, F, Na, Mg, Al, Si, ...) in cultural heritage objects.

In this respect PIGE can be considered a “sidekick” of PIXE



Sherlock Holmes and Doctor Watson



Batman and Robin



Frodo and Sam

Lapis-lazuli pigment in paint layers



“Maddonna dei fusi”, Leonardo da Vinci (1501)

Lapis-lazuli is a blue pigment, mainly composed of lazurite ($3\text{Na}_2\text{O} \cdot 3\text{Al}_2\text{O}_3 \cdot 6\text{SiO}_2 \cdot 2\text{Na}_2\text{S}$)

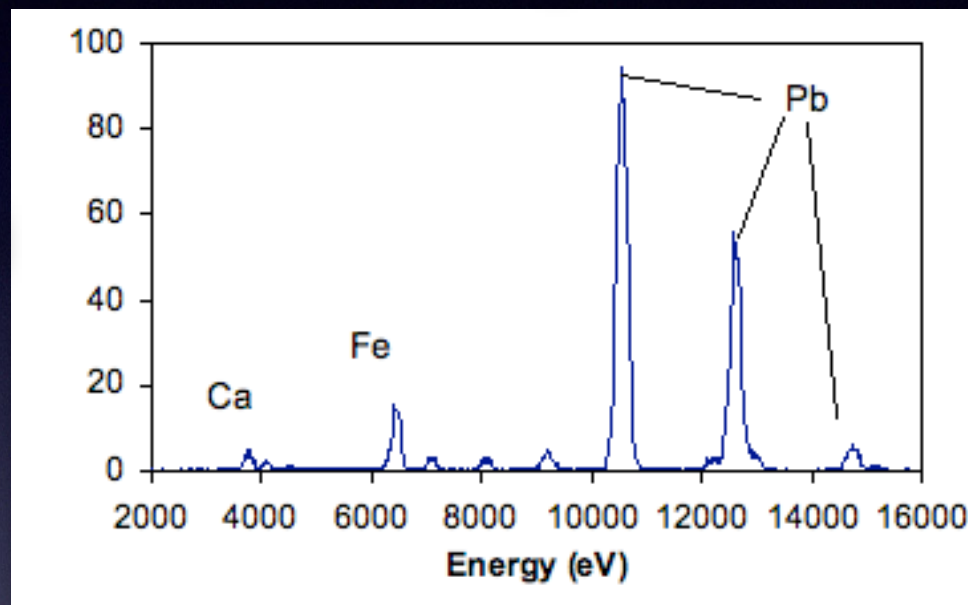
Limited possibility of identifying lapis-lazuli by PIXE in canvas and wood paintings:

- *low-energy X-rays absorption in the varnish and in the paint layer itself*
- *signal interference from other pigments*

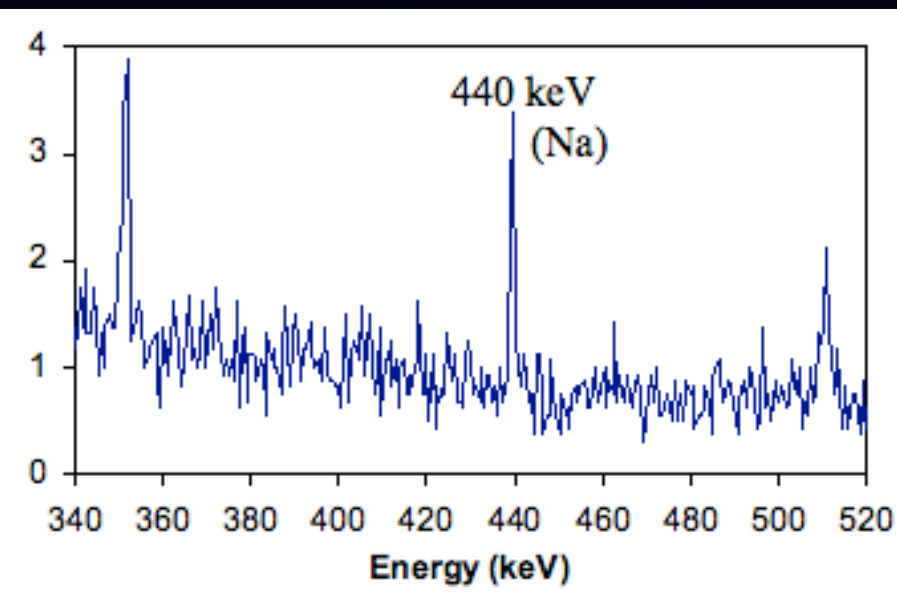
Lapis-lazuli pigment in paint layers

Original
Blue pigment mixed
with Lead white
(Ca and Fe from
the varnish)

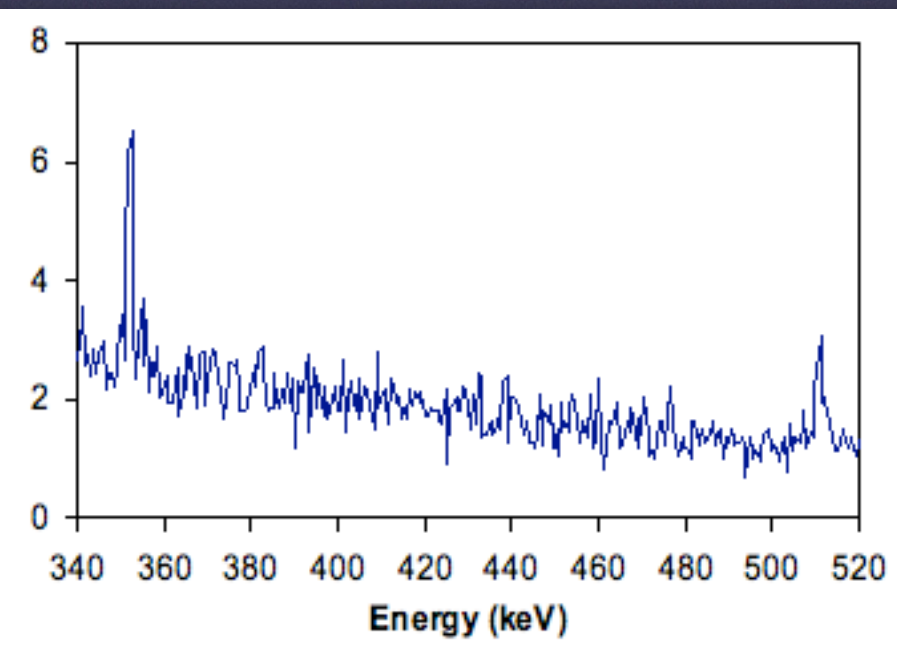
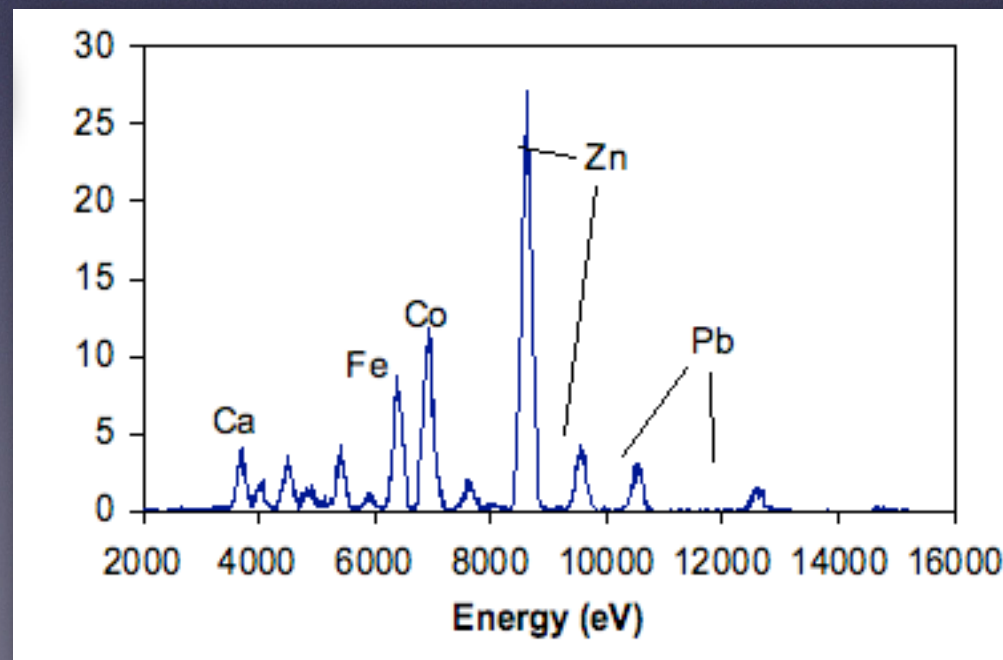
PIXE spectra



PIGE spectra



Restored
Cobalt blue and
Zinc white (used
only from XIX
century!)



Analysis of ancient Roman glasses

Quantification of sodium is of great importance for the characterisation of ancient glasses

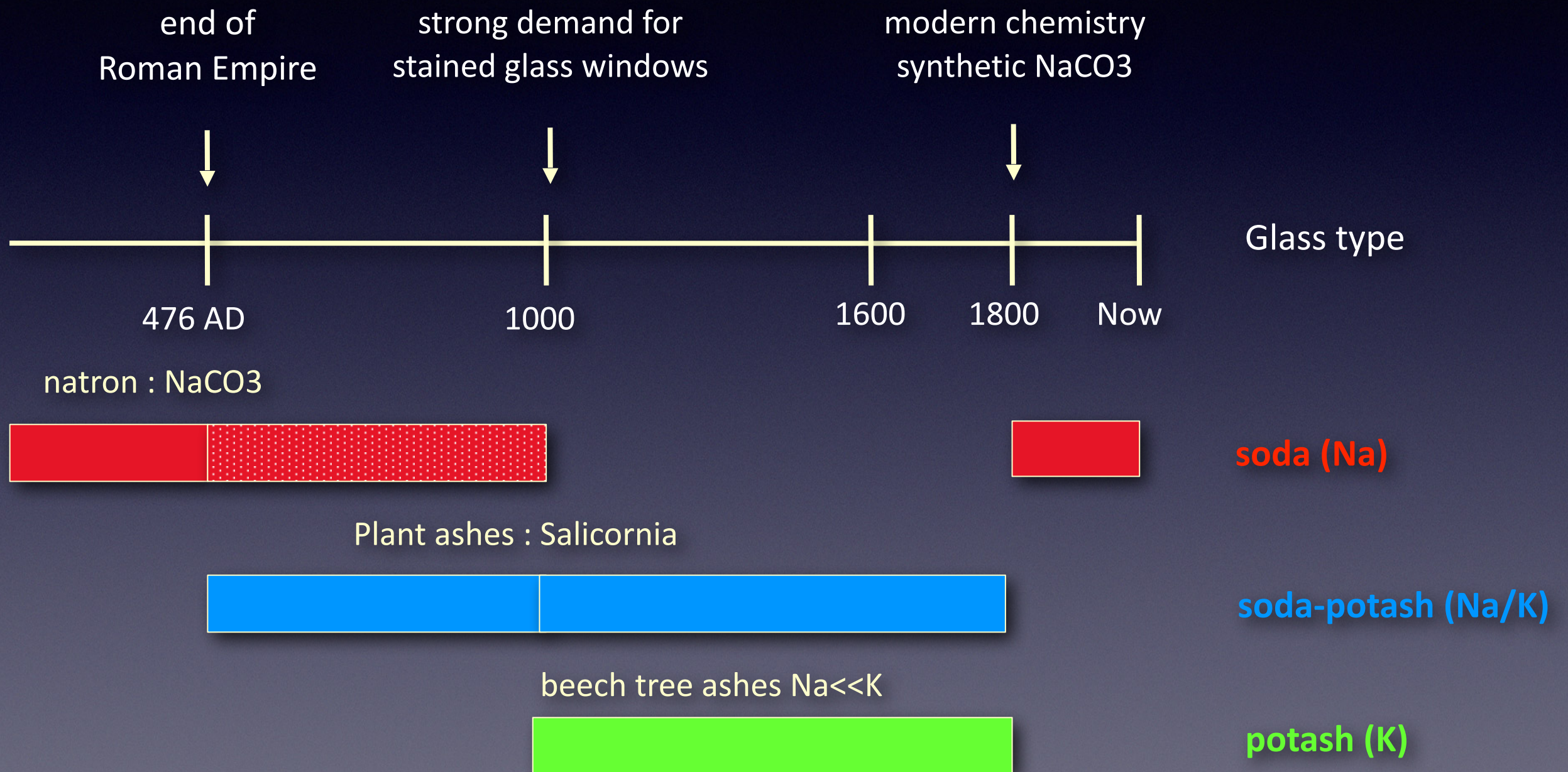


Roman glass mosaic tesserae from Villa Adriana, Tivoli (Italy)

There are two basic typologies of Western glasses:

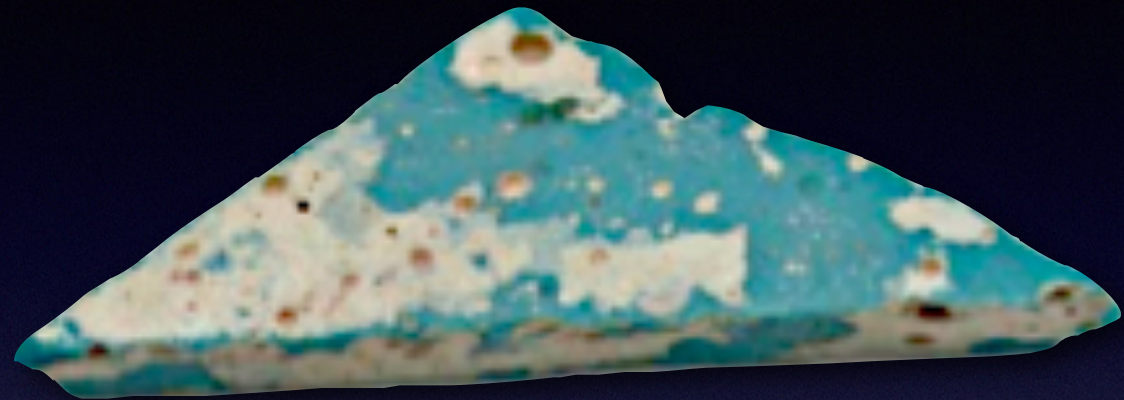
- **natron**
(high Na_2O , low K_2O and MgO content)
Roman and High Middle Ages
- **plant ash**
(low Na_2O , high K_2O content)
since Middle Ages

Evolution of glass manufacture technology



Sodium in Roman glasses

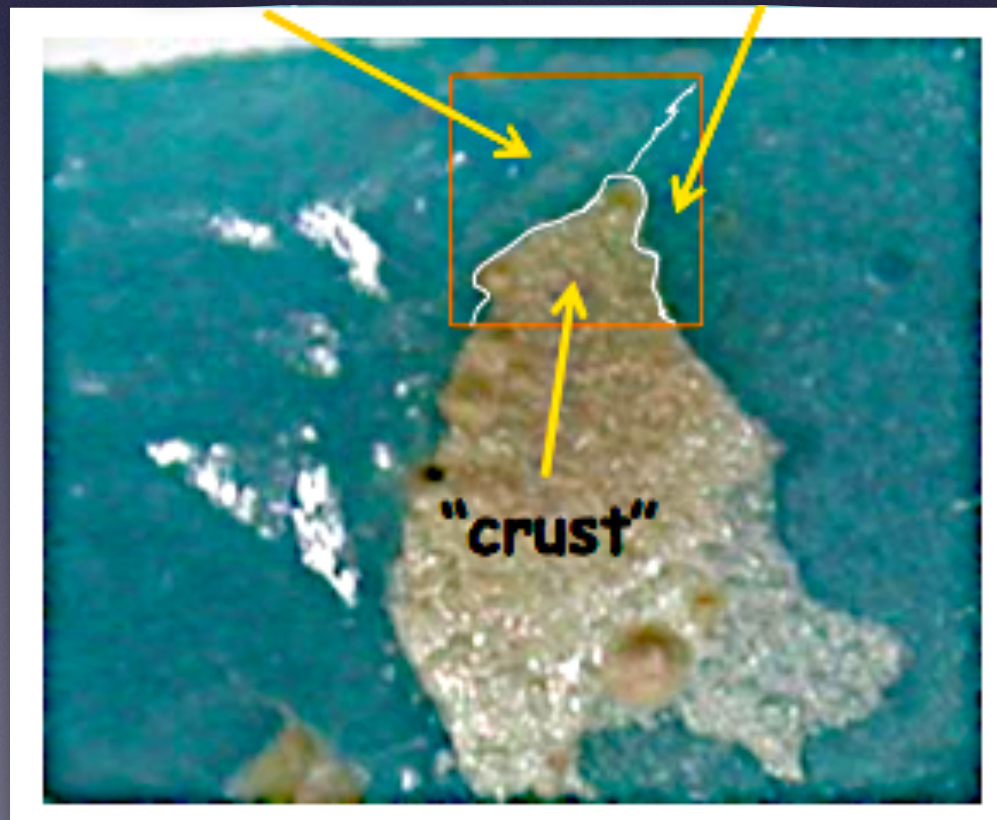
X-rays from the lightest elements strongly absorbed by crusts and *patinae*



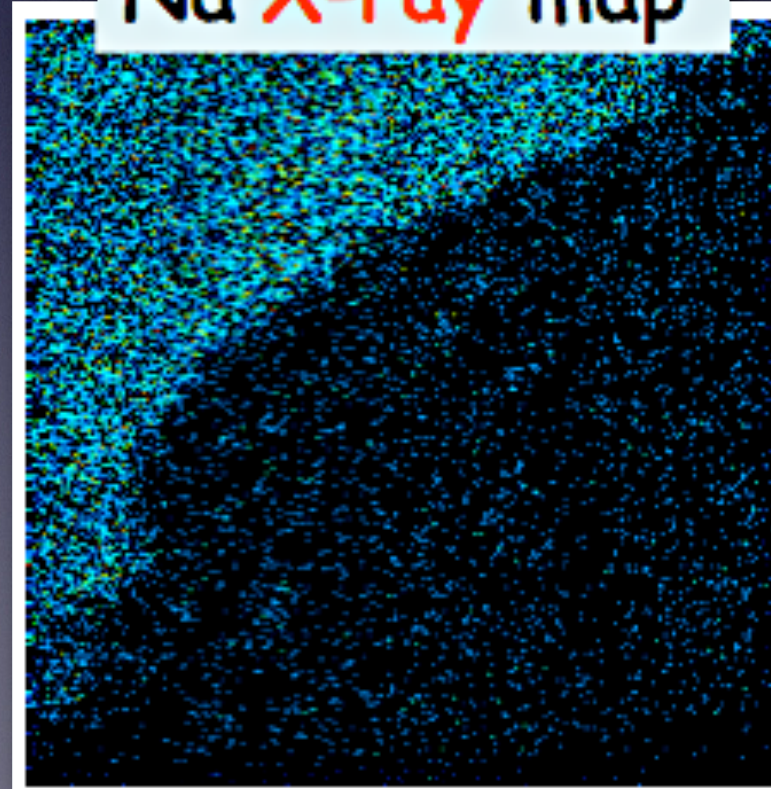
Roman glass mosaic tesserae

“freshly cut”
zone

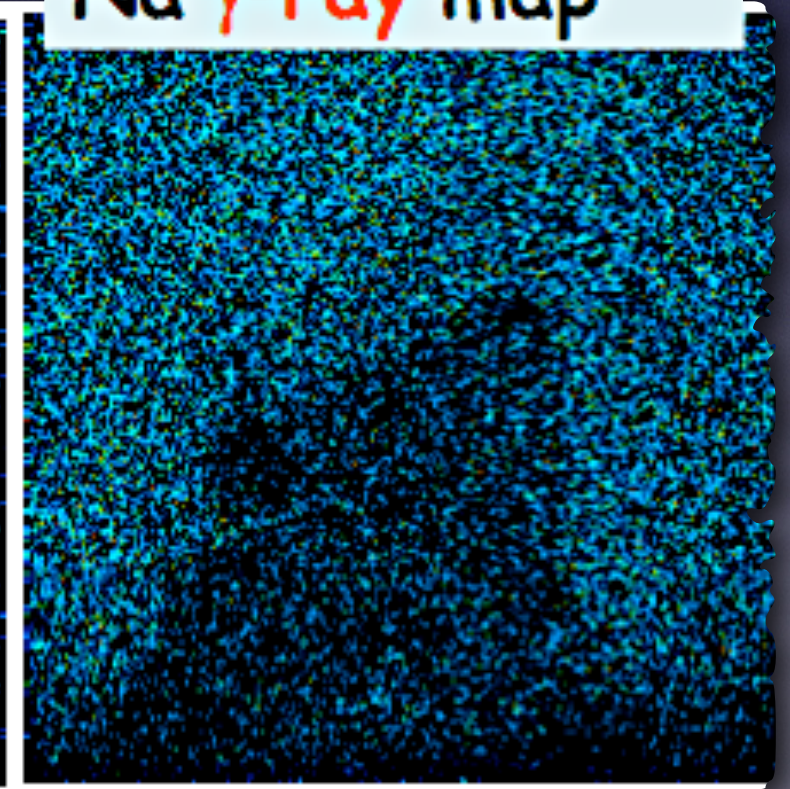
coloured but more
opaque zone



Na X-ray map



Na γ -ray map

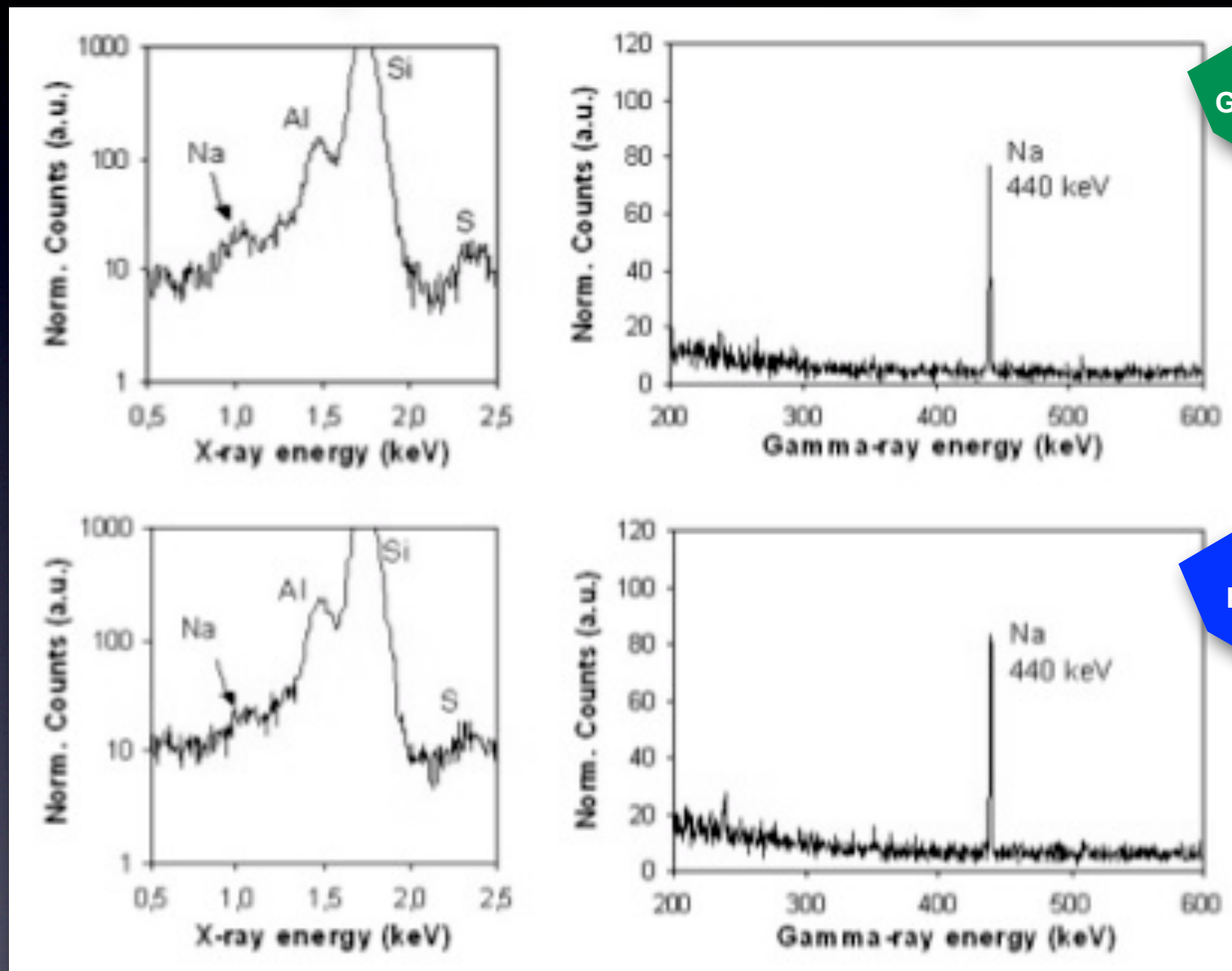


2 mm

Sodium in Roman glasses

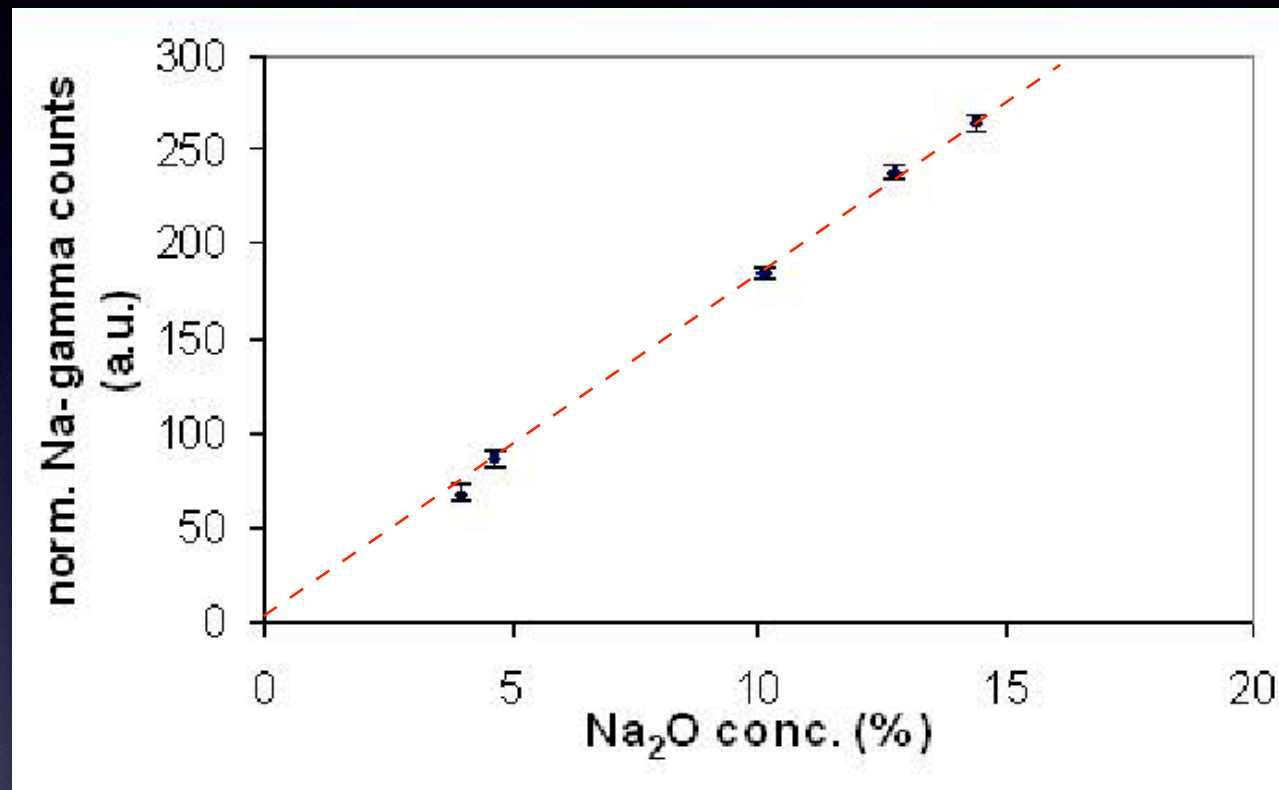
PIXE spectra

PIGE spectra



X-rays from the lightest elements strongly absorbed by crusts and *patinae*

Sodium in Roman glasses



Estimate of Na content by comparing gamma-ray yields to those of thick glass standards (NIST SRM) with certified Na₂O concentration

Concentration ranges perfectly compatible with the typical Roman soda-lime-silica glass

glass colour	main oxides (%)			
	Na ₂ O	SiO ₂	CaO	PbO
green	~20	55-60	5-9	1-3
blue	~20	60-65	5-9	<0.1
turquoise	~20	55-60	5-9	<0.3
yellow	~15	55-60	5-9	5-8
red	~10	35-40	5-9	30-35

Complementary PIXE/RBS

Whereas PIXE and Rutherford Backscattering Spectroscopy (RBS) separately give only partial information, in samples with a layered structure these analyses can be performed simultaneously and their synergic use permits to derive detailed data about composition and elemental depth distribution of the analysed material (aka “Total IBA”)



PIXE strenghts

- High sensitivity
- Excellent specificity

RBS strenghts

- Traceable accuracy
- Excellent depth resolution

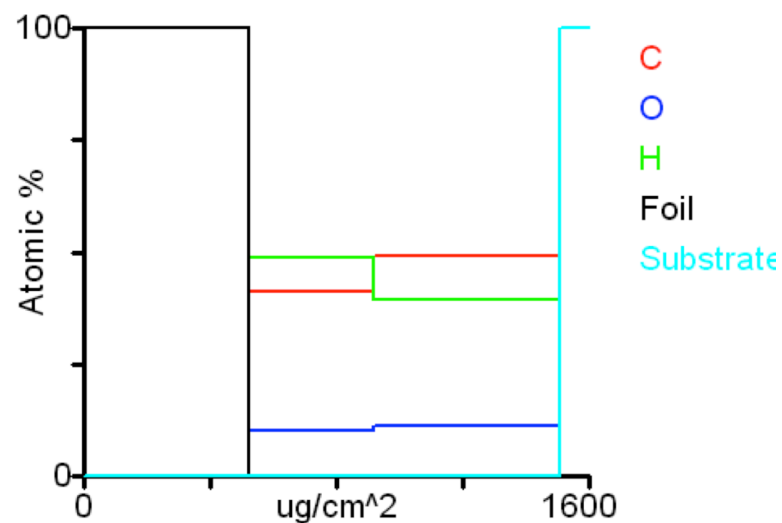
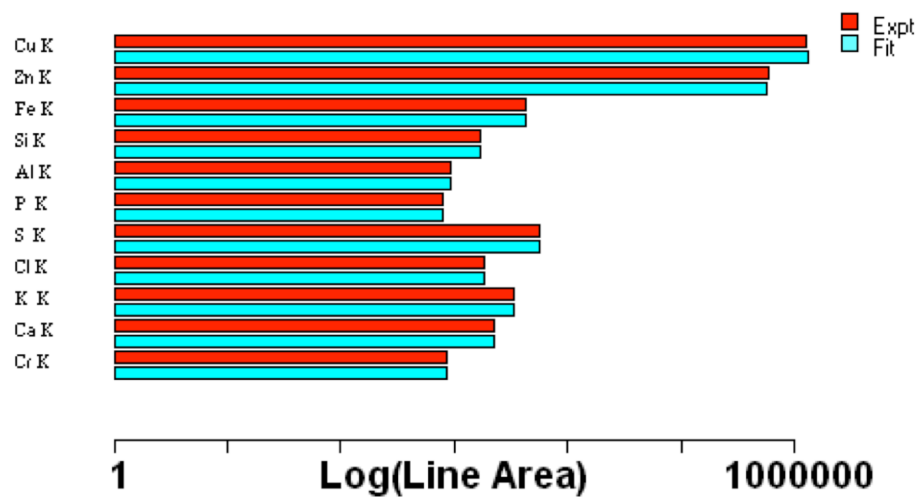
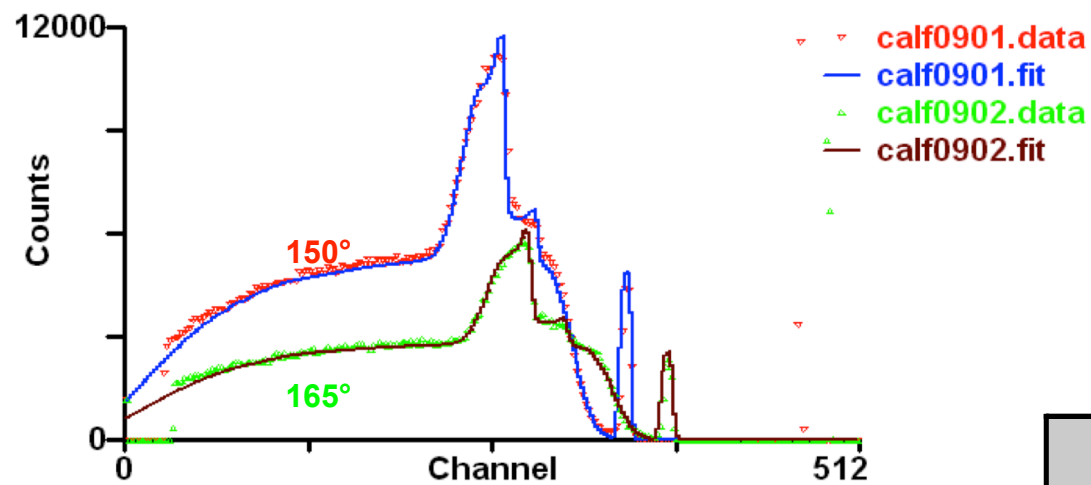
RBS weaknesses

- Low sensitivity
- Poor mass resolution

PIXE weaknesses

- Poor traceability
- Poor depth resolution

“Total IBA” of 1-layered brass test sample

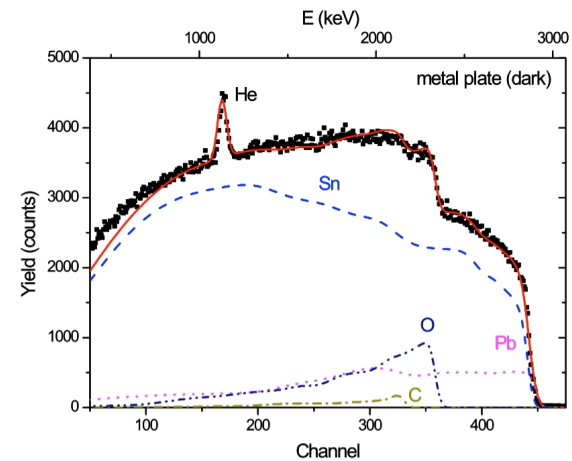


	DataFurnace	SIMNRA	GUPIX
Gilding	Cu 94% Zn 2% Fe 1%, 510 µg/cm	Cu 89% Zn 11%, 390 µg/cm	
Mordant	H 40-49% C 41-49% O 10-11%, 1.0 mg/cm	H 51% C 41% O 8%, 1.0 mg/cm	
Bulk	Cu 65% Zn 35%	Cu 65% Zn 35%	Cu 66%, Zn 34% H&Q 0.946

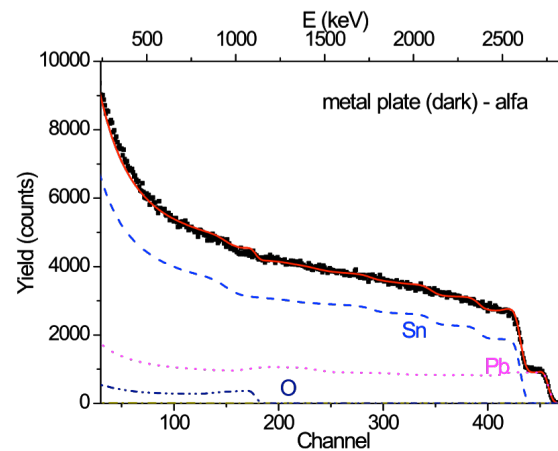
Analysis of stratigraphies in cultural heritage by PIXE/RBS analysis



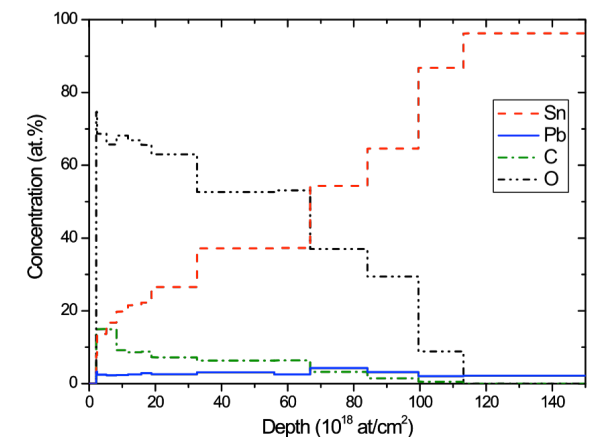
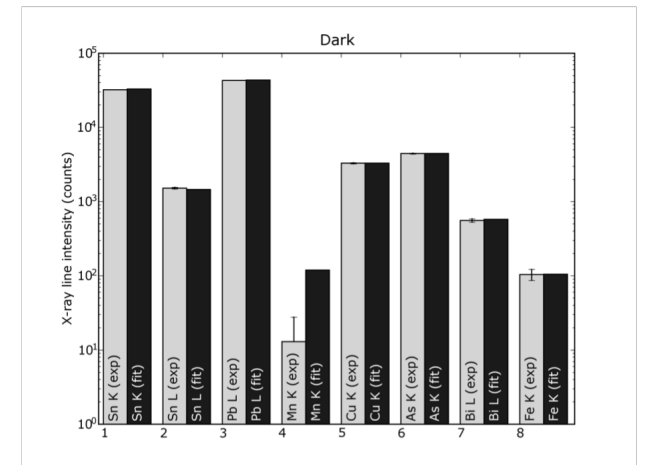
"View from the Window at Le Gras", the oldest surviving camera photograph ("heliography") created by Nicéphore Niépce (in 1826 or 1827) at Saint-Loup-de-Varennes



Fitted RBS spectrum for 3 MeV H^+ beam on the dark spot (corroded area). Calculated partial spectra for each element are also shown



Fitted RBS spectrum for 3 MeV $^4He^+$ beam on the dark spot (corroded area). Calculated partial spectra for each element are also shown



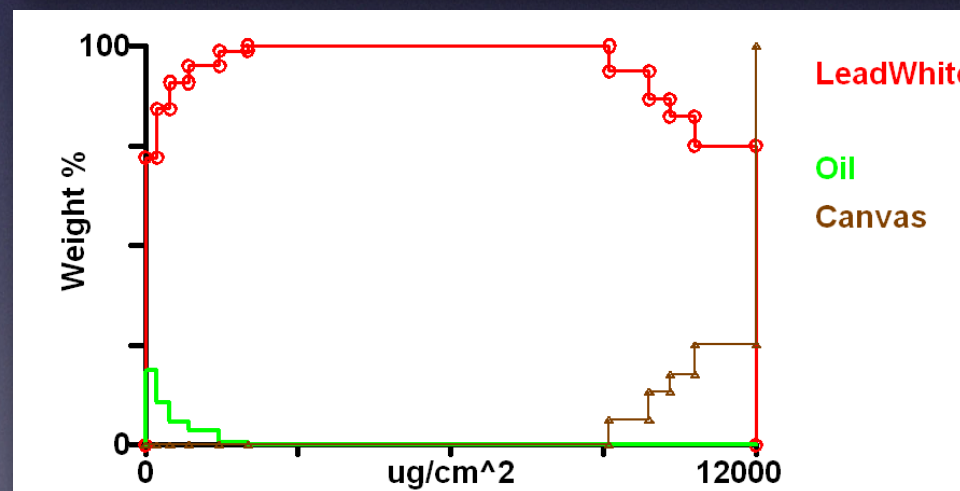
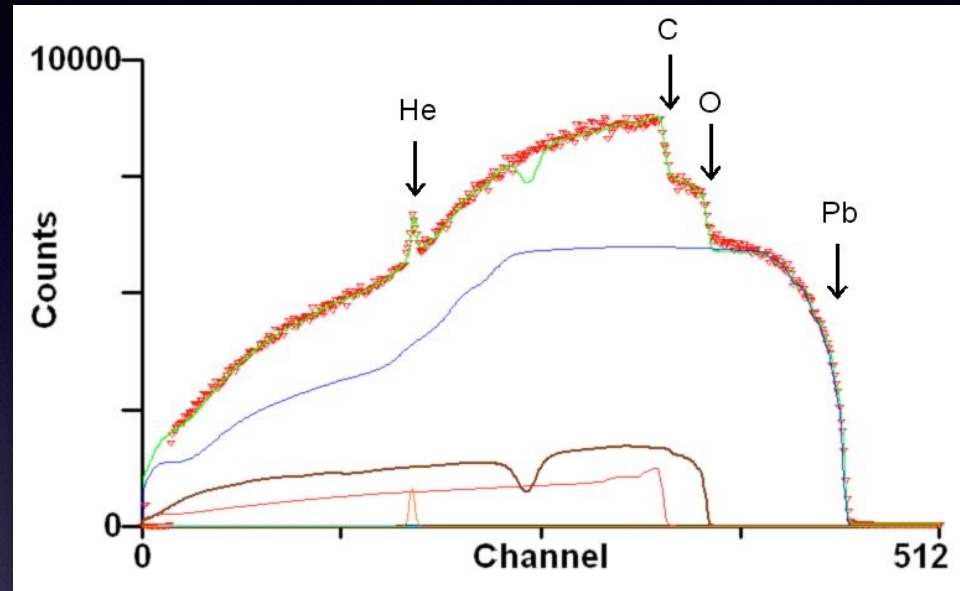
Concentration profiles for the dark spot (corroded area), as obtained from a simultaneous fit to 3 MeV proton PIXE and RBS, and 3 MeV alpha RBS.

PIXE/RBS analyses reveal that the corrosion products are lead oxides in a Sn/Pb matrix

Characterization of paint layers by simultaneous PIXE/RBS analysis



“La Bohémienne”, Frans Hals (1630)



The canvas is schematized as carbon plus chalk (CaCO₃)

Ochre pigment (ematite) detected and quantified thanks to simultaneous PIXE/RBS measurements: $440 \cdot 10^{15}$ atoms/cm² Fe₂O₃ in $7000 \cdot 10^{15}$ atoms/cm² of oil (C₁₃O₅)

Thanks for your
attention!